CHAPTER 5

Scenarios and Information for Policymakers

Lead Authors:
N.R.P. Harris
D.J. Wuebbles

Coauthors:
J.S. Daniel
J. Hu
L.J.M. Kuijpers
K.S. Law
M.J. Prather
R. Schofield

Contributors:
J.B. Burkholder
E.L. Fleming
Ø. Hodnebrog
R. Hossaini
C.H. Jackman
D. Phoenix

Chapter Editors:
M. McFarland
G.J.M. Velders

[Formatted for double-sided printing.]

CHAPTER 5

SCENARIOS AND INFORMATION FOR POLICYMAKERS

Contents

SCIENTIFIC SUMMARY

A new baseline scenario for ozone-depleting substances (ODSs) is presented in Chapter 5 that reflects our current understanding of atmospheric mixing ratios, production levels, and bank sizes. Elimination of future emissions, from either production or existing banks of various ODSs, is applied to this scenario to evaluate the maximum impacts of various hypothetical policy options including phase-outs and destruction (see Table S5-1). Some specific findings corresponding to this table include:

- **Emissions from the current banks (taking 2015 as being current) over the next 35 years are projected to lead to greater future ozone depletion and climate forcing than those caused by future ODS production.** Capture and destruction of these banks could avoid 1.8 million Ozone Depletion Potential-tonnes (ODP-tonnes) of future emission through 2050; this compares with an estimated 1.6 million ODP-tonnes of emissions that have occurred over the last decade (from 2005–2014).

- **Of all of the ODS banks, the banks of halons in 2015 are projected to contribute most to ozone depletion over the next 35 years (as Equivalent Effective Stratospheric Chlorine, EESC), while chlorofluorocarbon (CFC) and hydrochlorofluorocarbons (HCFC) banks are expected to contribute most in terms of Global Warming Potential-weighted (GWP-weighted) emissions.**

- **If future production and all ODS 2015 banks are considered, HCFCs represent the halocarbon group that contributes most to future GWP-weighted emissions. HCFCs can be reduced in the future by both bank recapture and destruction and by production elimination.**

Table S5-1. Summary of mitigation options for accelerating the recovery of the ozone layer and reducing CO_2-equivalent emissions. The table gives the reductions in integrated EESC (Equivalent Effective Stratospheric Chlorine) and integrated CO_2-equivalent emissions relative to the baseline scenario that can be achieved for mitigation options beginning in 2015 or 2020. The integrated EESC is defined as the total EESC amount integrated from 2015 until the time EESC returns to the 1980 level (before 2050 for all scenarios). Bank recapture and destruction is assumed to be 100% effective and either applies to the bank existing in 2015 or the bank existing in 2020. Any potential contribution from very short-lived substances is neglected. These calculations use the lifetimes derived from SPARC, 2013 (Stratosphere-troposphere Processes And their Role in Climate).

Substance or Group of Substances	Reductions (%) in Integrated Midlatitude EESC Integrated from 2015 until EESC Returns to 1980 Levels		Reduction in Cumulative GWP-Weighted Emissions from 2015 to 2050 (Gigatonnes of CO_2-equivalent)	
Bank recapture and destruction in 2015 or 2020:	**2015 bank**	**2020 bank**	**2015 bank**	**2020 bank**
CFCs	8.9	5.3	4.7	3.3
halons	12	6.8	0.2	0.2
HCFCs	6.4	5.5	4.6	4.6
Production elimination from 2015 onward:				
HCFCs	6.4		7.8	
CH_3Br (only quarantine and pre-shipment)	5.3		0.0	
Total emissions elimination from 2015 onward:				
CCl_4	9.8		1.2	
CH_3CCl_3	0.0		0.0	
HFCs	0.0		Up to 165*	

* Reduction relative to hypothetical future upper range scenario and would depend on actual growth rate of HFC use.

- **The impact on ozone-layer recovery of further policy actions on already controlled ozone-depleting substances is becoming smaller.** Nonetheless, if all ODS emissions – including those emanating from many widely dispersed banks – were to be stopped in 2015, then the return to 1980 midlatitude EESC values would be brought forward to 2036 compared with 2047 in the baseline scenario.

- **Updated Ozone Depletion Potentials (ODPs) are almost all numerically smaller, ranging from no change (for carbon tetrachloride, CCl_4) to more than a factor of two smaller (for CFC-115), with most of these smaller by 10–30% than the values reported in WMO (2011).** These changes largely reflect the revised estimate for the atmospheric lifetime of CFC-11 (from 45 to 52 years) reported in SPARC (2013); CFC-11 is the reference gas in determining ODPs so this change affects all ODPs. Uncertainties in the atmospheric lifetimes, the fractional release values, and atmospheric chemistry generally result in overall uncertainties in ODPs on the order of 30% for the CFCs and CCl_4, but are higher for HCFCs and halons (about 60% for the HCFCs and halon-1301, to over 80% for halon-1202 and halon-1211).

- **New atmospheric model studies continue to emphasize that ODPs for very short-lived substances (VSLS) that contain bromine or chlorine are strongly dependent on the geographic location and season of emission.** Impacts from VSLS are much larger (with ODPs approaching values of 1) if emissions occur in regions close to convective regions in the tropics. There is still insufficient research available to confidently compare the mitigation options of anthropogenic VSLS emissions with those of the longer-lived halogenated hydrocarbons; overall the VSLS have smaller ODPs than longer-lived ODS. However, if long-lived controlled halocarbons (and their banks) follow their projected decline, then chlorine- and bromine-containing anthropogenic VSLS emissions will play a relatively larger role in future ozone depletion, but the absolute effects are smaller than that of ODSs today while remaining uncertain.

- **The projection of CCl_4 remains more uncertain than projections for other ODSs due to our incomplete understanding of the current CCl_4 budget (likely a missing source; see Chapter 1).** In the scenarios examined (see table above), CCl_4 human-related emissions from 2015 through 2050 are comparable to those of the HCFCs in terms of ODP-weighted emissions and are about 10% in terms of GWP-weighted emissions. It is expected that future emissions of CCl_4 will remain an important factor in the evolution of EESC.

- **The total anthropogenic emissions of methyl bromide (CH_3Br) have declined in response to controls of the Montreal Protocol.** Overall, reported consumption has gone down from ~70,000 tonnes/yr in the late 1990s to ~13,000 tonnes/yr in 2012.

- **Quarantine and pre-shipment (QPS) uses of CH_3Br are exempted uses (not controlled) by the Montreal Protocol and in 2012 constitute an annual consumption of CH_3Br (~9,000 tonnes) that is larger than the annual consumption for 2012 from uses controlled by the Protocol (~4,000 tonnes).** The elimination of future emissions from QPS uses could bring forward the date of EESC return to 1980 levels by 1.1 years, smaller than the 1.6 years estimated in the previous Assessment. Critical-use exemptions continue to be granted, but at levels significantly reduced compared with four years ago. A continuation of critical-use exemptions at the current level would delay the return of EESC to 1980 levels by 0.2 years.

- **Carbon dioxide (CO_2), nitrous oxide (N_2O), and methane (CH_4) are each important to climate forcing and to the levels of stratospheric ozone (see Chapter 2).** In terms of the globally averaged ozone column, additional N_2O leads to lower ozone levels, whereas additional CO_2 and CH_4 lead to higher ozone levels. Ozone depletion to date would have been greater if not for the historical increases in CO_2 and CH_4. The net impact on ozone recovery and future levels of stratospheric ozone thus depends on the future abundances of these gases. For many of the scenarios used in the most recent Intergovernmental Panel on Climate Change (IPCC) Assessment (IPCC, 2013), global ozone

will increase to above pre-1980 levels due to future trends in the gases. Latitudinal and altitudinal responses are expected to vary. Note that scenarios used in IPCC consider a future with all three major greenhouse gases increasing and thus it is important to assess the net balance of these perturbations on stratospheric ozone.

- **Global Warming Potentials (GWPs) for a range of halocarbons have been updated based on IPCC (2013) and SPARC (2013).** The CO_2 Absolute Global Warming Potential (AGWP; the denominator for the GWP of other greenhouse gases) has increased by 6% compared to the previous Assessment (WMO, 2011). As a result, GWP values for many non-CO_2 greenhouse gases decreased slightly. GWPs also changed because of revised values for the lifetime and the radiative efficiency of the individual greenhouse gases. The revised SPARC-based lifetimes for a range of ODSs have been updated due to new analyses of observations and models and are included here; the largest differences in GWPs are found for CFC-11, CFC-115, halon-1301, halon-2402, and halon-1202. For hydrofluorocarbons (HFCs), some examples of the IPCC 100-year GWPs and the SPARC lifetime adjusted values are given below. The numbers in parentheses represent the effects of uncertainties in the SPARC lifetimes, radiative efficiency, and the AGWP for CO_2 based on 90% confidence. In addition, the IPCC (2013) stated uncertainties in the 100-year GWP for HFC-134a is ±35% (90% confidence) as representative for similar gases. The IPCC and updated GWPs that use the SPARC lifetimes are consistent within their uncertainties.

Substance	IPCC AR5 100-yr GWP	Updated 100-yr GWP (90% uncertainty range)
HFC-23	12,400	12,500 (8880–16,300)
HFC-32	677	704 (453–1070)
HFC-125	3170	3450 (2230–5140)
HFC-134a	1300	1360 (857–2050)
HFC-143a	4800	5080 (3460–7310)
HFC-152a	138	148 (96–211)

- **Global Temperature Potentials (GTPs) are discussed and values reported for the first time in a WMO-UNEP Ozone Assessment.** The GTP metric gives the relative temperature increase at a specified time horizon due to emissions of a greenhouse gas, relative to that caused by the same weight of CO_2 emissions. This metric may be useful as an alternative to GWPs. These metrics are different in construction and have both advantages and disadvantages. The revised SPARC-based lifetimes affect GTPs (relative to IPCC, 2013) in the same way as GWPs. The table below shows updated GTPs for the same HFCs listed above.

Substance	Updated 20-yr GTP	Updated 50-year GTP	Updated 100-year GTP
HFC-23	11,500	13,000	12,800
HFC-32	1440	154	98
HFC-125	6040	3350	1180
HFC-134a	3170	771	214
HFC-143a	7110	5390	2830
HFC-152a	191	26	21

- **The current direct radiative forcing (RF) from ODS halocarbons (CFCs, halons, and HCFCs) is about 0.33 W m^{-2} and is near its expected peak.** The RF is projected to decrease to about 0.20 W m^{-2} by about 2050, depending on the particular emission scenario adopted. By 2100, the radiative forcing from these halocarbons is projected to be near 0.10 W m^{-2} independent of the specific emission scenarios considered here.

- **While HFCs currently constitute less than 1% of the radiative forcing on climate (0.02 W m^{-2}), if the current mix of HFCs is unchanged, increasing demand could imply a radiative forcing for HFCs as high as 0.4 W m^{-2} by 2050.** For all scenarios (Special Report on Emissions Scenarios (SRES) and Representative Concentration Pathway (RCP)) used in the recent IPCC Assessments, the HFC radiative forcing increases by 0.1 W m^{-2} or less by 2050; however, these scenarios did not consider recent market trends. Scenarios based on projections of HFC markets yield radiative forcings that range from 0.16 W m^{-2} to 0.4 W m^{-2} by 2050.

- **Replacements of the current mix of high-GWP HFCs with low- or zero-ODP, low-GWP compounds, could lead to a decrease in the radiative forcing on climate over the coming decades, possibly by as much as 0.07 W m^{-2} by 2030 relative to baseline scenarios assuming continued growth in high-GWP HFC production.** Such reductions are comparable to possible reductions in radiative forcing for some other non-CO$_2$ emissions (e.g., for black carbon emissions). Even by 2050, the RF from the low-GWP replacement compounds would be negligibly small. For the uses projected, such replacements are likely to have a negligible effect on stratospheric ozone, despite some replacements containing chlorine or bromine and having non-zero ODPs.

- **The impact of HFC mitigation on future climate change that only considers radiative forcing of HFCs through a particular year is underestimated if the future commitment to climate forcing in the HFC banks is neglected.** This bank size represents a substantially larger fraction of the cumulative HFC production and emission than was the case for CFCs in the 1980s; this is because current and projected applications for HFCs emit those HFCs much more slowly than applications historically did for CFCs.

- **Unsaturated HFCs (also known as hydrofluoro-olefins, HFOs) are replacement compounds for long-lived HCFCs and HFCs.** Unsaturated HFCs have short atmospheric lifetimes (days) and small GWPs (<10). Atmospheric degradation of one of these substances (HFC-1234yf) produces the persistent degradation product trifluoroacetic acid (TFA). While the environmental effects of TFA are considered negligible over the next decades, potential longer-term impacts could require future evaluations due to the environmental persistence of TFA and uncertainty in future uses of HFC-1234yf.

- **CFC-316c ((E)- and (Z)- isomers of cyclic 1,2-C$_4$F$_6$Cl$_2$) are possible ODS replacement compounds, and have long lifetimes (75 and 114 years), with correspondingly high ODPs (0.46 and 0.54) and GWPs (4160 and 5400).**

- **Emissions of biogenically produced bromocarbons will likely increase as a result of changes in the management of their human-related production (e.g., marine aquaculture).** However, uncertainties in all natural emissions and in transport to the stratosphere are large, making it difficult to quantify their effects on ozone.

- **Current emissions from aviation and rockets have only a small effect on total ozone (<1%). However, new technologies and potential market growth in aviation and rockets will require further assessment as they could potentially lead to effects on ozone.**

- **Geoengineering the climate system via anthropogenic increases of stratospheric sulfate aerosols within the next few decades would be expected to deplete stratospheric ozone, with the largest effects in the polar regions.** The current level of understanding of how other possible geoengineering approaches would affect the stratosphere is limited.

- **The proposed cosmic-ray-driven breakdown of CFCs in ice particles is of negligible importance in polar ozone loss.**

5.1 INTRODUCTION

The series of WMO Ozone Assessments have reported the success of the control measures introduced under the Montreal Protocol. These have included striking reductions first in the rate of increase in atmospheric ozone-depleting substances (ODSs) and subsequently in the total amount of ODSs in the atmosphere (see Chapter 1). Signs of an increase in stratospheric ozone amounts are emerging (Chapter 2), pointing to the success of these measures in reducing ozone depletion and hence limiting the resulting increases in surface UV radiation. As successive Amendments and adjustments to the Montreal Protocol have been introduced, opportunities for further significant measures affecting stratospheric ozone have become scarcer. Accordingly, policy-relevant issues are now largely concentrated on (i) issues connected with new compounds with the potential to deplete ozone and (ii) the other atmospheric effects of ODSs and their replacements. In addition, the Montreal Protocol and its Amendments have at this point contributed more to climate change mitigation than any other existing international agreement.

In this section, the main points from the WMO Ozone Assessment (2011) are first summarized. Then, the objectives and the contents of this chapter are described.

5.1.1 Main Issues from WMO-UNEP 2010 and Other Reports

In several respects, this chapter is an update of Chapter 5 in WMO (2011). In that chapter, Ozone Depletion Potentials (ODPs) and Global Warming Potentials (GWPs) for ODSs and their replacements were updated. New scenarios were generated to explore the potential impacts of hypothetical ODS and nitrous oxide (N_2O) emissions reductions on future ozone depletion and climate forcing. The WMO (2011) chapter additionally included assessments of some processes and activities (e.g., from rockets or from the possible uses of geoengineering as a response to climate change) that may affect future ozone levels through mechanisms that do not necessarily involve the emission of chlorine- and bromine-containing source gases. It was found that some of these processes could affect future ozone levels more than future emissions of controlled ODSs. The impact of the Montreal Protocol on climate forcing was discussed. Finally, the chapter showed how the Montreal Protocol and its Amendments and adjustments had averted many profound changes to Earth and its atmosphere. In particular, because many ODSs are potent greenhouse gases, the Montreal Protocol has successfully avoided larger potential changes to the Earth's climate. Two specific issues raised there are worth mentioning as they are looked into again here.

First, the effects of the accelerated phase-out of HCFCs (hydrochlorofluorocarbons) agreed to by the Parties to the Montreal Protocol in 2007 were projected as a reduction in cumulative HCFC emissions between 2011 and 2050 of 0.6–0.8 million ODP-tonnes, equivalent to bringing forward the year in which Equivalent Effective Stratospheric Chlorine (EESC) returns to 1980 levels by 4–5 years. In addition, the accelerated HCFC phase-out was projected to reduce emissions by 0.4–0.6 gigatonnes of carbon dioxide-equivalents ($GtCO_2$-eq) per year averaged over 2011–2050. The *net* climate benefit is determined, in part, by the climate impact of the compounds used to replace the HCFCs. If high GWP HFCs (hydro-fluorocarbons) were to be used without mitigation, it was estimated that the HFC growth could result in GWP-weighted emissions up to 8.8 $GtCO_2$-eq per year by 2050. This amount is comparable to the GWP-weighted emissions of chlorofluorocarbons (CFCs) at their peak in 1988. The projected radiative forcing in 2050 from these compounds (up to 0.4 watts per square meter (W m^{-2})) could be reduced by using replacement compounds with lower GWP values that also have low ODPs.

Second, the options available for further reductions in future halocarbon emissions were recognized as becoming more limited. However, for reducing the risk of future increases in atmospheric concentrations, the Assessment showed it would be important to minimize any leakage of CFCs and halons from banked storage (or "banks," the largest source of current ODP-weighted emissions of ODSs). A delay of four years, from 2011 to 2015, in the capture and destruction of the estimated CFC and halon banks was estimated to reduce the potential ozone and climate benefits from these actions by about 30%.

Since the last WMO Assessment, several reports have addressed topics of direct interest for this chapter:

1) *The UNEP synthesis report, "HFCs: A Critical Link in Protecting Climate and the Ozone Layer" (UNEP, 2011).* It concluded that limiting the future growth of HFCs could result in unrealized emissions (emissions that would have otherwise occurred) corresponding to as much as 7–19% of the CO_2 emissions that year. Alternative technological options exist that minimize the climate impact of HFCs. Issues related to future scenarios in HFC and other ODS alternatives are addressed in this chapter.

2) *The SPARC report, "Lifetimes of Stratospheric Ozone-Depleting Substances, Their Replacements, and Related Species" (SPARC, 2013).* This report provides a thorough and consistent re-assessment of the lifetimes for a number of halocarbons as well as in-depth analysis of the associated uncertainties (Chapter 1, Box 1-1). These values are discussed in Chapter 1 and are used in the metric and scenario evaluations presented in this chapter.

3) *Reports produced by the UNEP Technology and Economic Assessment Panel (TEAP).* These reports continue to assess the technological and economic possibilities for phasing in commercially available replacements for ODSs (e.g., UNEP, 2013).

4) *The Fifth Assessment Report of the Intergovernmental Panel on Climate Change, "Climate Change 2013 – The Physical Science Basis" (IPCC, 2013).* This report includes updated values of metrics such as Global Warming Potentials. These are updated in this chapter using the SPARC (2013) lifetimes.

5.1.2 Objectives of This Assessment

The overall aim of this chapter is to present policy-relevant information. It includes an assessment of the possible options available to policymakers related to protection of stratospheric ozone (and effects on climate from halocarbons). In Section 5.2, recent developments in the understanding of the main ozone-depleting compounds, anthropogenic and natural, are summarized with emphasis on their importance for future stratospheric ozone depletion, other impacts such as the role of their breakdown products, and their influence on climate. The impacts of real and potential replacement products are similarly discussed. Special attention is given to the additional complexities associated with evaluating the effects from short-lived substances with spatially and temporally varying sources and sinks. Finally in Section 5.2, other potential influences on stratospheric ozone (e.g., other atmospheric changes, rockets, geoengineering) are considered.

Simple quantitative measures have been used to provide information about the effect of emissions from human activity on the atmosphere. These include Ozone Depletion Potentials (ODPs), Global Warming Potentials (GWPs), and radiative forcing (RF), which can be used to compare the relative effect of individual gases, as well as Equivalent Effective Stratospheric Chlorine (EESC) which is a measure of the combined impact of all chlorine- and bromine-containing gases. Estimates of these are discussed in Section 5.3, and updated values are presented based on the recently updated estimates of atmospheric lifetimes (SPARC, 2013). In addition, newer measures, such as Global Temperature change Potentials (GTPs), are discussed here for the first time in a WMO Assessment.

Section 5.4 concludes the chapter with an examination of a range of scenarios. These are compared to a new baseline that is consistent with the existing observational record for atmospheric concentrations of halocarbons and the current limits on emissions contained in the Montreal Protocol. The scenarios investigate effects of hypothetical changes in emissions and are illustrative of potential mitigation actions such as controls on banks (see Box 5-1). The halocarbon lifetimes used are those reported in SPARC (2013). The baseline emission scenario for CO_2, methane (CH_4), and N_2O is taken as the RCP6.0 scenario (van Vuuren et al., 2011; IPCC, 2013). The sensitivity of the calculated impact on the stratosphere is investigated by additionally using the RCP4.5 and RCP8.5 scenarios. (Representative Concentration Pathways are well established in the climate community and used as a basis for climate modeling experiments (van Vuuren et al., 2011; Chapter 4).) EESC is used where possible and additional calculations are performed using a two-dimensional (2-D) coupled chemistry-radiation-dynamics model (Fleming et al., 2011).

Box 5-1. Halocarbon Banks

The bank of a manufactured compound is defined as the quantity of that compound stored in equipment and products and held as chemical inventory. The size of the bank will increase as long as the production of a compound is larger than the release into the atmosphere. Any compound produced and kept in equipment will either increase the size of the bank or be used to compensate for leakage. Leakage is the amount released to the environment by physical leakage or by accidental leakage occurring in regular use, accidents, and maintenance.

For ODS and their replacements, bottom-up estimates of the banks are calculated on the basis of the total amount of equipment and products manufactured per year per country (or per region), and their assumed charges (or contents in the case of products). These bottom-up estimates are generally less accurate than either the amount of a given compound produced or the amount in the atmosphere, which is accurately known from atmospheric measurements. An alternative way to estimate the bank is by taking the difference between the amount produced and the amount released to the atmosphere.

Banks tend to decrease when products and equipment are taken from the market or their use stops. In the absence of specific measures, there will be leakage of the contents of the products to the environment. This release can be avoided by recovery and capture. The captured material can either be used or destroyed. Reporting the amounts of ODSs recovered, recycled, or destroyed is not required under the Montreal Protocol, leading to uncertainty in the size of the bank. However, the success of this option can be limited as a result of either cost or logistical problems. TEAP report XX/8 2009 describes the options for destroying ODS chemicals for different regions and a range of scenarios (UNEP, 2009).

Scenarios of future banks and their composition are based on assumptions of economic development, patterns in society (e.g., number of coolers in supermarkets, air conditioners, etc.), and the expected market penetration of alternative compounds and technologies. Containment, recovery and recycling, and destruction at the end of product life can reduce emissions to the atmosphere. This can be achieved by reducing leakage during operation and use and/or by ensuring high rates of recovery and capture at the end of the useful lifetime of equipment. The potential impact of such controls on atmospheric concentrations of CFCs, halons, HCFCs, and HFCs are investigated in Section 5.4.

5.2 ISSUES OF POTENTIAL IMPORTANCE TO STRATOSPHERIC OZONE AND CLIMATE

5.2.1 Halocarbons Controlled Under the Montreal Protocol

The success of the Montreal Protocol in limiting the atmospheric abundance of ODSs is now well documented. Implementation of its measures has resulted in significantly lower EESC than would otherwise have occurred (WMO, 2011 and preceding reports) as well as reductions in radiative forcing of climate change. Chapter 1 in this report finds that this success in limiting CFC and halon abundances has continued, though it notes large discrepancies between top-down and bottom-up emission estimates for halon-2402 and carbon tetrachloride (CCl_4). In WMO (2011), leakage of CFCs and halons from their banks (see Box 5-1) was found to be the largest source to the atmosphere, and so the main policy option presented was to reduce the leakage. This issue is investigated further in Section 5.4. Revised ODPs and GWPs for the CFCs and halons are presented in Section 5.3 based on the recommendations for the lifetimes made in SPARC (2013).

Part of the decrease in CFC usage in the 1990s was achieved by finding chemical substitutes for CFCs, including HCFCs and HFCs. Due to their lower, but non-zero ODPs, the HCFCs were defined by the Parties as transitional compounds and a first phase-out schedule for them was established in 1992. In order to accelerate the reduction in EESC, accelerated phase-out schedules for HCFCs were agreed under the Montreal Protocol in 2007. The implementation of these measures has been occurring gradually since that time, and it is expected that the overall effects will be observed as a decrease in first the growth rate

and then the atmospheric abundance of HCFCs. Chapter 1 reports that the increases over 2009–2012 for the main three HCFCs are smaller than those for 2006–2009. Presumably this has occurred in anticipation of the introduction of new measures following the accelerated phase-out agreement in 2007. Updated atmospheric measurements and lifetimes for HCFCs are used in the revised ODPs and GWPs presented and discussed in Section 5.3 and the scenarios presented in Section 5.4.

An inconsistency in the carbon tetrachloride (CCl_4) budget was reported in WMO (2011), as the decline in atmospheric CCl_4 concentrations was less than expected. Chapter 1 in this Assessment concludes that this discrepancy remains as there is a continued imbalance between the emissions of CCl_4 inferred from the observed changes in global concentration and the bottom-up estimates of the anthropogenic emissions. This difference cannot solely be explained by adjusting the atmospheric lifetime. Chapter 1 suggests that there may be ongoing anthropogenic emissions in the Northern Hemisphere. The implications of this uncertainty on future EESC are discussed further in Section 5.4.

Atmospheric methyl bromide (CH_3Br) results from anthropogenic and natural emissions. The partitioning between them has been the subject of much debate in the past (WMO, 2003, 2007. 2011). The continued decline in tropospheric CH_3Br amounts is caused by reductions in the controlled industrial production, consumption, and emission (see Chapter 1 for further analysis of the CH_3Br emissions and budget). The anthropogenic uses fall into three categories: (1) the controlled applications (soil and postharvest fumigation and commodity disinfestation); (2) quarantine and pre-shipment (QPS) exempted applications, which are reported under the Montreal Protocol; and (3) feedstock uses exempted but reported under the Montreal Protocol. The annual global total consumption for non-QPS uses of CH_3Br has decreased steadily as a result of the implementation of the Montreal Protocol, from over 50,000 tonnes/yr in the late 1990s to about 4,000 tonnes/yr in 2012 (Figure 1-6-6 of UNEP, 2013). This compares to a change in total consumption from about 70,000 tonnes/yr to about 20,000 tonnes/yr over the same period. Critical-use exemptions for the controlled uses are applied for by developed country (non-Article 5) Parties and have been granted annually since 2005. Fewer critical-use exemptions are being granted, as alternative approaches are more often available. The phase-out of controlled uses in Article 5 Parties by 1/1/2015 may result in additional applications for critical-use exemptions in the coming years (four Article 5 Parties have already applied for critical-use exemptions for 2015). The annual use for QPS is currently about 9,000 tonnes and is approximately steady (UNEP, 2013; Figure 1-6-6). In general, use for QPS has decreased in non-Article 5 and increased in Article 5 Parties. Feedstock production is estimated at about 3,900 tonnes in 2012; however, this should not result in any significant emissions. Total global production in 2012 was 16,700 tonnes, down from 35,000 tonnes in 2006. Scenarios for possible future emissions of CH_3Br are discussed in Section 5.4.

5.2.2 Replacement Compounds

The majority of the reduction in ODS emissions has occurred as a result of not-in-kind technology, such as containment, recovery and recycling, and non-fluorocarbon solutions. However, some of the decrease in the use of CFCs, and now HCFCs, has resulted in increased HFC use, particularly in the refrigeration and air conditioning sectors and, to a lesser degree, in the foam and fire protection sectors. While most HFCs have GWPs similar to those of the HCFCs they are replacing, some have higher GWPs (UNEP, 2011). The potential growth in the use of these high-GWP HFCs has given rise to concerns about the possible climate impact of the growth in HFC use (and emission) by the year 2050 (Velders et al., 2009, 2012; WMO, 2011; UNEP, 2011; Wuebbles at al., 2013). To minimize the impact on the ozone layer and climate, HCFC replacements would ideally have low ODPs and GWPs, even if the replacements contain chlorine or bromine. Meeting such conditions implies that the replacement compounds have short lifetimes and/or weak IR absorptions. A number of possible compounds, many of which have low GWPs, are now being considered. Technical aspects of new compounds are assessed by TEAP once their commercial potential has been shown (UNEP, 2013). Scenarios of future replacement compounds are considered in Section 5.4 and the possible impacts on ozone depletion and climate are assessed.

1,2-dichlorohexafluorocyclobutane ($C_4Cl_2F_6$, CFC-316c) is a proposed replacement substance, especially as a refrigerant. Papadimitriou (2013) evaluated the most likely atmospheric removal processes for the (*E*)- and (*Z*)- isomers of CFC-316c in a series of laboratory studies. 2-D model calculations included in their work show that stratospheric photolysis is the predominant loss process for both isomers, with lifetimes of 75 and 114 years for the (*E*)- and (*Z*)- isomers, respectively (see Table 1-3). Ozone Depletion Potentials and Global Warming Potentials were also reported, demonstrating that both isomers are potent ozone-depleting substances and greenhouse gases (ODPs are 0.46 for (*E*)-R-316c and 0.54 for (*Z*)-R-316c; GWP_{100} are 4160 for (*E*)-R-316c and 5400 for (*Z*)-R-316c).

A number of short-lived compounds have been proposed as replacements for long-lived ODSs and hydrofluorocarbons (HFCs) (see Table 1-11). Some of these substances are halogenated VSLS (i.e., lifetimes <0.5 years) and were chosen due to their low ODPs and GWPs. An updated summary of the partial and total lifetimes of the proposed replacement substances is given in Table 1-11. Further discussion of the ODPs and GWPs for a number of these compounds is given in Section 5.3.

5.2.3 HFC-23

HFC-23 is an unwanted by-product in the manufacture of HCFC-22. A major and increasing use of HCFC-22 is as a feedstock in the production of other chemicals, the most important of which is polytetrafluoroethylene (PTFE). The amount of HFC-23 produced in HCFC-22 manufacturing is far larger than the small amounts currently required for its direct use in some low temperature refrigeration and fire protection equipment. HFC-23 emissions are sometimes not considered in the emissions total from the mix of HFCs used or predicted to be used. Global emissions of HFC-23 have risen since 2009 after a period of decrease (Chapter 1). HFC-23 is a strong infrared absorber, and has a long lifetime of 220 years and a high GWP (12,400 for a 100-year time horizon GWP) (IPCC, 2013). Its radiative forcing in 2012 was 0.005 W m^{-2}, about 25% of the RF from all HFCs (Chapter 1). The annual emission of 12.8 ktonne per year (Chapter 1) corresponds to 150 Gt CO_2-eq per year.

The fraction produced in HCFC-22 manufacture depends on the details of the manufacturing process. It is assumed to be at most 3% of the amount of HCFC-22 produced, and in optimal manufacturing conditions (which are difficult to maintain) it can be brought down to 1.5%. Atmospheric emissions can be avoided if the HFC-23 is incinerated, which makes it possible to recover hydrofluoric acid (HF), the raw feedstock. Globally, a significant fraction of the HFC-23 produced in HCFC-22 facilities has been incinerated since 2006, due to the fact that incineration projects in developing countries could be supported through the Kyoto Protocol Clean Development Mechanism (CDM). Future HFC-23 emissions will depend on the amount of HCFC-22 produced, the efficiency of avoiding unwanted HFC-23 byproducts, and whether the amount of residual HFC-23 incinerated increases or decreases. This is directly related to future policy choices including those related to the granting of new HFC-23 incineration credits in the CDM (Miller and Kuijpers, 2011) and on other initiatives to avoid and destroy HFC-23. The impact of different emission scenarios is discussed in Section 5.4. More information can be found in Chapter 1 and references therein.

5.2.4 Biogenically Produced Short-Lived Halocarbons

Biogenically produced very short-lived substances (VSLS) are thought to contribute significantly to the stratospheric halogen budget, particularly for bromine (Chapter 1). The main processes affecting the effectiveness of these compounds (emissions, convective transport, and chemical processing) could all change in the coming decades as a result of changes in climate or in human activities. Bromoform ($CHBr_3$) and methylene bromide (CH_2Br_2) are expected to remain the two most important species. Their emissions could increase as a result of changes in managed production (e.g., algae farming for food, pharmaceuticals, or carbon capture). Currently 99% of cultivation comes from 7 countries in Asia and the volume produced has grown by ~8%/yr since 1990 (FAO, 2012). A study in Malaysia found that while current bromocarbon

emissions from aquaculture are negligible, they could become significant in the next decade (>10% of regional seaweed emissions) (Leedham et al., 2013). With multiple ecosystem, dynamical, and chemical components contributing to oceanic VSLS emissions, predicting future emissions will be a major challenge.

Transport of these species into and across the tropical tropopause is the major way for them to enter the stratosphere. Tropical convection is thus a critical process in determining their flux into the stratosphere, and any changes in its strength or frequency as a result of a changing climate will affect their future stratospheric concentrations. These changes will happen in concert with any changes in the strength of the stratospheric circulation. The Coupled Model Intercomparison Project Phase 5 (CMIP5) climate models suggest that the flux of air into the stratosphere will increase at the same time as ozone depletion reduces and as greenhouse gas concentrations increase (see Figure 4-8 and related discussion). For shorter-lived species, some features of the convection are particularly important in determining how much of any emitted substance (or their reaction products) reaches the stratosphere: these include the overall mass transport in convection, the altitudes where the air flows into and out of the convection, the frequency of strong events (particularly the high altitude outflow), and the location of the convection relative to the emissions. These all have significant uncertainties associated with them (e.g., Schofield et al., 2011). In addition, the boundary layer mixing and stratospheric advection processes have been shown to cause significant differences in simulated VSLS reaching the stratosphere (Hoyle et al., 2011). Differences are amplified for shorter-lived compounds. The implications for the contribution of short-lived species to stratospheric chlorine and bromine amounts and to the calculation of ODPs are discussed in Section 5.3.

Modeling studies have shown that climate-driven changes to tropospheric transport may affect stratospheric VSLS loading (Dessens et al., 2009; Pyle et al., 2011). Hossaini et al. (2012a) calculate increased injection of $CHBr_3$ into the stratosphere for a 2100 simulation based on the Representative Concentration Pathways (RCPs) 4.5 and 8.5 scenarios (IPCC, 2013; also see Chapters 2 and 4). This increase was largest under RCP8.5, a scenario with stronger warming, and mostly attributed to an enhanced convective mass flux in the tropical troposphere, which agrees qualitatively with earlier model studies (Stevenson et al., 2005; Dessens et al., 2009). Overall, Hossaini et al. (2012a) project an increase in the direct injection of bromine into the stratosphere contained in the five major VSLS of 0.3 ppt and 1.0 ppt Br under RCP4.5 and RCP8.5, respectively. These increases are attributed to both the dynamical and chemical perturbations, both of which carry large uncertainty, while climate-driven changes to emissions and changes in anthropogenic use were not considered. As discussed in Chapter 1, there remains significant uncertainty in the role of convection in determining the amount of bromine and chlorine reaching the lower stratosphere.

Changes in the tropospheric oxidizing capacity will impact the lifetimes of VSLS (SPARC, 2013), particularly those whose primary sink is through hydroxyl radical (OH) oxidation (e.g., CH_2Br_2, CH_2Cl_2). Hossaini et al. (2012a) find significant variation in projected tropical tropospheric [OH] between the RCP scenarios. The local lifetime of CH_2Br_2 (against oxidation) varies significantly (±40%) (e.g., see Figure 1-14). Despite OH production being favored under warm and humid conditions, tropical [OH] in 2100 is projected to decrease by 25% near the surface, due to a projected doubling of methane (CH_4) under RCP8.5. Voulgarakis et al. (2013) find similar [OH] decreases of −22 ± 4.6% from a multi-model intercomparison. Under more moderate climate scenarios, such as RCP2.6 and RCP4.5, models project an increase in tropospheric [OH] of up to ~10% below 500 hectoPascals (hPa) (Hossaini et al., 2012a; John et al., 2012; Voulgarakis et al., 2013). These studies underline the sensitivity of future OH concentrations and distribution to future CH_4 emissions. Results also depend on responses to relative decreases in nitrogen oxides ($NO_x = NO + NO_2$) and carbon monoxide (CO) in the different scenarios over polluted regions. In addition sub-annual and regional variations, such as the low ozone concentrations found (and low OH concentration inferred) in the West Pacific (Rex et al., 2014), could affect VSLS.

The future impact of VSLS on ozone has yet to be fully assessed. While some studies suggest a potential increase in bromine from VSLS toward the end of the century, stratospheric chlorine will have decreased substantially by 2100 due to the phase-out of the long-lived chlorinated source gases under the Montreal Protocol. Therefore, bromine-mediated O_3 destruction via the BrO + ClO catalytic cycle would be reduced.

5.2.5 Breakdown Products

Certain HCFCs, HFCs, HFEs (hydrofluoroethers), and HFOs (hydrofluoroolefins) can contribute to tropospheric ozone formation and degrade to produce toxic compounds. The atmospheric degradation of HCFCs, HFCs, HFEs, and HFOs is initiated by reaction with OH radicals leading to the formation of halogenated carbonyl compounds, which undergo further oxidation to yield HF, HCl, CO_2, and, in some cases, trifluoroacetic acid (TFA, $CF_3C(O)OH$) (e.g., see prior Assessments such as IPCC/TEAP 2005; WMO, 2011). There is a special concern regarding the production of TFA because of its possible effects on life in aquatic environments (see the discussion in WMO, 2011). The chlorine production is considered in the discussion of EESC in Section 5.4; the effects on HF and CO_2 are likely to be extremely small. Examples of halocarbons that lead to the formation of TFA (and related compounds) include: HCFC-123, HCFC-124, HFC-125, HFC-134a, HFC-227ea, and HFO-1234yf (Young and Mabury, 2010). While it is well established that TFA is a ubiquitous natural component in rivers, lakes, and other surface water bodies, uncertainties remain, as discussed in WMO (2011), regarding its natural and anthropogenic sources, long-term fate, and abundances. TFA formation depends on whether CF_3CFO or CF_3CClO are formed as intermediates in the parent compound degradation. The sole atmospheric fate of CF_3CFO is hydrolysis to give TFA (Wallington, et al., 1994). The atmospheric fate of CF_3CClO is hydrolysis, to give TFA, or photolysis. For halogenated propenes, HFOs, if there is a fluorine atom on the central carbon, the TFA yield is expected to be high; such as found with $CF_3CF=CH_2$ (HFO-1234yf) (Papadimitriou et al. 2011; Wallington et al., 2010). On the other hand, if there is a hydrogen on the central carbon atom there is no TFA formation, such as in $CF_3CH=CHF$ (HFO-1234ze) or $CF_3CH=CHCl$ (trans-1-chloro-3,3,3-trifluoropropylene or tCFP; also referred to as HFO-1233zd) or HFC-152a. While some studies suggest that the extensive use of some TFA source compounds could dramatically increase the amount of TFA in wetlands (e.g., Luecken et al., 2010; Henne et al., 2012), the potential effects on associated ecosystems remains unclear and may not be as large a problem as initially envisioned (Boutonnet et al., 1999; Benesch et al., 2002; WMO, 2007, 2011). UNEP (2010) concluded that even when added to existing amounts from natural sources, risks from TFA (and the more toxic monofluoroacetic acid (MFA)) from halocarbons to humans and organisms in the aquatic environment are judged to be negligible. Nonetheless, there remains significant uncertainty about the potential effects of TFA in the future environment.

5.2.6 Nitrous Oxide, Methane, and Carbon Dioxide

Any future changes in halogen concentrations will be taking place against the backdrop of other atmospheric changes. From a stratospheric chemistry and circulation standpoint, the most important direct changes are likely to be those of CH_4, N_2O, and CO_2 (also see Chapters 2 and 4). The concentrations of these gases have changed and are continuing to change as a result of human activities (IPCC, 2013). Continued changes in the stratospheric concentrations of these gases will lead to changing odd hydrogen (HO_x) and NO_x concentrations during the period that halogen levels are falling. At the same time, continued increases in the CO_2 concentrations will lead to stratospheric cooling, which will slow the ozone chemical loss rates. Increases in CO_2 also are projected to cause a strengthening of the stratospheric Brewer-Dobson circulation, which will redistribute ozone.

In general the chemical effects of these three gases occur in different locations in the stratosphere, but overall the increases in CH_4 and CO_2 will have the opposite effect on stratospheric ozone as that of N_2O. Future ozone levels will be strongly dependent on the actual future emissions and concentrations of these gases. How ozone will change as the future concentrations of these gases change is explored in Section 5.4 (see also Section 2.4).

5.2.7 Stratospheric Water Vapor

Stratospheric water vapor is critically important for the gas-phase chemistry, the particle distribution, and the radiative balance of the stratosphere. The large majority of stratospheric water vapor

enters the stratosphere in the tropics in the form of either CH_4 or H_2O. However, it can also enter the lowermost stratosphere through mixing processes around the extratropical tropopause. One such process is direct injection through midlatitude convection. Increased midlatitude convection could thus result in increased injection of water vapor and a greater occurrence of ice crystals. While EESC remains high, there is thus a chance of enhanced chemical destruction of ozone by catalytic halogen chemistry on these additional surfaces (Anderson et al., 2012). The comprehensive measurements by the Aura Microwave Limb Sounder (MLS) satellite instrument (Schwartz et al., 2013) confirmed that the lower stratosphere over North America is episodically moist (as seen in the aircraft campaigns reported in Anderson et al., 2012). However, Schwartz et al. (2013) caution that chemical ozone depletion as a result of convectively enhanced H_2O of the scale suggested by Anderson et al. (2012) does not seem readily apparent or likely in the current stratosphere; moreover, dilution effects from low O_3 values lofted by tropospheric air would complicate the detection and attribution issues. Comparison of the Aura MLS observations with the CLaMS model (Chemical Lagrangian Model of the Stratosphere) further suggest that the annual cycle in water above 360 K at northern midlatitudes is dominated by horizontal transport of water vapor from low latitudes (Ploeger et al., 2013). The importance of northern midlatitude convection in the lower stratosphere is therefore unclear. Two points can be made with confidence: any chemical ozone depletion (i) is already included in the changes seen in the existing observational record; and (ii) will continue to reduce as EESC decreases.

Future stratospheric water vapor levels will be affected by any changes in the amount of water entering the stratosphere in the tropics. This could occur through changes in the large-scale structure of the tropical tropopause layer (Davis and Rosenlof, 2012; Randel and Jensen, 2013); and in the strength of the vertical transport of tropospheric air associated with features such as the Asian monsoon anticyclone (Ploeger et al., 2013). Such changes are included implicitly in the discussions in Sections 2.4 and 3.5. Given the uncertainties in possible future changes of stratospheric water vapor, the effect on ozone depletion is not investigated further with the simple models in this chapter.

Finally, it has been proposed that the observed correlation between stratospheric water levels and higher tropospheric temperatures implies a positive feedback of stratospheric water vapor on climate, with one-third of the feedback resulting from increases in water vapor entering the stratosphere in the tropics and the rest occurring from increases entering through the extratropical tropopause (Dessler et al., 2013).

5.2.8 Stratospheric Aerosols

Stratospheric aerosols can have a significant influence on stratospheric ozone (e.g., Solomon et al., 1996; Chapter 2). The stratospheric aerosol layer has been increasing during the volcanically quiescent period of 2000–2009 by ~3.8% (Nagai et al., 2010). This has been shown to have a direct climate impact (Solomon et al., 2011). The increase is probably caused by the cumulative effect of minor volcanic eruptions with subsequent transport of sulfur dioxide (SO_2) into the stratosphere (Vernier et al., 2009; Neely et al., 2013). The impact of tropospheric pollution is now thought to be small (Siddaway and Petelina, 2011; Vernier et al., 2011; Section 8.4.2.2 in IPCC, 2013; Chapter 4). Changes in anthropogenic carbonyl sulfide (COS) emissions could also affect future background aerosol levels (Brühl et al., 2012). Other than in the discussion on geoengineering below, the effect on stratospheric ozone of possible changes in the stratospheric aerosol layer is not considered further in this chapter and so represents a source of uncertainty in the results presented.

5.2.9 Other Proposed Influences on Stratospheric Ozone

Aviation

Since WMO (2011), studies have continued toward understanding the effects of emissions from commercial aviation on ozone in the upper troposphere and lower stratosphere (UTLS) and on climate (e.g., see Brasseur et al., 2013, Holmes et al., 2011; Lee et al., 2009). Aircraft emit gases and particles into the atmosphere, especially in the region of the UTLS. These emissions include carbon dioxide,

nitrogen oxides, water vapor, sulfates, and soot. The gases and soot tend to have a positive radiative forcing (RF), a surface warming effect, while other particles like sulfates produce a negative RF, a surface cooling effect. NO_x produces ozone in the UTLS that then leads to additional OH production in the troposphere and a resulting decrease in methane. Current commercial aviation emissions are estimated to increase UTLS ozone at northern midlatitudes by 5–7% (2.3–9.1% in the range of models from recent studies: Olsen et al., 2013; Brasseur et al., 2013; Skowron et al., 2013). The net effect on the total ozone column, however, is small, an increase of less than 0.3% globally- and annually-averaged. By 2050, current studies using a scenario that includes technology advances in aviation efficiency suggest the effect of aviation on UTLS ozone could increase to as much as 11% (Olsen et al., 2013; Brasseur et al., 2013). The effect on the total ozone column remains small (<1%).

Supersonic aircraft fly at higher altitudes, where they emit NO_x and H_2O into the stratosphere at altitudes where they can be mixed upwards and globally (instead of being flushed out of the lowermost stratosphere within a season as for subsonic aircraft). Thus high-flying supersonic aircraft can have potentially much greater impacts on ozone and climate forcing. There are no current plans for development of commercial supersonic aircraft, although the technology for supersonic business jets is continuing to be developed, and future growth should be monitored.

ROCKETS AND SUB-ORBITAL VEHICLES

WMO (2011) raised the potential importance of emissions from rockets. Cryogenic rocket engines using liquid oxygen and liquid hydrogen produce water and nitric oxide. Solid rocket motors (SRMs) have emissions of hydrochloric acid (HCl) and alumina (Al_2O_3) and so have more impact on ozone than the cryogenic engines. These SRM emissions can lead to destruction of the ozone in the rocket exhaust plumes (Ross et al., 2009; Voigt et al., 2013). The present-day loss in the globally averaged total ozone column due to these rockets is estimated at ~0.03%, insignificant compared to other processes (Ross et al., 2009). It would take a large increase in the frequency of launches for the impact on ozone to become significant compared to the impacts of other influences. A recent forecast for the commercial sector (currently about 25% of the total) is an increase from about 20 to 30 launches per year (FAA, 2013).

A number of suborbital, reusable vehicles (SRV) are being developed for use for satellite launches and/or for passengers. It is still early in the development of these technologies and so it is hard to predict future usage and growth in the number of launches. One study developed three scenarios (baseline, constrained, and growth) based on different assumptions about cost, level of consumer interest, and governmental/industrial demand (FAA, 2013). In these scenarios, the number of flights ten years after the first year of regular SRV operation ranged from about 250 to 1600. Newer propellants are being considered in the private space market, many of which are liquid oxygen (O_2) with alcohol (FAA, 2011). The effect on stratospheric ozone will depend on the number of launches, the propellant used, and the flight profiles. Few studies have addressed the effects of these vehicles and their potential environmental impacts.

GEOENGINEERING OF CLIMATE

A variety of ideas have been proposed to mitigate the climate effects of rising greenhouse gases concentrations (geoengineering). One of these, the creation of additional particles in the stratosphere, would directly impact stratospheric ozone (Tilmes et al., 2008, 2009). Other methods have indirect effects on stratospheric ozone and are not considered further here.

Stratospheric particles reflect a small amount of the incoming solar radiation back to space, and so lead to a reduction in the incident solar energy reaching the Earth and a resultant surface cooling. An enhancement of the stratospheric particle layer, e.g., following volcanic eruptions, increases this cooling effect. The effect is well established, because the surface of the Earth is observed to cool as a result of the high sulfate aerosol loading in the years following major volcanic eruptions (WMO, 2011; Graf et al., 1998; Free and Lanzante, 2009; IPCC, 2013), although it has recently been suggested that the volcanic response may have been overestimated by as much as a factor of two (Canty et al., 2013).

Increases in stratospheric particles affect the radiative balance in the stratosphere, with consequent changes in the dynamics and in the chemistry (through changes in photolysis rates). In addition, stratospheric chemistry is perturbed by heterogeneous reactions that occur on particle surfaces, with impacts on the HO_x, NO_x, ClO_x, and BrO_x chemical cycles. Three-dimensional models have individually simulated the stratospheric response following the Mt. Pinatubo eruption (the best observed) with some success (e.g., Heckendorn et al., 2009; see also Chapter 2, Section 2.3.4). However, the large inter-model variation in the dynamical response to forcings (SPARC CCMVal, 2010) limits our confidence in the predictive capability of the current models.

The main type of artificial perturbation that has been considered is an augmentation of the background sulfate aerosol layer through the injection of sulfur (Crutzen et al., 2006; Wigley, 2006; WMO, 2011). The observed changes with volcanic eruptions give confidence in our qualitative understanding of the impacts of elevated sulfate aerosol. However, quantitative studies are limited to date. Recent modeling studies of an artificially perturbed stratospheric aerosol layer have concentrated on scenarios defined in the Geoengineering Model Intercomparison Project (GeoMIP) (Kravitz et al., 2011), with nearly all GEOMIP studies to date focusing on impacts on climate rather than stratospheric ozone. Results from four models using the two GEOMIP scenarios that include stratospheric aerosol (Pitari et al., 2014) indicate reductions in total column ozone of a few percent, with the larger losses at high latitudes, consistent with earlier studies based on different scenarios (Heckendorn et al., 2009; Tilmes et al., 2009). The chemical ozone loss is calculated to decrease as the availability of ClO_x and BrO_x decreases. This effect may be offset by any increase in the input of chlorine- and bromine-containing VSLS into the stratosphere (Tilmes et al., 2012; see Section 5.2.4).

Consideration is also being given to particles with different optical properties that could substantially increase the amount of light scattered back to space thereby reducing the mass required for injection (Katz, 2011) or that reduce the absorption of solar radiation by the particles hence leading to a reduced impact on the stratospheric circulation (Ferraro et al., 2011). Such particles could be more effective in producing a surface cooling than sulfate aerosol. The heterogeneous chemistry occurring on the surface of new particles is poorly known (Pope et al., 2012). The surface coating of a particle and how it evolves under stratospheric conditions will be important for the heterogeneous reaction rates. For example, a coating of sulfuric acid (H_2SO_4) on a particle's surface would tend to make the heterogeneous chemistry that occurs more like that of sulfate aerosol. However, the effect on the optical properties would likely be small. If the particles became significantly larger, the sedimentation rate would in general increase and the stratospheric lifetime would shorten.

In our discussion, we have not considered other potential effects of the stratospheric particle geoengineering approach on climate and other aspects of the environment. Overall the gaps in our current understanding of the full impacts of possible geoengineering approaches on stratospheric ozone preclude us from making a full assessment with confidence. Thus, there is still the potential for significant risks to the ozone layer, both known and unknown, from solar radiation management through the use of stratospheric particles.

POLAR OZONE DEPLETION BY COSMIC RAYS

A series of papers (most recently Lu (2013, 2014)) have repeated the hypothesis that cosmic rays can promote the breakdown of organic and inorganic halogenated compounds, including CFCs, on ice and other stratospheric particles in polar regions, with the resulting chlorine compounds playing the dominant role in polar ozone loss. The recent papers have been published despite a number of previous papers showing that this hypothesis is inconsistent with established knowledge of the stratosphere (Harris et al., 2002; Patra and Santhanam, 2002; Grooß and Müller, 2011; Müller and Grooß, 2014 and references therein). Lu (2013) and his earlier papers rely principally on correlations of observed variables (e.g., ozone, temperature, cosmic ray flux) with no quantitative evidence that the proposed mechanism makes a significant difference to the well established understanding of polar ozone loss based on mechanisms demonstrated in laboratory and field measurements as well as model studies (e.g., see Chapter 3). Among other things there is no evidence that the hydrophobic CFC-11 or CFC-12 molecules are absorbed into the

particles in large enough amounts for cosmic-ray-produced electrons to dissociate them (Harris et al., 2002). Nor can the mechanism explain the observed distributions and correlations of long-lived trace gases such as the CFCs, N_2O, and CH_4 which show that CFC depletion occurs in the middle and upper stratosphere at low and midlatitudes and not in the polar lower stratosphere (Grooß and Müller, 2011). The fundamental problem with the hypothesis is that it ignores most of the work that has been done over the last 30–40 years as reported in the series of WMO Assessments prepared in support of the Montreal Protocol. This hypothesis should be rejected.

5.3 METRICS FOR CHANGES IN OZONE AND CLIMATE

For the purpose of this Assessment, metrics are defined as tools used for quantifying and comparing impacts of emissions from human activity. Typically they aggregate and simplify complex information about different gases, placing them on a common scale to simplify comparison of impacts. Metrics such as Equivalent Effective Stratospheric Chlorine (EESC) and Ozone Depletion Potentials (ODPs) have proven to be important tools in policy considerations for stratospheric ozone (see Box 5-2), while other metrics, including radiative forcing (RF) and Global Warming Potentials (GWPs), have proven to be useful tools in climate-policy-related studies (see Box 5-3). These metrics have all been used in past assessment of ozone and climate including the WMO Assessments. In addition, newer metrics, such as Global Temperature change Potentials (GTPs), are introduced in the discussion below.

One advantage of metrics is that they are straightforward to communicate. Some of these metrics express the integrated impact of a given gas relative to that for the release of the same mass of a reference compound (generally CFC-11 for ODPs and CO_2 for GWPs and GTPs). For these metrics using such relative indices, some uncertainties in translating emissions into absolute environmental impacts tend to cancel, and the relative benefits of controlling emissions of different gases are highlighted. However, it should be recognized that the metrics discussed here do not represent the full complexity of the chemistry and physics of the atmosphere (e.g., where and when the ozone depletion occurs). Their simplicity means some caution is required when interpreting the values derived (e.g., how much are these values dependent on the background atmosphere assumed in their derivation). Nonetheless, ODPs and GWPs have found widespread use in national regulatory actions and in international agreements such as the Montreal Protocol and the Kyoto Protocol.

5.3.1 Metrics for Changes in Ozone

Box 5-2 (next page) summarizes the basics of metrics used for describing changes in ozone, namely, Equivalent Effective Stratospheric Chlorine (EESC) and Ozone Depletion Potentials (ODPs).

UPDATING THE EVALUATION OF ODPS
There have been only a few published updates on ODP values since the last Assessment, with most of those concerning VSLS as discussed below. Papanastasiou et al. (2013) provide analyses of updated semi-empirical ODPs for several bromine-containing compounds (halon-1202, -1211, and -2402) using updated lifetimes computed with the NASA GSFC 2-D atmospheric model (Fleming et al., 2011). Their analyses produced somewhat different ODP values compared to WMO (2011): 1.95 for halon-1202 vs. 1.7 in WMO (2011), 8.1 for halon-1211 vs. 7.9 in WMO (2011), and 18.4 for halon-2402 vs. 13.0 in WMO (2011).

New scientific results affect the earlier ODPs, especially from the reanalysis of atmospheric lifetimes in SPARC (2013). The revised SPARC (2013) recommended lifetimes are based on calculations with atmospheric chemical transport models, analysis of observations at the surface and in the stratosphere, laboratory analysis of chemical reactions and photolysis rates, and on inverse modeling. In addition, the SPARC report provides uncertainties in the lifetimes of major halogenated ODSs. The uncertainties in the lifetimes are considerable, ranging from 3% to 33% (one standard deviation, 1σ; also see Velders and Daniel (2014) for further discussion on these uncertainties). The SPARC (2013) atmospheric lifetimes are

Box 5-2. Metrics for Ozone: The Basics

Equivalent Effective Stratospheric Chlorine (EESC)

EESC is a sum of the time-dependent chlorine and bromine derived from ODS tropospheric abundances, weighted to reflect their potential influence on ozone. EESC has become a standard benchmark for estimating ozone depletion relative to a base period, usually taken as 1980 (a time before major ozone depletion). EESC relates surface mixing ratios of chlorine- and bromine-containing ODSs to the stratospheric inorganic chlorine and bromine released from these gases in key regions of the stratosphere and thus to the amount of ozone they will destroy (Daniel et al., 1995; WMO, 1995, 1999, 2003, 2007, 2011; also see Chapter 1). EESC also accounts for the larger efficiency of bromine to destroy stratospheric ozone compared to chlorine (on a per-atom basis) and that different source gases release their chlorine and bromine at different rates and geographic locations. EESC has been reformulated (Newman et al., 2007) to account for the age-of-air spectrum and the age-of-air dependent fractional release values. Not only does this increase its accuracy, but EESC can also then be derived for various latitudes, including effects at midlatitudes or in the Antarctic vortex (Newman et al., 2009; WMO, 2011). The changes in integrated EESC and the date when EESC returns to 1980 levels have both been used in the previous WMO Assessments to quantify the relative impacts of future emissions of ODSs. In Section 5.4, EESC is used in the evaluation of scenarios for various assumptions about future emissions of halocarbons.

The EESC concept has been further revised (Daniel et al., 2010) to account for the effects of nitrous oxide (N_2O), the primary source for nitrogen oxides (NO_x = NO + NO_2) in the stratosphere. If this can be done accurately, it is useful because N_2O is increasing and is projected to continue to do so in the future. The NO_x produced from N_2O chemistry not only destroys ozone itself, it also reduces the efficiency of chlorine and bromine in destroying ozone by tying up these halogens in chlorine nitrate ($ClONO_2$) and bromine nitrate ($BrONO_2$) reservoir gases. Projected decreasing levels of reactive chlorine (Cl_y) similarly ties up less reactive nitrogen (NO_y; note that reactive nitrogen does not include N_2O, only the more reactive forms of atmospheric nitrogen) in $ClONO_2$, especially in the lower stratosphere, increasing the efficiency of N_2O to destroy ozone at those altitudes (Ravishankara et al., 2009). However, there is also a decreasing efficiency of N_2O in ozone depletion in the future climate due to the projected CO_2-induced cooling of the stratosphere and enhancement of the stratospheric circulation (Rosenfield and Douglass, 1998; Plummer et al., 2010). The expected decrease, by 2100, in the effectiveness of a unit N_2O emission to destroy ozone ranges from 10–20% (Daniel et al., 2010) to 50% (Plummer et al., 2010). Although these interactions will potentially lead to a complicated relationship between EESC and ozone depletion, we investigate the usefulness of this effect in Section 5.4. Future changes in emissions of methane, as well as potential emissions of other gases and particles, can further complicate the interpretation of EESC but are not considered in the EESC index at this time.

EESC is calculated as in previous Assessments. The only difference between the calculations in WMO (2011) and those here is that we now use an age spectrum for both midlatitude (3-year mean age) and Antarctic conditions (5.5-year mean age), while a full age spectrum was not used before. In both cases, we assume the width of the spectrum is equal to half of the average age (Newman et al., 2007). A complete discussion of the other aspects of the EESC calculation can be found in Chapter 5 of WMO (2011). As in that Assessment, we assume the relative impact of bromine compared to chlorine for ozone destruction, typically referred to as alpha (α), is 60 at midlatitudes and 65 in polar regions.

Ozone Depletion Potentials (ODPs)

The concept of Ozone Depletion Potentials (ODPs) (Wuebbles 1981, 1983; Solomon et al. 1992; the various WMO Assessments) arose as a means of determining the relative ability of a chemical to destroy ozone. Steady-state ODPs are defined as the change in global ozone for a sustained unit mass emission of a specific compound relative to the change in global ozone for the sustained unit mass emission of CFC-11 ($CFCl_3$). This is equivalent to assuming an infinitesimal emission pulse and integrating over the entire decay of the compound. ODPs are an integral part of national and international

Box 5-2, continued.

considerations on ozone-protection policy, including the Montreal Protocol and its Amendments. ODPs provide an important and relatively straightforward way of analyzing the potential for a new chemical to affect ozone relative to the chlorofluorocarbons (CFCs) and other chlorine-, bromine- and iodine-containing halocarbons. It is also now being applied to non-halogenated compounds like nitrous oxide (N$_2$O) (Ravishankara et al., 2009; Fleming et al., 2011; WMO, 2011) and methane (CH$_4$) (Fleming et al., 2011). ODPs are currently determined by two different means: calculations from chemical transport models (CTMs) of the global atmosphere, and the semi-empirical approach that depends primarily on observations rather than models (Solomon et al., 1992; WMO, 2003, 2007, 2011). Both approaches have been shown to give very similar ODP values in previous Assessments.

Advantages and disadvantages of using ODPs have been discussed in the prior WMO Assessments. Because ODPs are defined relative to the ozone loss caused by CFC-11, it is generally thought that the ODP values demonstrate less sensitivity to photochemical modeling errors than do absolute ozone loss calculations, but this is only strictly true for other chlorine-containing compounds with similar atmospheric lifetimes. Interpretation of non-halocarbon ODPs could be particularly problematic. For example, ODPs are normally derived relative to the current atmosphere, but there could potentially be some differences in values if they were calculated relative to a future atmosphere with different background composition, temperatures, or circulation.

Originally, the evaluation of ODPs was conducted largely for chemicals with atmospheric lifetimes sufficiently long (> ~1 year) that they are well mixed throughout the troposphere after surface release, and a significant portion of the surface emissions can still reach the stratosphere. However, many of the compounds being considered either for new applications or as replacements for substances controlled under the Montreal Protocol are now designed to be very short lived, on the order of days to a few months, so as to reduce the impacts on ozone and climate. Many of these very short-lived substances (VSLS) still contain chlorine, bromine, or iodine, and can be vertically transported into the lower stratosphere particularly through the tropical troposphere. A major complication with VSLS is that the compounds can decompose into inorganic halogen compounds in the uppermost tropical troposphere, and hence an important uncertainty is the degree to which the inorganic halogens (e.g., HBr, HOBr) are scavenged during the removal of water vapor in ascent. Another issue is that basic assumptions of referencing to CFC-11 to cancel transport and other errors in the model clearly break down since the chemical removal processes are so different; nonetheless there is high value for policymakers in being able to use the modified form of the ODP concept for VSLS.

Due to the difficulties in calculating the dynamical and chemical processes affecting such short-lived compounds, three-dimensional (3-D) models fully representing the troposphere and stratosphere need to be used to predict the halogen loading and resulting effects on global ozone. As a result, the definition of ODPs has been revised for VSLS (Wuebbles et al., 2001; WMO, 2003, 2011; Pisso et al., 2010). The ODPs derived for VSLS now account for variations that can occur in the ODP as a function of where and when (geographic location and time of year) the compound is emitted. The most important factor in evaluating the ODP of VSLS is shown to be geographical distribution, or latitude, of the surface emissions because gases emitted at higher latitudes are less likely to reach the stratosphere before destruction than gases emitted in the tropics (Bridgeman et al., 2000; Olsen et al., 2000; Wuebbles et al., 2001). The discussion of updates to ODPs thus reflects this change in definition for VSLS.

compared to those from WMO (2011) in Table 5-1 (also see discussion of atmospheric lifetimes in Chapter 1). There are a number of differences, but the most important one to the derivation of ODPs is the change in lifetime of CFC-11 from 45 years to 52 years (+15%); CFC-11 is in the denominator in ODP derivation, so this change in lifetime decreases the values of all ODPs in WMO (2011) by 15%. Revisions in the lifetimes for other gases produce the other differences found in ODP values for "This Assessment" found in Table 5-2.

The age-of-air spectrum from Newman et al. (2007) and the age-of-air dependent fractional release factors (FRFs, defined as age of-air-dependent ODS decomposition rates; also see Chapter 1) from

Table 5-1. Atmospheric lifetimes and fractional halogen release factors relative to WMO (2011) for long-lived halocarbons. In this Assessment, lifetimes are based on SPARC (2013). Fractional release factors (midlatitude conditions) used in this Assessment are based on the previous Assessment (WMO, 2011), but we also show in the table those for the 10 compounds updated in Laube et al. (2013) using a mean age of air of 3 years. Lifetime uncertainties are based on SPARC (2013) lifetimes as evaluated by Velders and Daniel (2014). Also see Chapter 1 for further discussion on atmospheric lifetimes.

Halocarbon	Atmospheric Lifetime (years)			Fractional Release Factors	
	WMO (2011)	This Assessment	Lifetime uncertainty (1σ)[c]	This Assessment	Laube et al. (2013)
Annex A-I					
CFC-11	45	52	±22%	0.47	0.35
CFC-12	100	102	±15%	0.23	0.19
CFC-113	85	93	±17%	0.29	0.22
CFC-114	190	189	±12%	0.12	
CFC-115	1020	540	±17%	0.04	
Annex A-II					
halon-1301	65	72	±13%	0.28	0.26
halon-1211	16	16	±29%	0.62	0.52
halon-2402	20	28	±19%	0.65	
Annex B-II					
CCl$_4$	26 [a]	26 [a]	±17%	0.56	0.42
Annex B-III					
CH$_3$CCl$_3$	5.0	5.0 [a]	±3%	0.67	0.61
Annex C-I					
HCFC-22	11.9	12	±16%	0.13	0.07
HCFC-123	1.3				
HCFC-124	5.9				
HCFC-141b	9.2	9.4	±15%	0.34	0.17
HCFC-142b	17.2	18	±14%	0.17	0.05
HCFC-225ca	1.9				
HCFC-225cb	5.9				
Annex E					
CH$_3$Br	0.75 [a,b]	0.8 [a]	±17%	0.60	
Others					
halon-1202	2.9	2.5	±33%	0.62	
CH$_3$Cl	1.0 [a]	0.9 [a]	±18%	0.44	

[a] Losses due to oceanic and soil processes are taken into account using values from WMO (2011). The partial lifetime for CCl$_4$ is 44 years for atmospheric loss (from SPARC, 2013) and is assumed to be 95 years for oceanic loss and 195 years for soil loss for a total lifetime of 26 years. The partial lifetime for CH$_3$CCl$_3$ is 5.0 years for atmospheric loss (from SPARC, 2013). The total lifetime for CH$_3$Br is 1.5 years for atmospheric loss (from SPARC, 2013), 3.1 years for oceanic loss, and 3.3–3.4 years for soil loss. The partial lifetime for CH$_3$Cl is 1.3 years for atmospheric loss (from SPARC, 2013) and 3 years for oceanic and soil loss.

[b] In Table 5-1 a lifetime of 0.7 years is reported. In the scenarios calculations, however, a value of 0.75 years is used to be consistent with natural emission estimates from WMO (2011).

[c] These are 1-σ lifetimes, taken from Velders and Daniel (2014), which are calculated when only the uncertainties in the atmospheric loss rates (inverse of the atmospheric lifetime) from SPARC (2013) are taken into account. A 1-σ uncertainty implies that there is an approximately 68% chance that the actual lifetime will fall within that range. The exclusion of other loss rate uncertainties is relevant for CCl$_4$, for which the uncertainty could change if the uncertainty in the partial lifetime due to oceanic loss (82–191 years (WMO, 2011)) would be taken into account.

Newman et al. (2006) were used in WMO (2011) for discrete ages-of-air for midlatitude (3 year) and Antarctic (5.5 year) conditions. A new analysis of the FRF for ten ODS by Laube et al. (2013) gives values that are on average about 20% smaller than those derived by Newman et al. (2006) (see comparison in Table 5-1). These have not been adopted for this Assessment although their effect on ODP values is considered in the following discussion and in Chapter 1.

In Table 5-2, the steady-state semi-empirical ODPs for longer-lived halocarbons (those with an atmospheric lifetime greater than 0.5 year) are shown using the atmospheric lifetimes from WMO (2011) and those derived using the lifetimes from SPARC (2013). In general the derived ODP values in Table 5-2 are almost all smaller numerically (ranging from no change (for carbon tetrachloride, CCl_4) to more than a factor of two smaller (for CFC-115), with most smaller by 10–30% than the values reported in WMO (2011), as expected given the longer lifetime for CFC-11. The one major exception is halon-2402, for which the lifetime in SPARC (2013) is appreciably longer than in WMO (2011).

The use of the Laube et al. (2013) FRFs also affects the semi-empirical ODPs, as shown by the values in parentheses in Table 5-2 (based on Velders and Daniel, 2014). Using both the lifetimes from SPARC (2013) and the fractional release values from Laube et al. (2013) results in small changes in ODPs of most species compared with the values reported in WMO (2011). The ODPs of the HCFCs show larger changes: the ODP of HCFC-22 decreases by 37%; that of HCFC-141b, by 40%; and that of HCFC-142b, by 64%. ODPs calculated from the fractional release values of Laube et al. (2013) and using the SPARC (2013) lifetimes are consistent with the assessed values in the Montreal Protocol and WMO (2011) except for HCFC-22, HCFC-141b, and HCFC-142b, all of which have much smaller values using the Laube et al. fractional release values. Uncertainties in the atmospheric lifetimes, the fractional release values, and atmospheric chemistry generally result in overall uncertainties on the order of 30% for the CFCs and CCl_4, but are much higher for HCFCs and halons (roughly 55–58% for the HCFCs and halon-1301 to over 80% for halon-1202 and halon-1211), based on analyses by Velders and Daniel (2014). The 95th percentile confidence intervals are also shown in the table, as taken from Velders and Daniel (2014). They are shown when using the "most likely" and "possible" lifetime uncertainty ranges as presented in SPARC (2013).

Table 5-3 shows analyses of the spatial dependence in ODPs for VSLS primarily based on results using different versions of the National Center for Atmospheric Research (NCAR) global 3-D model (Wuebbles et al., 2009, 2011; Patten and Wuebbles, 2010; Youn et al., 2010; Patten et al., 2011). Note that this model calculates an atmospheric lifetime of 53.7 years for CFC-11, so the published ODPs would not be significantly affected by the revised SPARC (2013) lifetime for CFC-11. In these studies, the VSLS examined all have quite small ODPs based on emissions occurring primarily at midlatitudes. New approaches for estimating VSLS ODPs have been developed since WMO (2011) based on Lagrangian models (Tegtmeier et al., 2012; Pisso et al., 2010; Brioude et al., 2010), with findings similar to previous studies, except for emissions in the tropics, where a different treatment of convection may allow for more VSLS (and their products) to reach the stratosphere.

In addition to these lifetime estimates, Patten and Wuebbles (2010) evaluated the lifetimes and ODPs of (*E*)-1-chloro-3,3,3-trifluoropropylene ((*E*)-CHCl=CHCF$_3$, HCFC-1233zd(*E*)) and (*E*)-1,2-dichloroethylene ((*E*)-CHCl=CHCl), assuming industrial emissions were to occur over all land surfaces in the latitude range 30°N to 60°N. These compounds are proposed foam blowing agents and electronic cleaning substances. Based on 3-D chemical transport model (CTM) calculations, the atmospheric lifetime of HCFC-1233zd(*E*) was 40 days with an ODP of 0.00034. The model-calculated lifetime is shorter than the boundary layer local lifetime given in Table 1-11 (250 days) and longer than the 26-day lifetime reported in Sulbaek Andersen et al. (2008) that was calculated using a specific OH concentration. For (*E*)-CHCl=CHCl the calculated lifetime and ODP were 12.7 days (6.7-day local lifetime in Table 1-11) and 0.00024, respectively. Patten et al. (2011) evaluated the lifetime and ODP of 2-bromo-3,3,3-trifluoropropene (CH_2=CBrCF$_3$), a suggested halon replacement for use in fire extinguishers. They reported a global annually averaged lifetime of 7 days and an ODP of 0.0028, when emissions were distributed between 30°N to 60°N, compared to the 3.9-day local lifetime given in Table 1-11. The differences in the model-calculated and estimated local lifetimes given in Table 1-11 highlight the dependence on the OH climatology used for the lifetime estimate.

Table 5-2. Ozone Depletion Potentials (ODPs) for long-lived halocarbons. Shown are the ODP values assumed in the Montreal Protocol, the ODPs updated in the previous Assessment (WMO, 2011), and the values determined in this Assessment based on the atmospheric lifetimes from SPARC (2013). Values shown as "This Assessment" are based on the fractional release factors from WMO (2011). The ODPs in parentheses are those using the fractional release factors from Laube et al. (2013). In general the derived ODP values in the Assessment are almost all smaller numerically (ranging from no change (for carbon tetrachloride, CCl_4) to more than a factor of two smaller (for CFC-115), with most smaller by 10–30% than the values reported in WMO (2011), as expected given the longer lifetime for CFC-11. The one major exception is halon-2402, for which the lifetime in SPARC (2013) is appreciably longer than in WMO (2011).

Halocarbon	ODP in Montreal Protocol	Semi-Empirical ODP		Uncertainties (95% confidence interval) (from Velders and Daniel, 2014)	
		WMO (2011)	This Assessment	Possible (±)	Most Likely (±)
Annex A-I					
CFC-11	1.0	1.0	1.0		
CFC-12	1.0	0.82	0.73 (0.81)	34%	30%
CFC-113	0.8	0.85	0.81 (0.82)	34%	30%
CFC-114	1.0	0.58	0.50	37%	30%
CFC-115	0.6	0.57	0.26	34%	32%
Annex A-II					
halon-1301	10.0	15.9	15.2 (19.0)	61%	57%
halon-1211	3.0	7.9	6.9 (7.7)	90%	82%
halon-2402	6.0	13.0	15.7	80%	71%
Annex B-II					
CCl_4	1.1	0.82	0.72 (0.72)	34%	30%
Annex B-III					
CH_3CCl_3	0.1	0.16	0.14 (0.17)	52%	36%
Annex C-I					
HCFC-22	0.055	0.04	0.034 (0.024)	69%	58%
HCFC-123	0.02	0.01			
HCFC-124	0.022				
HCFC-141b	0.11	0.12	0.102 (0.069)	68%	57%
HCFC-142b	0.065	0.06	0.057 (0.023)	67%	56%
HCFC-225ca	0.025				
HCFC-225cb	0.033				
Annex E					
CH_3Br	0.6	0.66 [a]	0.57	78%	69%
Others					
halon-1202		*	1.7	96%	88%
CH_3Cl		0.02	0.015		

[a] This value was based on the lifetime of CH_3Br of 0.8 year shown in the ODP table in WMO (2011).

* The value of 2.2 in Velders and Daniel (2014) is attributed to WMO (2011); the value was not in Table 5-1 of WMO (2011) but can be inferred from the fractional release and lifetimes shown in that table.

Table 5-3. Ozone Depletion Potentials (ODPs) for emissions from given latitude bands over land for short-lived halocarbons (very short-lived substances, VSLS) based on analyses from 3-D models. ODPs are from the papers, but modeled lifetimes for CFC-11 were similar to the SPARC (2013) values, so no correction was necessary. See Chapter 1, Table 1-5, for local lifetimes of such VSLS.

VSLS	Reference	Latitudes of Emissions	Reported Annual Lifetimes (days)	ODPs
nPB [1]	Wuebbles et al. (2009, 2011)	30°N – 60°N	24.7	0.0049
		60°S – 70°N	19.6	0.011
TCE [2]	Wuebbles et al. (2011)	30°N – 60°N	13.0	0.00037
PCE [3]	Wuebbles et al. (2011)	30°N – 60°N	111	0.0050
BTP [4]	Patten et al. (2011)	30°N – 60°N	7.0	0.0028
		60°S – 60°N	4.3	0.0052
HFO-1233zd [5]	Patten and Wuebbles (2010)	30°N – 60°N	40.4	0.00034
tDCE [6]	Patten and Wuebbles (2010)	30°N – 60°N	12.7	0.00024
CF_3I [7]	Youn et al. (2010)	30°N – 60°N	5.0	0.008
		20°S – 20°N	1.1	0.016
CH_3I [8]	Youn et al. (2010)	30°N – 60°N	13.6	0.017
CH_2Br_2 [9]	Tegtmeier et al. (2012)	20°S – 13°N	120	3 – 4
$CHBr_3$ [10]	Tegtmeier et al. (2012)	20°S – 20°N	26	1 – 5

[1] n-propyl bromide (C_3H_7Br)
[2] trichloroethylene (C_2HCl_3)
[3] perchloroethylene (C_2Cl_4)
[4] 2-bromo-3,3,3-trifluoropropene ($CH_2 = CBrCF_3$)
[5] (E)-1-chloro-3,3,3-trifluoropropylene ((E)-$CHCl=CHCF_3$) (also called tCFP)
[6] (E)--1,2-dichloroethylene ((E)-$CHCl=CHCl$)
[7] iodotrifluoromethane
[8] methyl iodide
[9] dibromomethane
[10] tribromomethane

Earlier studies (Wuebbles et al., 1999, 2001; Olsen et al., 2000; Bridgeman et al., 2000) have shown that the ODPs for short-lived compounds depend greatly on when or where the emissions occur, with the largest ODPs being found for emissions in the tropics. Although it is generally expected that most emissions from anthropogenic emissions of VSLS will occur at northern midlatitudes, there is no guarantee of this and the locations of future emissions could change. ODPs for tropical emissions of two VSLS compounds from Tegtmeier et al. (2012) are also presented in Table 5-3. The compounds examined, CH_2Br_2 and $CHBr_3$, are important contributors to lower stratospheric reactive bromine (especially through natural oceanic sources, see Chapter1), and have large ODPs for emissions occurring in the tropics.

The recent modeling studies also re-emphasize the point that VSLS ODPs are very dependent on the location of emissions, and not just the latitude; for example, by co-location with efficient vertical transport by deep convection into the stratosphere (semi-empirical ODPs as a function of specific locations of emissions based on Brioude et al. (2010) are shown in Table 5-4). Brioude et al. (2010) showed that these factors are more important than regional variations in VSLS losses by OH or photolysis. Using CO-like emissions to represent anthropogenic VSLS, they estimated ODPs for various compounds and found maximum ODPs over the Indian sub-continent varying from 0.079 in winter to 0.29 in summer for n-propyl bromide (C_3H_7Br or nPB) and from 0.13 in winter to 0.83 in summer for

CH_3I. Pisso et al. (2010) applied their new methodology to an nPB-like tracer with a lifetime of 20 days. They also found higher ODPs over southeast Asia in the summer (and over western Pacific in winter). In July in the tropics (30°N–30°S), ODPs varied from 0.33 in runs with convection to 0.17 in runs with no convection. Locally, values over southeast Asia are as high as 1.00. In general the results from these Lagrangian studies predict higher ODPs regionally compared to the global model results. These differences highlight uncertainties in simulating the transport of VSLS, with boundary layer mixing, convection depth, and advection strength all possibly leading to local differences in VSLS delivery to the stratosphere (e.g., see Hossaini et al., 2012b; Feng et al., 2011; Hoyle et al. 2011). The global model studies (e.g., Wuebbles et al., 2011) used a full chemical treatment for VSLS and CFC-11 degradation in the stratosphere and more realistic degradation and wet deposition schemes for VSLS in the troposphere than the Lagrangian-based studies (e.g., Tegtmeier et al., 2012; Pisso et al., 2010), leading to less VSLS reaching the stratosphere. Overall, these results point to potentially more important impacts from VSLS if emissions occur in regions close to convective regions in the tropics.

Ravishankara et al. (1994) estimated that HFCs and other halocarbons with CF_3 groups, such as HFC-23, -125, and -134a, could lead to ODPs of at most 0.0005 because of degradation product reactions. While the fluorine in HFCs is largely thought to be inert to ozone, it can destroy a small amount of ozone (Ravishankara et al., 1994). This can occur by (barely) catalytic cycles involving $FO_x = F + FO$ and $CF_3O_x = CF_3O + CF_3O_2 + CF_3O_2NO_2$ families (e.g., Lary, 1997). Recent updates to relevant reaction rates suggest that the upper limits of the ODPs for such compounds are likely to be smaller (Sander et al., 2011), indicating that these compounds (not containing chlorine, bromine, or iodine) are unlikely to have a significant effect on stratospheric ozone.

Table 5-4. Estimated annual-mean Ozone Depletion Potentials (ODPs) for short-lived halocarbons (very short-lived substances, VSLS) as a function of specific emissions location. The numbers in brackets show the seasonal variability. These semi-empirical ODP estimates are based on the Lagrangian model study of Brioude et al. (2010) (the numbers shown are from the Supplementary materials of the published paper). The ODP estimates for $CHBr_3$ have been reduced by a factor of 3.1 compared with the Brioude et al. (2010) Supplement values owing to an error discovered after publication.

Species	North America	Europe	East Asia	Indian Subcontinent
C_2H_5Br	0.1300 [0.0780 – 0.2000]	0.1100 [0.0610 – 0.1700]	0.2100 [0.1000 – 0.3100]	0.4600 [0.3400 – 0.6300]
CH_2CBrCF_3	0.0035 [0.0008 – 0.0077	0.0013 [0.0006 – 0.0024]	0.0052 [0.0011 – 0.0130]	0.0440 [0.0130 – 0.0830]
n-C_3H_7Br	0.0235 [0.0150 – 0.0320]	0.0150 [0.0070 – 0.0260]	0.0420 [0.0190 – 0.0600]	0.1700 [0.0790 – 0.1300]
C_2HCl_3	0.0004 [0.0001 – 0.0007]	0.0001 [0.0001 – 0.0002]	0.0006 [0.0002 – 0.0013]	0.0041 [0.0013 – 0.0079]
CCl_3CHO	0.0008 [0.0005 – 0.0010]	0.0004 [0.0002 – 0.0008]	0.0014 [0.0007 – 0.0022]	0.0062 [0.0026 – 0.0110]
CH_3I	0.0360 [0.0130 – 0.0650]	0.0140 [0.0072 – 0.0210]	0.0660 [0.0220 – 0.1500]	0.4200 [0.1300 – 0.8300]
CF_3I	0.0068 [0.0022 – 0.0120]	0.0034 [0.0013 – 0.0061]	0.0120 [0.0020 – 0.0310]	0.0940 [0.0290 – 0.1900]
C_3F_7I	0.0028 [0.0007 – 0.0064]	0.0015 [0.0005 – 0.0031]	0.0033 [0.0006 – 0.0100]	0.0390 [0.0140 – 0.0670]
CH_2ClI	0.0047 [0.0011 – 0.0110]	0.0024 [0.0007 – 0.0050]	0.0051 [0.0009 – 0.0150]	0.0660 [0.0240 – 0.1100]
$CHBr_3$	0.130 [0.094 – 0.201]	0.106 [0.074 – 0.158]	0.216 [0.123 – 0.310]	0.581 [0.387 – 0.806]

5.3.2 Metrics for Changes in Climate

Box 5-3 summarizes the basics of metrics used for describing changes in climate, namely, Global Warming Potentials (GWPs) and Global Temperature change Potentials (GTPs).

Box 5-3. Metrics for Climate: The Basics

Global Warming Potentials (GWPs)

Many metrics are based on the concept of radiative forcing (RF), which is itself a metric. RF has been commonly used to compare different forcing agents (e.g., emissions of gases and particles) affecting climate in assessments of climate change (e.g., IPCC, 1990, 1995, 1996, 1999, 2000, 2001, 2007, 2009, 2013). Traditionally, the use of radiative forcing as a metric has been based on there being a clear relationship between the globally averaged forcing and the globally averaged annual mean surface temperature response at equilibrium. IPCC reports now also use Effective Radiative Forcing (ERF) to compare different climate change mechanisms (Forster et al. in IPCC 2007; Myhre et al., 2013). Forcings can only be accurately compared in a global mean sense, and not all forcings necessarily have the same efficiency or "efficacy" in causing climate to change. The IPCC 5th Assessment Report accounts better for the effects of efficacy by using the concept of ERF. For RF, all surface and tropospheric conditions are assumed to be constant, while for ERF, all physical variables can respond to perturbations except for those concerning the sea surface temperatures and sea ice. The basis for ERF is to account for the rapid adjustments in the troposphere that occur in the climate system such as the effects on clouds. The inclusion of these adjustments makes ERF a better indicator of the eventual temperature response, especially from particles and other forcings on climate that have strong atmospheric responses on short timescales or have large spatial variations. By including many of the rapid adjustments that differ across forcing agents, the ERF concept includes much of their relative efficacy and therefore leads to more uniform climate sensitivity across agents than the traditional RF concept (Myhre et al., 2013). Because the rapid adjustments included in ERF differ in strength across climate models, the uncertainty range for ERF estimates tends to be larger than the range for RF estimates (Myhre et al., 2013). Nonetheless, for well-mixed gases, there is no significant difference between RF and ERF.

The Global Warming Potential (GWP) metric arose out of analyses done for the first IPCC Assessment and is still the most widely used emission metric and the general standard for metric discussion in Climate Assessments (IPCC 1990, 1996, 1999, 2007). It represents the radiative forcing for either pulse or sustained emissions above the current background levels by integrating the radiative forcing over a specific time interval and comparing that integral to the forcing from an equal mass emission of carbon dioxide. GWPs for different gases can be compared for evaluating their relative potential for affecting climate over a given timescale. The Kyoto Protocol and other climate-related policymaking also compares the effects of different emissions using GWPs with a 100-year time horizon, effectively mapping all greenhouse gas emissions into "CO_2-equivalent emissions." It has become common practice to use the 100-year time horizon for analyses of GWPs, but the choice of time horizon has no direct scientific basis (IPCC, 1990; Wuebbles, 1995; Myhre et al., 2013). Its choice is a value judgment since it depends on the relative weight assigned to effects at different times. Other important choices include the background atmosphere underlying the GWP calculations, and the way indirect effects and feedbacks are considered (Myhre et al., 2013).

Essentially, GWPs are a relative measure of the total energy added to the climate system by a component in question relative to that added by CO_2. The GWP is approximately equal to the ratio (normalizing by the similar expression for CO_2) of the *equilibrium temperature response due to a sustained emission* of the species or to the *integrated temperature response for a pulse emission* (assuming efficacies are equal for the gases that are compared) (Myhre et al., 2013; also see O'Neill, 2000; Prather, 2002; Peters et al., 2011; Azar and Johansson, 2012).

Box 5-3, continued.

However, GWPs do not lead to equivalence with the temporal evolution of the temperature response or that of other climate variables. As a result, despite its existing use in policy considerations, there have been many critiques of the GWP concept. Metrics beyond radiative forcing and GWPs have been proposed but have not yet been used for policy decisions. The most prevalently discussed alternative metric is Global Temperature change Potential, also referred to as Global Temperature Potential (GTP).

Global Temperature change Potentials (GTPs)

The GTP metric (Shine et al., 2005; Shine et al., 2007) gives the relative temperature increase on a per unit mass of emissions basis due to emissions of a greenhouse gas relative to that due to CO_2 emissions for the chosen time horizon. GTP takes into account the thermal inertia and response of the climate system, and provides a measure of the temperature responses of the different components for a specific time horizon. GTP is an end-point measure based on temperature change for a selected year. As with GWPs, the choice of time horizon has a strong effect on the metric. Like GWPs, GTPs can be used for weighting the emissions to obtain "CO_2 equivalents."

GWPs and GTPs are fundamentally different by construction (see Figure 5-1) and different numerical values can be expected. By accounting for the climate sensitivity and the exchange of heat between the atmosphere and the ocean, GTPs include physical processes that GWPs do not. GTPs account for the slow response of the (deep) ocean, thereby prolonging the response to emissions beyond what is controlled by the decay time of the atmospheric concentration. GTPs include both the atmospheric adjustment timescale of the component considered and the response timescale of the climate system. However, GTPs also incorporate extra uncertainties relative to GWPs from including the climate response in the analysis, e.g., GTP values can be significantly affected by assumptions about the climate sensitivity and heat-uptake by the ocean (also see discussion in Myhre et al., 2013). As such, GTPs are sensitive to the specific climate model used in their derivation (e.g., see Olivié and Peters, 2013) and to the background scenario used in the analyses. As a result, the relative uncertainty ranges are potentially much wider for GTPs compared to GWPs.

Peters et al. (2011) provide additional useful insights to the GWP and GTP emissions metrics. They found that GWPs are a useful measure of the energy entering the climate system. GWPs and GTPs should be different as GTPs are an instantaneous measure while GWPs are an integrated measure of the system; that is, for the GTP the pathway of the forcing following a pulse emission is important, whereas the GWP depends only on the integral of the forcing. The ultimate choice of emission metric(s) and time horizon(s) depends on policy objectives. To the extent that limiting integrated temperature change over a specific time horizon is consistent with the broader objectives of climate policy, the analysis by Peters et al. suggests that the GWP concept represents a relatively robust, transparent, and policy-relevant emission metric, except for the short-lived gases, but GWPs are quite small for such gases.

ANALYSES OF GWPS AND GTPS

Updated GWPs and GTPs for many compounds based on the analyses in IPCC (Myhre et al., 2013) are shown in the Appendix in Table 5A-1. Also shown are the atmospheric lifetimes and radiative efficiencies used in these analyses. Hodnebrog et al. (2013) provide further descriptions of the analyses of radiative efficiencies for many halocarbons and related compounds (the IPCC values for the GWPs and GTPs are largely based on those in Hodnebrog et al.). Absolute GWP and GTP (AGWP and AGTP) are the absolute integral of RF (W m^{-2} yr; using ERF if possible) and the absolute temperature change (°C) for a kilogram emission of the greenhouse gas. Climate-carbon feedbacks (i.e., feedbacks between climate change and the carbon cycle) are included in the AGWP and AGTP of CO_2, but not for the AGWP of the non-CO_2 gases; see discussion below. In the new IPCC analyses, there is an increase of approximately 1% and 6% relative to IPCC (2007) and WMO (2011) in the AGWP for CO_2 for integrations of 20 and 100

years, respectively. As a result, many of the GWP values decrease slightly, but they also change because of changes in the lifetime and the radiative efficiency of the named greenhouse gas. This is the first time that values are provided for GTPs in the Ozone Assessment. The derivation of GTP in IPCC (2013) assumes a climate sensitivity of 1.06°C (W m^{-2})$^{-1}$, equivalent to a +3.9°C equilibrium response to 2 × CO$_2$, toward the higher end of the traditional range in climate sensitivity of 1.5 to 4.5°C for doubling of CO$_2$.

The IPCC (2013) GWP and GTP values do not include the changes in atmospheric lifetimes recommended by SPARC (2013). Table 5-5 adjusts the IPCC GWPs and GTPs for the 24 halocarbons with recommended lifetimes from SPARC (2013). Halon-1211 and CCl$_4$ were the only ODSs for which the lifetime was unchanged. The changes in GWPs and GTPs are roughly proportional to the changes in atmospheric lifetimes. Although there are some differences for all of the gases (except halon-1211 and CCl$_4$), the largest differences in GWPs and GTPs relative to Table 5A-1 are found for CFC-11, CFC-115, halon-1301, halon-2402, halon-1202, HFC-125, and HFC-143a.

Uncertainties in GWP values based on the uncertainties given for radiative efficiencies, perturbation lifetimes, and in the AGWP for the reference gas CO$_2$ are estimated in IPCC AR5 Chapter 8 (Myhre et al., 2013). The uncertainty in GWPs for gases with lifetimes of a few decades is estimated to be approximately ±25% and ±35% for 20 and 100 years, respectively. Velders and Daniel (2014) report uncertainties on a number of ODSs; their results suggest that the uncertainties differ substantially for different ODSs. Table 5-6 shows the estimated uncertainty ranges in 20-year and 100-year GWPs for several HFCs, first due to uncertainties in the SPARC (2013) lifetimes by themselves, and then in combination with other uncertainties in evaluation of the full range of uncertainties.

For shorter-lived gases, the uncertainties in GWPs will be larger but the GWP values are also smaller. For GTPs, few uncertainty estimates are currently available in the literature. In IPCC, the results from Joos et al. (2013), Reisinger et al. (2010, 2011), and Boucher (2012) were used to assess an uncertainty for methane for a 100-year GTP of ±75% (as compared to a range of 14 to +22% for 100-year GWPs, based on Olivié and Peters (2013)). The uncertainty in GTPs for longer-lived gases is much smaller (e.g., −17 to +24% for N$_2$O). We do not attempt to show the range of uncertainties for GTPs in this Assessment.
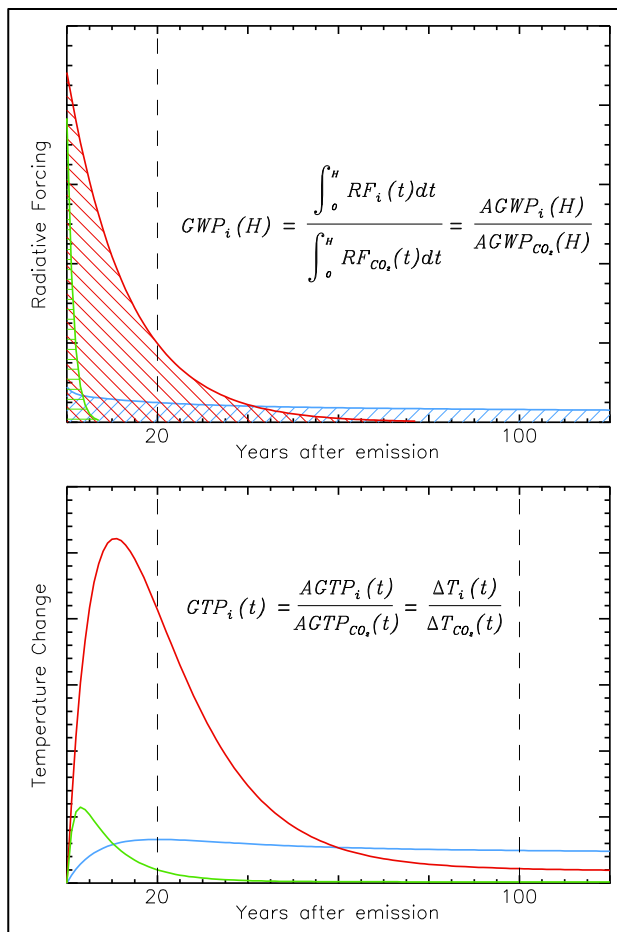
$$GWP_i(H) = \frac{\int_o^H RF_i(t)\,dt}{\int_o^H RF_{CO_2}(t)\,dt} = \frac{AGWP_i(H)}{AGWP_{CO_2}(H)}$$

$$GTP_i(t) = \frac{AGTP_i(t)}{AGTP_{CO_2}(t)} = \frac{\Delta T_i(t)}{\Delta T_{CO_2}(t)}$$

Figure 5-1. (a) The Absolute Global Warming Potential (AGWP) is calculated by integrating the RF due to emission pulses over a chosen time horizon; e.g., 20 and 100 years (vertical lines). The GWP is the ratio of AGWP for component *i* over AGWP for the reference gas CO$_2$. The blue-hatched field represents the integrated RF from a pulse of CO$_2$, while the green and red fields represent example gases with 1.5-year and 13-year lifetimes, respectively. (b) The Global Temperature change Potential (GTP) is based on the surface temperature response at a selected year after pulse emission of the same gases; e.g., 20 or 100 years (vertical lines). See IPCC (2013) Supplementary Material Section S8.11 for equations for calculations of GWP and GTP as used here.

Table 5-5. GWPs and GTPs of various halocarbons based on the SPARC (2013) atmospheric lifetimes. Except for the HFCs, the lifetimes are also found in Table 5-1.

Halocarbon	SPARC (2013) Lifetime (years)	GWP 20-yr	GWP 100-yr	GTP 20-yr	GTP 50-yr	GTP 100-yr
Annex A-I						
CFC-11	52	7090	5160	7160	5480	2920
CFC-12	102	10800	10300	11300	11000	8590
CFC-113	93	6560	6080	6830	6510	4860
CFC-114	189	7710	8580	8180	9010	8530
CFC-115	540	5780	7310	6210	7500	8290
Annex A-II						
halon-1301	72	7930	6670	8160	7160	4700
halon-1211	16	4590	1750	3950	1130	297
halon-2402	28	3920	2030	3730	1900	615
Annex B-II						
CCl_4	26	3480	1730	3280	1570	479
Annex B-III						
CH_3CCl_3	4.8	555	153	298	32	21
Annex C-I						
HCFC-22	12	5310	1780	4230	847	265
HCFC-141b	9.4	2590	800	1900	285	114
HCFC-142b	18	5140	2070	4530	1490	387
Annex E						
CH_3Br	0.8	9	2	3	<1	<1
Others						
halon-1202	2.5	719	196	285	35	27
CH_3Cl	0.9	40	11	13	2	2
HFC-23	228	10800	12500	11500	13000	12800
HFC-32	5.4	2530	704	1440	154	98
HFC-125	31	6280	3450	6040	3350	1180
HFC-134a	14	3810	1360	3170	771	214
HFC-143a	51	7050	5080	7110	5390	2830
HFC-152a	1.6	545	148	191	26	21
HFC-227ea	36	5250	3140	5140	3180	1260
HFC-245fa	7.9	2980	882	2040	259	124

Values of the GWP and GTP metrics are dependent on what processes are included. Ideally all indirect effects should be taken into account. The indirect effects of CH_4 on its own lifetime, tropospheric ozone, and stratospheric water have been traditionally included in its GWP (Prather, 1994; IPCC, 1995). The indirect effect of N_2O on its own lifetime has been considered since the IPCC 3rd Assessment Report (Prather, 1998; IPCC, 2001; Prather and Hsu, 2010). The WMO Assessments (e.g., WMO, 2007, 2011) have considered the indirect effects on stratospheric ozone from various halocarbons. In Table 5-7, indirect GWPs based on IPCC (2013) for various halocarbons are updated using the approach for the ozone response first developed by Daniel et al. (1995). The resulting values are similar to those found in the previous Assessments.

Table 5-6. For selected HFCs, lifetime and full uncertainty estimates of the 20- and 100-year GWPs using the SPARC (2013) lifetimes. The number ranges represent the effects of only considering uncertainties in the SPARC lifetimes, while the "full uncertainty" ranges include also uncertainties in the radiative efficiency (10%, from Myhre et al., 2013) and the AGWP for CO_2 (from Joos et al., 2013). The GWP uncertainties are calculated as in Myhre et al. (2013) (see Supplementary Material Section 8.SM.12 in IPCC (2013) for details), except that new information about lifetime uncertainties from SPARC (2013) is included here. The uncertainty estimates are representative of a 5 to 95% (90%) confidence interval. In addition, note that the IPCC (2013) stated uncertainties in the 100-year GWP for HFC-134a is ±35% (90% confidence) as representative for similar gases. The IPCC and updated GWPs that use the SPARC lifetimes are consistent within their uncertainties.

Halocarbon	SPARC (2013) Lifetime (years)	GWP 20-yr			GWP 100-yr		
		Best Estimate	Lifetime Uncertainty	Full Uncertainty	Best Estimate	Lifetime Uncertainty	Full Uncertainty
HFC-23	228	10800	10700–11100	8640–13100	12500	11800–14000	8880–16300
HFC-32	5.4	2530	2030–3530	1810–3650	704	551–1010	453–1070
HFC-125	31	6280	5840–7110	4930–7800	3450	2720–4830	2230–5140
HFC-134a	14	3810	3300–4690	2890–4980	1360	1040–1930	860–2050
HFC-143a	51	7050	6780–7690	5600–8620	5080	4340–6790	3460–7310
HFC-152a	1.6	545	431–718	386–750	148	117–195	96–211

Table 5-7. Indirect GWPs from ozone depletion (direct forcing from ODS, themselves, is not included) taken from IPCC (2013). Approach is taken from Daniel et al., 1995, assuming a radiative forcing due to ozone depletion in 2011 of −0.15 W m^{-2} (IPCC, 2013). Uncertainty in this radiative forcing leads to an uncertainty in these GWPs of ±100%.

SUBSTANCE	GWP 100-yr
CFC-11	−2640
CFC-12	−2100
CFC-113	−2150
CFC-114	−914
CFC-115	−223
HCFC-22	−98
HCFC-123	−37
HCFC-124	−46
HCFC-141b	−261
HCFC-142b	−152
CH_3CCl_3	−319
CCl_4	−2110
CH_3Br	−1250
halon-1211	−19000
halon-1301	−44500
halon-2402	−32000
HCFC-225ca	−40
HCFC-225cb	−60

It is also important to consider feedbacks between climate and the carbon cycle, effectively the additional amount of CO_2 released from the warming caused by any greenhouse gas. Gillett and Matthews (2010) included climate-carbon feedbacks in calculations of the GWPs for CH_4 and N_2O and found that this increased the values by ~20% for the 100-year GWP. For GTPs they found an increase of ~80%. The AGWP for the CO_2 reference gas has included the climate–carbon feedback in the analyses of GWP in recent Assessments (WMO, 2011; IPCC, 2007, 2013). For the first time, Myhre et al. (2013) include analyses of these indirect climate-carbon feedback effects on GWPs and GTPs for many halocarbons. For many gases, the correction is sizeable, increasing the values of the GWPs and GTPs. However, uncertainties remain large, so more analysis is likely needed before this additional effect is included in policy considerations. Also, the GWPs for the combination of indirect effects on ozone depletion and climate-carbon feedbacks have not been evaluated.

5.4 SCENARIOS AND SENSITIVITY ANALYSES

This section presents an analysis of a set of scenarios and hypothetical test cases that may be of use to decision-makers. The existing Montreal Protocol and its Amendments and adjustments provide the backdrop and a framework for these analyses. Options evaluated include the elimination of future production and future emissions in advance of current controls, and the recapture and destruction of banks (see Box 5-1) in 2015 and 2020. Results are roughly linear, in that a decrease in 50% of future production will have about half the effect on ozone depletion and climate forcing as the scenario evaluated here in which all future production is eliminated. This Ozone Assessment does not evaluate the technical or economical feasibility of these options, but because of the linearity, these results can help guide policymakers in their environmental evaluation of feasible options.

5.4.1 Tools Used in Analyses of Ozone and Climate Effects

As in WMO (2011), both EESC and climate-chemistry modeling studies are used in the scenario analyses relating to ozone impacts. As discussed earlier, EESC is a metric that relates the tropospheric concentration of source gases to their chemically active stratospheric products that are available to destroy ozone. It has been shown (Daniel et al., 2010) that the halogenated ODS mitigation options have about the same percentage impact on integrated EESC as on integrated global stratospheric total column ozone. Because of the computational ease of calculating EESC, an EESC analysis allows for a fast and accurate method for comparing potential ODS mitigation options involving halogenated species without running a full atmospheric model.

Typically, EESC has only been used for halocarbon source gases. However, surface N_2O concentrations due to anthropogenic activity can also be included in EESC (Daniel et al., 2010). The calculation of N_2O's contribution to ozone depletion, and thus to EESC, is complicated by other chemical interactions, such as the concentration of atmospheric chlorine and stratospheric aerosols (Ravishankara et al., 2009), but these obstacles are similar to those encountered by the chlorine- and bromine-containing gases. In this chapter, we do not include N_2O in our standard EESC calculations, but we do include a set of sensitivity runs to show the degree to which the two-dimensional (2-D) modeled ozone response compares with the N_2O EESC response for an N_2O mitigation option.

The NASA/Goddard Space Flight Center (GSFC) 2-D coupled chemistry-radiation-dynamics model (Fleming et al., 2011) is used to evaluate the impact of various ODS and GHG scenarios on past and future ozone, including evaluation of the effects of changes of CO_2 and CH_4 that cannot readily be addressed by EESC as used here. While three-dimensional (3-D) climate-chemistry modeling studies would be ideal for these scenario/test analyses, the computational and time requirements make most of these studies prohibitive for this Assessment. The GSFC 2-D model provides realistic simulations of meridional transport in the stratosphere on timescales >30 days, as seen by good model agreement with a variety of observations in reproducing transport-sensitive features in the meridional plane (Fleming et al.,

2011). Since the computational efficiency of a zonally averaged 2-D model makes it possible to perform multiple long-term simulations in a reasonable amount of time, this 2-D climate-chemistry model is optimal for addressing the ozone-change scenarios discussed here. To be consistent with the model results reported in other Chapters, the model simulations presented here use the recommended chemical rate constants from Sander et al. (2011). Sensitivity simulations revealed that using the updated rate constants from SPARC (2013) resulted in a very minor impact on global total ozone, with changes $<\pm 0.2$ Dobson units (DU).

Radiative forcing is used to quantify the potential effects of the various scenarios on climate. The radiative forcing is calculated with a radiative transfer model using the spatial distribution of mixing ratios determined from observations or calculated in the given atmospheric chemistry-climate model. For the halocarbons, radiative forcing is determined by multiplying the surface mixing ratio by the appropriate radiative efficiency (see Appendix 5A, Table 5A-1). The radiative forcing of N_2O is based on the analyses in Annex II of IPCC (2013).

In addition to the previously discussed ozone depletion and climate metrics, integrated ODP- and GWP-weighted quantities are also shown in Table 5-8 as another comparative tool.

5.4.2 Background Scenario(s) for Ozone and Climate

To evaluate the impact of potential policy decisions on ozone depletion and climate change, a background or baseline scenario of mixing ratios from 1950 through 2100 has been developed for ODS halocarbons and N_2O (and CH_4 and CO_2 in the 2-D model), against which other scenarios are compared. These alternative scenarios are consistent with various mitigation options and are discussed in more detail in Section 5.4.3. The RCP6.0 scenario is used for the time evolution of CO_2, CH_4, and N_2O abundances in the background scenario.

The baseline scenario for the halocarbon ODSs is consistent with the current upper limits prescribed by the Montreal Protocol on Substances that Deplete the Ozone Layer, and it has been developed to be consistent with mixing ratio observations through the beginning of 2013 (see Chapter 1). In the years before atmospheric observations were made, mixing ratios have been estimated from reported production values and are very similar to values in WMO (2011). Future projections are determined from global lifetime estimates that have been recently updated (SPARC, 2013), future production amounts set to be the maximum allowed under the Montreal Protocol, and bottom-up bank estimates for 2008 are the same as were used in WMO (2011). It is assumed that future releases of halocarbons from equipment and applications will continue at the same fractional rate as estimated over the period 2005 through 2011.

Figure 5-2 compares the current baseline scenario and alternative scenarios (see Section 5.4.3 for a description of these scenarios) with the baseline scenario from WMO (2011). The most significant difference in terms of effects on EESC between the two baseline scenarios results from the longer estimated lifetimes for CFC-11 and CCl_4. These lead to slower atmospheric decay and thus an increased contribution to EESC in the future. Lifetime estimate changes have no effect on historical mixing ratios since those are constrained by observations. Some of the largest relative mixing ratio changes occur for the HCFCs. These are primarily caused by the lower base level against which future HCFC production and consumption in Article 5 Parties are referenced to in the current baseline compared with the one from WMO (2011); they are also partly due to a higher assumed level of production between 2009 and 2012 in the previous Assessment, before the freeze went into effect in 2013. The Article 5 base production level is defined in the Montreal Protocol as the average of the 2009–2010 production. In WMO (2011), it was estimated that the Article 5 base level for the HCFCs would be slightly more than 36 ODP-ktonnes; it is now known to be about 33 ODP-ktonnes. This affects the current HCFC production as well as the production and emissions for decades to come since the future limits on production and consumption are prescribed by the Montreal Protocol to be a decreasing fraction of this base level over time.

Changing concentrations of CO_2, CH_4, and N_2O also affect stratospheric ozone and should be considered in analyses of ozone. CO_2 and CH_4 have never been included in the EESC formalism, and N_2O's contribution to EESC has met with limited use. Therefore, in this chapter, we will consider the impact

Table 5-8. Comparison of scenarios and cases[a]: the year when EESC drops below the 1980 value for both midlatitude and Antarctic vortex cases, and integrated EESC differences (midlatitude case) relative to the baseline (A1) scenario[b]. Also shown are changes in integrated ODP- and GWP-weighted emissions and, for selected cases, integrated global ozone depletion from 2015−2050. Future changes in CH_4 and CO_2 may also significantly alter ozone levels, perhaps by amounts larger than any of the cases considered in this table. However, their effects are not included here because policy choices that would lead to reduced global O_3 depletion would require increased CH_4 and CO_2, which would increase climate forcing.

Scenario and Cases	Percent Difference in Integrated EESC Relative to Baseline Scenario for the Midlatitude Case		Year When EESC is Expected to Drop Below 1980 Value		Change in Cumulative ODP-Weighted[d] Emission: 2015−2050	Change in Cumulative GWP-Weighted[e] Emission: 2015−2050	Percent Difference in Integrated O_3 Depletion[f]: 2015−2050
	Midlatitude [b,c]			Antarctic vortex [c]	(Million tonnes CFC-11-equivalent)	(Billion tonnes CO_2-equivalent)	
	$\int_{1980}^{x} EESC\ dt$	$\int_{2015}^{x} EESC\ dt$					
Scenarios							
A1: Baseline scenario	-	-	2047.6	2073.3	0.0	0.0	
Cases[a] of zero production from 2015 onward of:							
P0: All ODS	−5.9	−20	2042.8	2069.5	−0.91	−9.0	−0.30
CFCs	0.0	0.0	2047.6	2073.3	−0.00	−0.00	-
halons	0.0	0.0	2047.6	2073.3	−0.00	−0.00	-
HCFCs	−1.8	−6.4	2046.3	2072.6	−0.22	−7.8	−0.12
CH_3Br for QPS	−1.6	−5.3	2046.5	2071.9	−0.13	−0.00	−0.07
CCl_4	−2.8	−9.8	2045.3	2071.6	−0.56	−1.2	−0.11
Cases[a] of zero emissions from 2015 onward of:							
E0: All ODS (does not include N_2O)	−12	−40	2036.5	2061.4	−2.72	−18.5	−0.75
CFCs	−2.6	−8.9	2045.0	2069.6	−0.86	−4.7	−0.20
halons	−3.4	−12	2044.8	2070.1	−0.76	−0.24	−0.16
HCFCs	−3.7	−13	2045.3	2072.2	−0.41	−12.4	−0.19
CCl_4 [g]	−2.8	−9.8	2045.3	2071.6	−0.56	−1.2	−0.11
CH_3CCl_3	0	0	2047.6	2073.3	−0.00	−0.00	-
CH_3Br for QPS	−1.6	−5.3	2046.5	2071.9	−0.13	−0.00	−0.07
Total anthropogenic N_2O [h]	-	-	-	-	−6.69	−104	−0.88
N_2O mitigation					−1.25	−19.5	−0.16
Cases[a] of full recovery of the 2015 banks of:							
B0: All ODS	−7.3	−25	2041.3	2065.7	−1.80	−9.6	−0.44
CFCs	−2.6	−8.9	2045.0	2069.6	−0.86	−4.7	−0.20
halons	−3.4	−12	2044.8	2070.1	−0.76	−0.24	−0.16
HCFCs	−1.9	−6.4	2046.8	2072.9	−0.19	−4.6	−0.07
Cases[a] of full recovery of the 2020 banks of:							
B0: All ODS	−4.7	−16	2042.4	2066.8	−1.39	−8.1	−0.38
CFCs	−1.5	−5.3	2045.6	2070.3	−0.64	−3.3	-
halons	−2.0	−6.8	2045.4	2070.6	−0.56	−0.18	-
HCFCs	−1.6	−5.5	2046.5	2072.7	−0.19	−4.6	-
CH_3Br sensitivity: [i]							
Same as A1, but CUEs continue at 2012 levels	+0.2	+0.7	2047.8	2073.5	+0.02	+0.00	-

Table 5-8, continued.

[a] Significance of ozone-depleting substances for future EESC was calculated in the hypothetical "cases" by setting production or emission to zero in 2015 and subsequent years or the bank of the ODS to zero in the year 2015 or 2020.

[b] EESC is integrated until it returns to 1980 levels, denoted as year "x."

[c] For midlatitude conditions, an average age-of-air of 3 years, corresponding fractional release values, and a bromine efficiency factor (alpha) of 60 are assumed. For Antarctic vortex conditions, an average age-of-air of 5.5 years, corresponding fractional release values, and an alpha value of 65 are assumed. In all cases, age spectra are applied as in Newman et al. (2007).

[d] Semi-empirical ODPs from Table 5-2.

[e] GWPs with 100-year time horizon (see Appendix 5A, Table 5A-1).

[f] Integrated globally averaged total column ozone changes are taken from 2-D model runs described in chapter.

[g] Banks are assumed to be zero. Emissions include uncertain sources such as possible fugitive emissions and unintended other emissions.

[h] The integrated ODP- and GWP-weighted emissions correspond to the reduction of anthropogenic N_2O emissions from a business-as-usual case to a strong mitigation case (see text).

[i] Same as A1 but critical-use exemptions continue at 2012 levels.

of these three gases in the 2-D model calculations, but not with the box model EESC analysis, except for a brief discussion of the estimated impact of N_2O on EESC. The baseline scenario chosen for these compounds is taken to be the RCP6.0 scenario. While RCP6.0 is a mitigation scenario, it represents one choice of a central scenario around which we can explore the sensitivity of our results to a stronger mitigation scenario (RCP4.5) and a business-as-usual scenario (RCP8.5). This sensitivity analysis has been performed to explore the impact of this choice on the results, but in general, it has little effect on the impacts of the halocarbon mitigation scenarios in terms of either depletion of globally averaged total ozone or on climate forcing changes. However, the scenario choice could have local effects on the structure of ozone changes with altitude and latitude.

5.4.3 Alternative Future Scenarios

Future scenarios have been developed that reflect the impacts of various mitigation options to further reduce future ozone depletion. Because halocarbons and N_2O are greenhouse gases, these scenarios will reduce climate forcing as well. For the ODS halocarbons, the mitigation options include capture and destruction of the banks (see Box 5-1), elimination of future production beginning in 2015, and elimination of future emissions beginning in 2015. Two sets of bank recapture scenarios have been performed, one for elimination of banks in 2015 and one for 2020. A comparison of these bank scenarios illustrates the reduced impact of the bank capture option on ozone and climate as the halocarbons are released into the atmosphere over this 5-year period and bank sizes are projected to decline for most ODSs. Because all post-2015 emission either originates from production after 2015 or from banks existing in 2015, the production elimination and bank capture and destruction scenarios can be approximately added together to reproduce the "no emission" scenario results. The reason that the results are not always perfectly additive is that some of the metrics quantified here are tied to the return of EESC to 1980 levels and this return time changes differently in each mitigation scenario. The production, bank, and emission scenarios are run for individual ODS groups to evaluate the impact of mitigation options for each group to the future ozone and climate metrics. These individual calculations allow for a straightforward evaluation of the relative importance of future production and bank sizes for each of the ODS groups considered.

Figure 5-2 shows future ODS concentration projections for the various mitigation options. The CFCs should have almost no additional production in the future scenarios and so all future emissions are assumed to originate from current equipment and applications. Thus, bank recapture and destruction is the only approach to reduce future mixing ratios of the CFCs. On the other hand, banks of CH_3Br and CCl_4
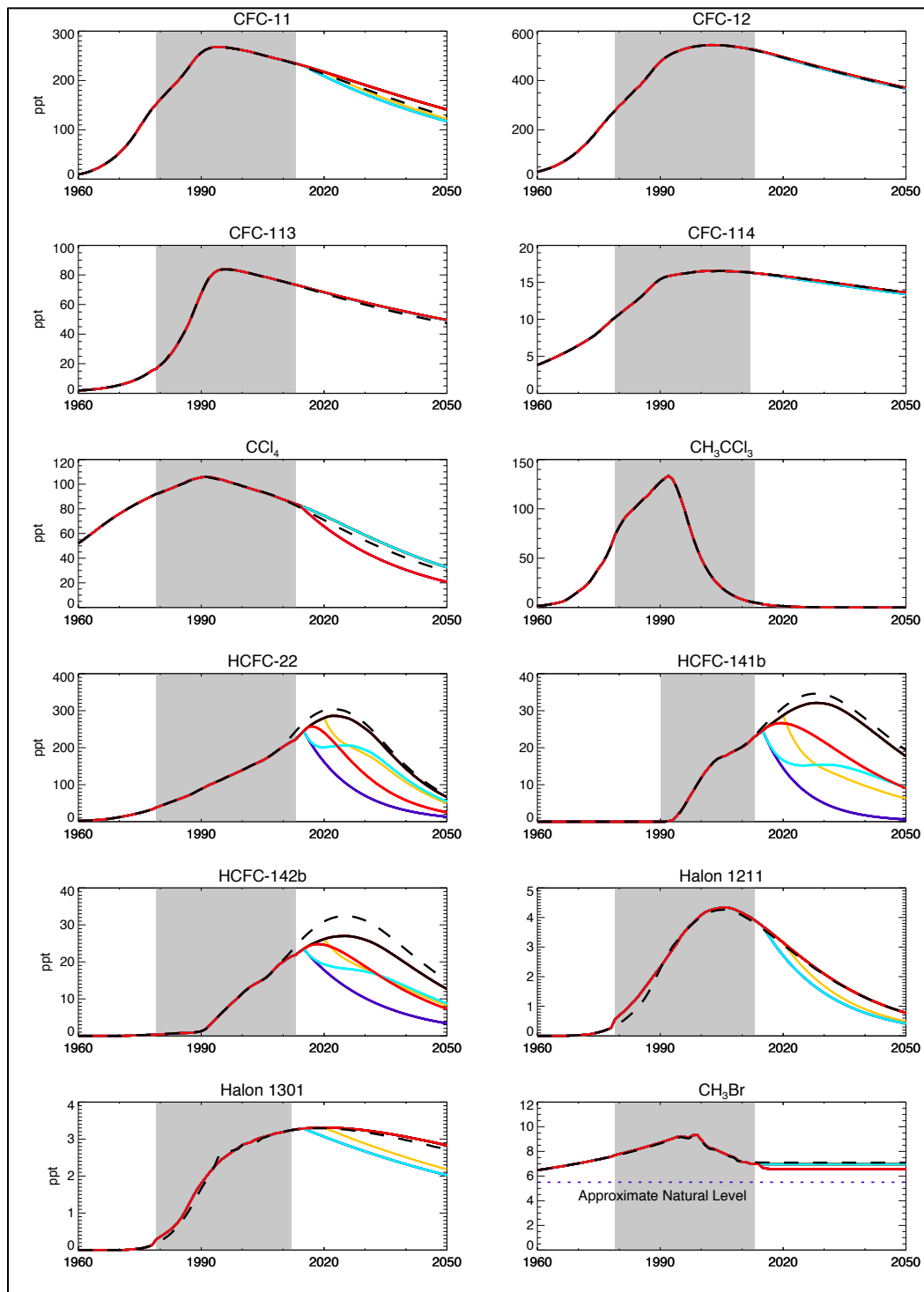
Figure 5-2. Comparison of current baseline halocarbon mixing ratios compared with those from the baseline scenario of WMO (2011); also shown are future mixing ratio projections for "no emission from 2015 onward," "bank capture and destruction in 2015," "bank capture and destruction in 2020," and "no production from 2015 onward" scenarios. Curves are color coded in the same manner as in Figure 5-3 (e.g., solid black is the baseline scenario). Shaded regions represent mixing ratios that are constrained to observational estimates (see Chapter 1; Chapter 5 Appendix 5A, Table 5A-2). The approximate natural concentration of CH_3Br is noted by the dashed dark blue line in the lower right-hand panel (see Chapter 1).

may be small compared with their annual production; for these compounds, eliminating production is the way to reduce their future mixing ratios. Of course, as discussed in Chapter 1, there is a discrepancy between top-down emissions estimates derived from CCl_4 mixing ratio observations and reported production, with reported production too small to be able to account for the observed trend in abundances even if all production were emitted immediately. Thus, to the extent that there is additional unidentified emission that does not come from reported production, elimination of that emission could reduce future EESC and ozone depletion. In this Assessment we adopt current emissions of CCl_4 from the top-down estimates and assume that future emissions will decline at 6% per year in the absence of additional controls. HCFCs can be noticeably reduced in the future by both bank recapture and destruction and by production elimination. It is important to recognize that only emissions resulting from QPS and critical-use exemptions (CUE) applications are considered in our scenario calculations. While controlled uses are thought to lead to small emissions in comparison to QPS emissions (see Chapter 1), we also neglect emissions associated with other activities, such as biomass burning and gasoline and biofuel usage. The baseline scenario for WMO (2011) is shown for comparison in Figure 5-2.

Figure 5-3 shows the impacts of the different mitigation options on total midlatitude EESC. The "No Future Emissions" curve represents the EESC levels to which we are committed even if no ODSs are emitted from 2015 on. This limiting case assumes no further production and no release from existing banks. Both future production and current banks contribute to the elevation of EESC above this level in our baseline scenario approximately equally as shown by the various curves. The difference between the "Zero 2015 Bank" and "Zero 2020 Bank" curves illustrates the impact on EESC of waiting 5 years to capture and destroy the banks; this difference is largest just after 2020 and shrinks over time. Velders and Daniel (2014) have quantified the EESC uncertainty in a scenario that is similar to the baseline scenario shown in Figure 5-3. That calculated uncertainty is determined from uncertainty estimates in all the terms that are used in the EESC calculation. It is found that the 2-σ fractional EESC uncertainty when considering the "most likely" lifetime ranges is comparable to the maximum difference between the baseline scenario and the zero emissions scenario. Overall, the most important single factor to future EESC uncertainty is the uncertainty in the lifetimes of the ODSs.

Table 5-8 shows, as in WMO (2011), how different specific mitigation options affect integrated EESC, ODP- and GWP-weighted emissions, and the return to 1980 EESC levels. In terms of future emissions, HCFCs, halons, CFCs, CCl_4, and CH_3Br all contribute noticeably to increasing future integrated
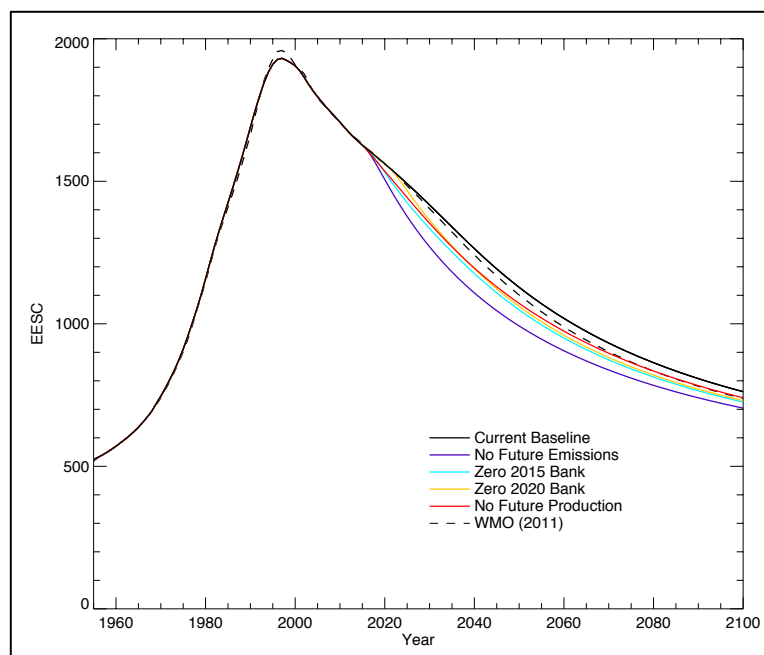
Figure 5-3. EESC for the current baseline scenario (midlatitude conditions) compared with EESC from the WMO (2011) baseline scenario; also shown are four alternative scenarios that reflect current mitigation alternatives considered in this Assessment. Velders and Daniel (2014) have quantified the uncertainty in a similar EESC scenario considering uncertainties in all contributing terms; they found that the 2-σ uncertainty values in the future vary somewhat over time, but are less than 15% when the most likely lifetime ranges are considered and the curves are normalized at 1980 EESC levels.

Global average total ozone change from 1950
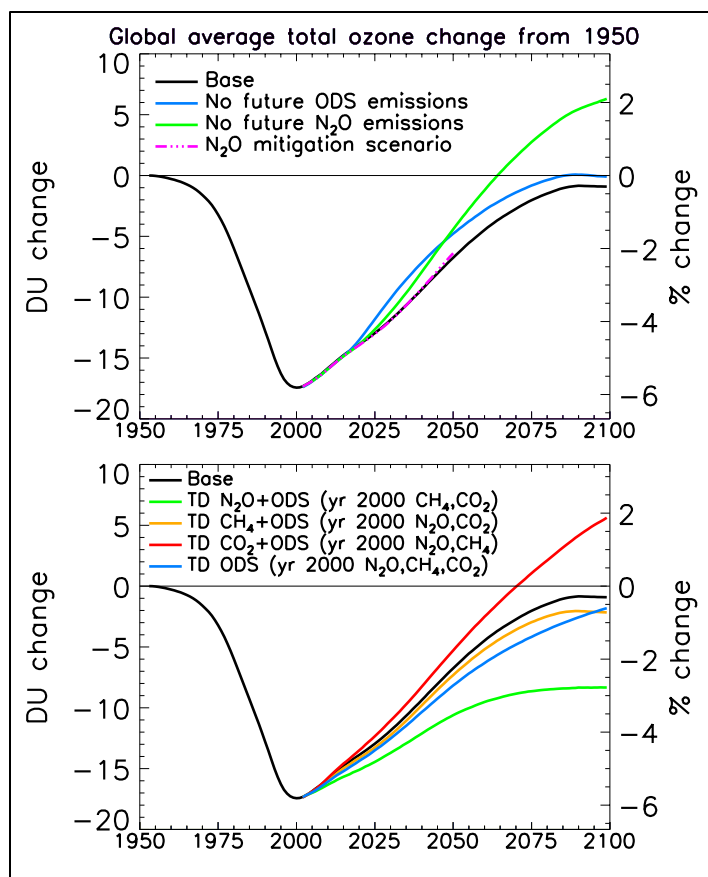
Figure 5-4. Model calculations of the globally averaged total column ozone difference relative to 1950. Upper panel: the baseline scenario, a scenario of no future ODS emissions (blue), no future human-related N_2O emissions (green), and the N_2O mitigation scenario from UNEP (2013) (red dashed-dotted). Bottom panel: the impact due to only the decreasing ODSs, with CO_2, CH_4, and N_2O fixed at 2000 levels (blue), and the separate impacts due to future increasing CO_2 (red), CH_4 (yellow), and N_2O (green) in the presence of decreasing ODSs. The RCP6.0 scenario was used for the greenhouse gases. As stated in the text, these scenarios are different than those presented in Chapter 2.

EESC, where the integration is stopped once total EESC drops below 1980 levels. If all ODS emissions were to be eliminated beginning in 2015, EESC for midlatitudes would return to 1980 levels 11 years sooner than in the baseline scenario. The most significant projected emissions for determining the return time arise from current halon, CFC, and HCFC banks and future production of HCFCs, and CH_3Br. Future emissions of CCl_4 are also projected to be important, but as discussed in Chapter 1 and in this chapter, the sources of these emissions are uncertain. Production of CH_3Br has been eliminated for many historical uses. However, production for quarantine and pre-shipment (QPS) applications is not controlled and is currently the largest remaining emissive anthropogenic component of CH_3Br production. The elimination of future emissions from QPS uses could bring forward the date of EESC return to 1980 levels by 1.1 years, smaller than the 1.6 years estimated in the previous Assessment. Critical-use exemptions for CH_3Br also continue to be granted, but emissions arising from this production are substantially smaller than those from QPS activities. A continuation of critical-use exemptions at the current level would delay the return of EESC to 1980 levels by 0.2 years. For climate considerations, HCFCs play the largest role in future integrated GWP-weighted emissions, contributing almost two-thirds of the total by the ODS halocarbons. These emissions result primarily from future HCFC production, but current banks are also important. Future CFC emissions represent most of the remaining cumulative GWP-weighted emissions through 2050 and are due almost exclusively to current banks.

Table 5-8 also shows the changes in integrated global ozone levels for selected scenarios run with the 2-D model. Figure 5-4 (top panel) shows the two most significant scenarios: 1) no future ODS emissions, and 2) no future human-related N_2O emissions. Also shown is the effect of more modest N_2O mitigation on future ozone. Unlike the ODS halocarbon scenarios, this N_2O alternative mitigation scenario does not assume complete elimination of future production or emission. N_2O has a number of sources but a major one results from the use of fertilizers, i.e., it is to a large degree a by-product of global food production, and because there are no replacements for this use, we have adopted the "concentrated

mitigation" scenario from UNEP (2013) for the alternative mitigation scenario here to compare with the baseline. Even though the reduction in N_2O is only a fraction of the total anthropogenic emissions, the results here are qualitatively consistent with WMO (2011): the impact of all anthropogenic N_2O emissions is very significant compared with the sum of all halocarbon emissions in terms of both ozone depletion and climate. When integrated through 2050, elimination of all anthropogenic N_2O emissions leads to a slightly larger reduction in future CO_2-equivalent emissions than would the elimination of all ODS halocarbon emissions. In terms of integrated ODP-weighted emissions, elimination of anthropogenic N_2O has about half the effect of an elimination of all ODS halocarbon emissions. The alternative N_2O mitigation scenario has an obviously smaller impact on global ozone by 2050. N_2O's impact becomes relatively more important over time because the halocarbon production and consumption is phased out by the Montreal Protocol, while N_2O is projected to continue growing under many future scenarios, including those considered here. It must be recognized, however, that the quantitative impact of N_2O emissions mitigation depends on the baseline scenario chosen (RCP6.0 here). A higher baseline scenario will increase the impact of N_2O mitigation on future climate forcing and ozone depletion.

Figure 5-5 shows the relative importance of historical and future projected N_2O abundances on EESC relative to that of the ODS halocarbons for the baseline scenario used in the chapter. This exemplifies the increasingly important role that N_2O is expected play in the future if its emissions are not reduced. A similar response is seen in the 2-D model calculations of ozone with increasing N_2O but CO_2 and CH_4 fixed at 2000 levels, with increasing ozone flattening and even starting to decrease in the later part of the 21st century (Figure 5-4, bottom, green line). The upper panel of Figure 5-4 shows the relative impact of reducing or eliminating future N_2O emissions compared with that of eliminating future halocarbon ODS emissions on global average total ozone. While total future N_2O emissions cause substantially more depletion in the future than do future halocarbon ODS emissions, many of the N_2O emissions are expected to be very difficult to eliminate (UNEP, 2013). If the UNEP (2013) N_2O mitigation scenario is adopted, which was only analyzed to 2050 (Figure 5-4, top, red dash-dotted line), there is little difference relative to the baseline scenario and much less change than if the no future ODS emissions scenario were adopted (blue line). Again, however, the impact of N_2O mitigation is expect to grow past 2050, while that of ODS halocarbon mitigation will decrease.

It is important to recognize that any future increases in CO_2 and CH_4 not only will have a substantial impact on climate forcing, but also are expected to lead to higher levels of globally averaged total ozone than if these greenhouse gases remained constant. So while CO_2 and CH_4 are likely not considered candidates for altering future ozone depletion themselves, it is important to be aware that policy options for halocarbon ODSs and for N_2O will be made against a backdrop of potentially large ozone changes due to CO_2 and CH_4. The effects on ozone due to increasing CO_2 and CH_4 are discussed in detail in Chapter 2; a summary of the important mechanisms and ozone responses is provided here.
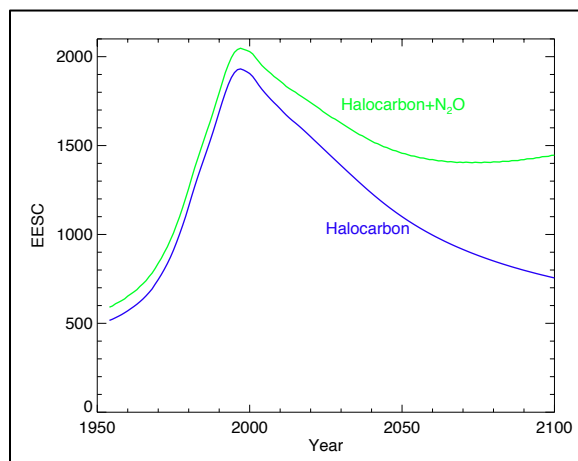

Figure 5-5. Comparison of EESC calculated from halocarbons alone using the midlatitude baseline scenario (Halocarbon), and with the addition of the N_2O contribution (Halocarbon+N_2O) using the formula from Daniel et al. (2010) for including N_2O in EESC.

For most of the scenarios examined, increases in ozone arising from CO_2 and CH_4 increases may be comparable to or larger than the additional depletion caused by N_2O increases. This behavior can be seen from the 2-D model calculations of global total ozone using the RCP6.0 scenario shown in Figure 5-4 (bottom). This illustrates the individual effects of future increases in CO_2 (red line), CH_4 (yellow line), and N_2O (green line) in the presence of decreasing ODSs, and can be compared with the impact due to only the decreasing ODSs (in which the GHGs are all fixed at 2000 levels, blue line). As shown by comparing the red, yellow, and green lines with the blue line in Figure 5-4, increasing CO_2 leads to a substantial global ozone increase by 2100 (+2% relative to 1950) primarily due to stratospheric cooling, which reduces the ozone chemical loss rates (Haigh and Pyle, 1979). Note that these results are for global ozone and that more localized changes may differ (see below and Chapter 2). Another factor is that future CO_2-induced stratospheric changes will indirectly affect ozone by somewhat mitigating the ozone depletion caused by N_2O (see Box 5-2 and Section 2.4.3.1).
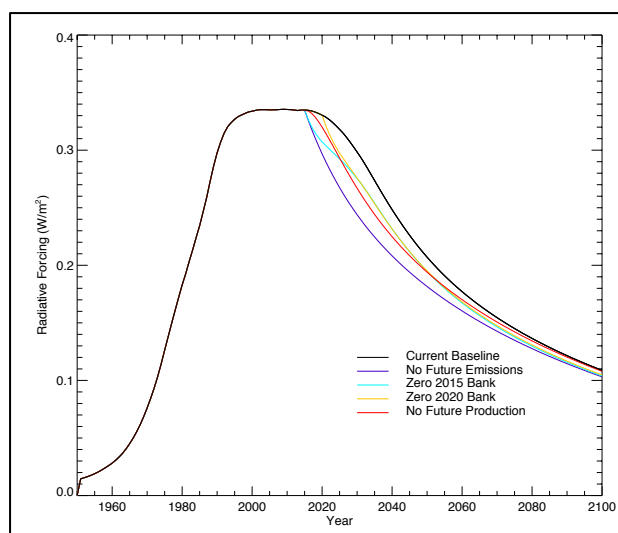
Compared to CO_2, methane loading leads to a smaller global total ozone increase (yellow line in Figure 5-4, bottom). CH_4 causes ozone to increase by: 1) mitigation of the chlorine-ozone loss cycles in the stratosphere, and 2) enhanced NO_x-induced ozone production in the troposphere and lowermost stratosphere following CH_4 oxidation (Brasseur and Solomon, 2005, and see Section 2.4.3.1). For total column ozone, these processes dominate the ozone reductions caused by the CH_4-enhanced HO_x-ozone loss cycles that are important primarily in the upper stratosphere (Revell et al., 2012). The slight decline of the CH_4-induced total ozone change during the late 21st century in Figure 5-4 is caused by the decrease in methane in the RCP6.0 scenario. As atmospheric chlorine levels decline through the 21st century, future methane-induced changes in total ozone will be increasingly determined by the NO_x-ozone production cycle in the troposphere and lowermost stratosphere. The large range in CH_4 among the RCP scenarios, mainly due to the very high methane of RCP8.5 (Section 2.4.3.2), is projected to produce a large range of future tropospheric ozone responses. For example, in 2100, CH_4 increases of 1.9–2.0 ppm (approximately the increase from present day to 2100 in RCP8.5) are projected to increase tropospheric column ozone by 3.5–5 DU (10–13%) (Brasseur et al., 2006; Kawase et al., 2011).

The baseline scenario, with all ODS and GHG effects included, gives an ozone level in 2100 that is slightly less (by 1 DU) than in 1960 (Figure 5-4, black line). This is generally similar to the CMIP5 CHEM multi-model mean for the RCP6.0 scenario, in which stratospheric column ozone is 4 DU less in 2100 than 1960 (Eyring et al., 2013, see also Section 2.4.1). Scenarios with higher levels of CO_2 and CH_4 may cause ozone to obtain higher globally averaged levels than historically observed despite the fact that N_2O levels contribute several DU of ozone depletion by 2100. This is seen in the CMIP5 multi-model mean for the RCP8.5 scenario, in which global stratospheric column ozone in 2100 is greater (by 2 DU) than in 1960 (Eyring et al., 2013). Also, the Special Report on Emissions Scenarios (SRES) A1B (medium) scenario used in the CCMVal-2 simulations (also used in WMO (2011) and Section 2.4.1 of this Assessment) had higher levels of CO_2 and CH_4, and lower N_2O compared with RCP6.0; these factors all contribute to higher global ozone (by ~5 DU) in the A1B scenario during the mid to late 21st century (compare baseline simulations in Figure 2-24 (A1B) and Figure 5-4 (RCP6.0) which are from the same model). However, the ozone response to GHG forcing will likely differ in altitude and region. For example, the CO_2-driven enhancement of the stratospheric circulation will increase lower stratospheric ozone at middle to high latitudes (Li et al., 2009). While global and midlatitude ozone may rise above historical levels, the CO_2-driven circulation enhancement may lead to ozone decreases in the tropical lower stratosphere after 2050, as seen in the CCMVal-2 and CMIP5 simulations for different GHG scenarios (SPARC CCMVal, 2010; Eyring et al., 2013; see also Sections 2.3.5 and 2.4.1).

It is sometimes argued that the future projected "super-recovery" of stratospheric ozone, which can occur under certain scenarios of CO_2 and CH_4 future increased abundances, is a reason to not be concerned about increasing N_2O. Scientifically however, it is clear that N_2O increases in the future will lead to lower ozone levels (greater depletion) than if anthropogenic N_2O emissions were mitigated. Depending on the particular $CO_2/CH_4/N_2O$ scenario, this may mean that levels of global total ozone before intervention from human emissions will never be attained again, or that there will be a delay in reaching those levels.

5.4.4 Radiative Forcing on Climate

Figure 5-6 shows the impacts of the various mitigation scenarios on the radiative forcing on climate from the ODS halocarbons. These curves represent the same scenarios as were shown in Figure 5-3 for their impacts on EESC. The relative shapes and positions of the various scenarios are similar to their EESC contributions. It is currently projected that ODS halocarbon climate forcing will decline from its current peak of 0.33 W m^{-2} to close to 0.1 W m^{-2} by 2100, with little dependence on the particular scenario because of controls already adopted under the Montreal Protocol. In the next few decades, the particular scenario can make a somewhat larger impact on radiative forcing reductions compared with the baseline scenario. One of the consequences of the controls on ODSs is that HFCs, climate forcing agents themselves, have become prevalent replacement compounds. These are discussed in the next section. Velders and Daniel (2014) have quantified the RF uncertainties for a scenario very similar to the baseline scenario considered here. They considered uncertainties in a wide variety of factors that go into estimating past and future concentrations, as well as a 5% uncertainty in the radiative efficiency of each compound. That analysis suggests a 2-σ uncertainty of about ±0.02 W m^{-2} from the present through 2100, when considering the "most likely" range of lifetimes. This uncertainty is controlled primarily by the radiative efficiency uncertainty in the past and current time, while lifetime uncertainties dominate further in the future.

Figure 5-6. Time series of historical and projected radiative forcing from long-lived ODS halocarbons. The radiative forcing projections for the primary mitigation scenarios considered in this Assessment are also shown.

Figure 5-7 shows the derived direct radiative forcing on climate from 2010 to 2050 due to ODSs and other compounds (note that there would be additional indirect forcing due to effects on ozone). The top panel shows the RF due to CFCs and HCFCs to 2050 based on assuming the emissions follow the Montreal Protocol (RF values from Annex II of IPCC, 2013).

The second panel shows the RF for HFCs under various assumptions and demonstrates that increasing RF from HFCs could essentially compensate (or more than compensate) for the decrease in RF from ODSs. The RF curves for HFCs for the RCP scenarios are based on IPCC (2013); these scenarios give lower RFs than those from Velders et al. (2009). Another scenario projecting HFCs growth is taken from Gschrey et al. (2011), which used various sources of information, including the Gross Domestic Product (GDP) and population data underlying the SRES scenarios (IPCC, 2000). Much larger RFs are given in the High and Low scenarios from Velders et al. (2009), which were also based on GDP and population data underlying the SRES scenarios, plus other information, including: the rapid observed growth in demand, substantiated by atmospheric observations; information about products and equipment using HCFCs and HFCs in developing countries; reported increases in consumption of HCFCs in developing countries; replacement patterns of HCFCs by HFCs as reported in developed countries; accelerated phase-out schedules of HCFCs in developed and developing countries; and increases in reported use of HFC-134a in mobile air conditioning in developed and developing countries. The Velders et al. (2009) High scenario describes what happens if the developing world follows the same path in transitioning from CFCs and HCFCs to HFCs (and not-in-kind alternatives) as we have seen in the developed world in the past decade (up to 2009). This in combination with large population and economic
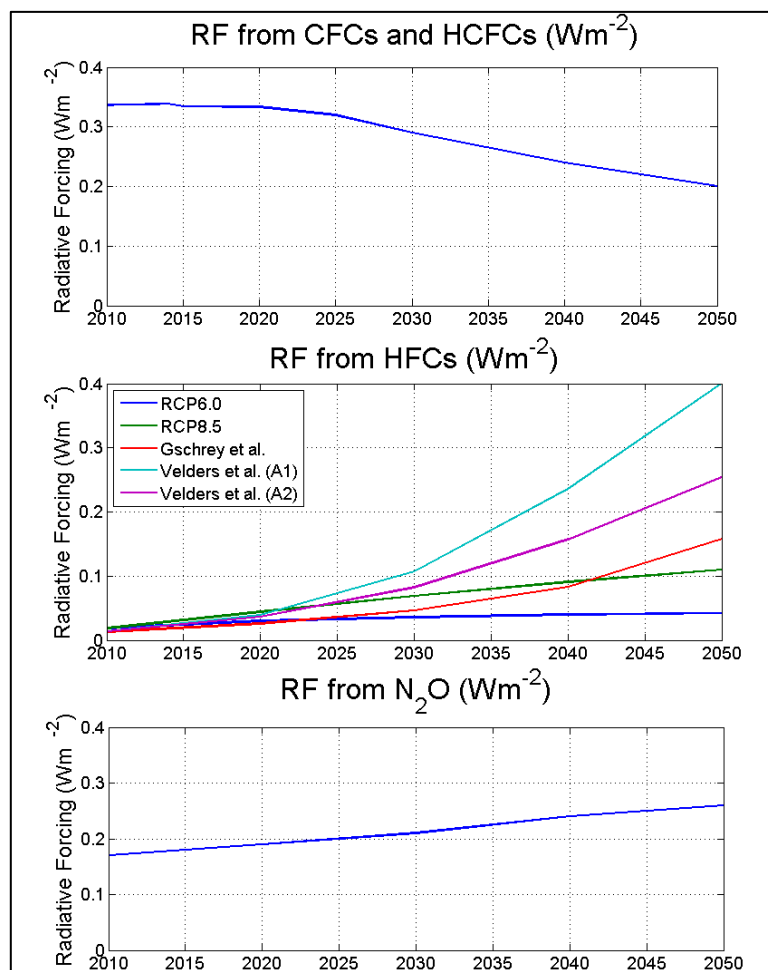
Figure 5-7. Radiative forcing (given as Effective RF) projections for CFCs and HCFCs (following the Montreal Protocol) and the degree to which these decreases might be offset by HFC and N_2O increases. Except for some of the HFC scenarios, the values are based on the scenarios used in Annex II of IPCC (2013). The HFC scenarios represent a range of assumptions and calculations (e.g., see Velders et al. 2009; Gschrey et al., 2011). The Velders et al. A1 and A2 scenarios correspond to the high and low scenarios, respectively, used in Figure 5-8.

growth result in a larger RF for HFCs. If more alternative (low GWP) technologies get a larger market, share the contributions of HFCs to RF will be smaller than in this scenario.

The bottom panel shows the projected growth in RF from N_2O based on the RCP6.0 scenario from IPCC (2013). The increase in N_2O concentration for this scenario results in a direct increase in RF of about 0.09 W m^{-2} by 2050 relative to 2010 (from 0.17 to 0.26 W m^{-2}). This is smaller than, but comparable to, the decrease in RF from ODSs over this time period. By comparison the RF changes for CO_2 and CH_4 for the same scenario over this time period are 1.1 (from 1.8 to 2.9) and 0.05 (from 0.48 to 0.53) W m^{-2}, respectively.

5.4.5 Replacements for High-GWP HFCs

The special report on HFCs by UNEP (2011) found that the climate benefits of the Montreal Protocol could be offset by future increases in the use of the HFCs with longer lifetimes and higher GWPs (those with GWP 100-year values greater than 1000, e.g., including HFC-134a, -143a, and -125). While HFCs are not currently a significant contributor to radiative forcing on climate, they could become important within the next few decades if no action is taken. Switching away from the use of such higher-GWP HFCs to alternatives with much lower GWPs could effectively reduce the effects of halocarbons on climate by 2050. In WMO (2011), a set of different scenarios was considered based on Velders et al. (2009, 2012) that show the phase-out of the higher-GWP HFCs could be an important contributor to reducing future radiative forcing. The analyses can be taken a step further (Wuebbles et al., 2013) by examining a realistic mix of compounds for replacing the uses of the higher-GWP HFCs. As stated in the previous section, the Velders et al. studies assumed growth in HFC use is much larger than in the IPCC (2013) analyses.

Various unsaturated halogenated hydrocarbons with very short atmospheric lifetimes have been recently proposed as substitutes for HCFCs (which are now being phased out under the Montreal Protocol) and longer-lived HFCs. These short-lived substances are expected to have extremely small effects on tropospheric and stratospheric ozone and on climate. Among the possible replacement chemical

compounds are (E)-CHCl=CHCF$_3$ (tCFP or HFO-1233zd; included in the ODP analyses in Table 5-3) and at least six possible HFOs: 2,3,3,3-tetrafluoropropene (CF$_3$CF=CH$_2$, HFO-1234yf); (E)-1,3,3,3-tetrafluoropropene ((E)-CHF=CHCF$_3$, HFO-1234ze(E)); (Z)-1,3,3,3-tetrafluoropropene ((Z)-CHF=CHCF$_3$, HFO-1234ze(Z)); (Z)-1,2,3,3,3-pentafluoropropene ((Z)-CF$_3$CF=CHF, HFO-1225ye(Z)); (E)-1,2,3,3,3-pentafluoropropene ((E)-CF$_3$CF=CHF, HFO-1225ye(E)); and (Z)-1,1,1,4,4,4-hexafluoro-2-butene ((Z)-CF$_3$CH=CHCF$_3$, HFO-1336mzz-Z). In the possible uses, HFO-1234yf can serve as a mobile air conditioning refrigerant; HFO-1234ze(E) can be used as a blowing agent and propellant; HFO-1233zd and HFO-1336mzz-Z can serve as blowing agents; HFO-1234ze(Z) has been suggested as a refrigerant (Brown et al., 2009); HFO-1225ye(Z) and -1225ye(E) have been also proposed as refrigerants (Hurley et al., 2007). The prospect of using HFO-1234yf and HFO-1234ze(E) has been discussed in the literature (UNEP, 2011; Velders et al., 2012). Three-dimensional modeling analyses by Wuebbles et al. (2013) show HFO-1233zd to have an atmospheric lifetime (for realistic locations of emissions) of 30.5 days, while the HFOs have lifetimes ranging from 9.2 days for HFO-1225ye to 17.3 days for HFO-1234ze. The 100-year GWPs range from 0.9 to 4.7 for these six compounds, assuming emissions occur spatially corresponding to current uses of HFCs (Wuebbles et al., 2013).

Scenarios for replacing HFCs with the low-GWP alternatives are developed in Wuebbles et al. (2013) based on the demand for such compounds (e.g., see Velders et al., 2009) with the assumptions that (i) production and consumption of HFCs decrease linearly starting in 2015; (ii) production and consumption of HFC-32, -125, -143a, -245fa, and -365mfc decrease to zero in 2035; (iii) production and consumption of HFC-134a decrease to zero in 2025; (iv) the demand for refrigerants from use of HFC-32, -125, -134a, and -143a is replaced by HFO-1234yf, -1234ze(Z), -1225ye(Z), or -1225ye(E) on a per mass basis; (v) the demand for blowing agents from the use of HFC-152a, -245fa, and -365mfc is replaced by HFO-1234ze(E), or HFO-1233zd on a per mass basis. With these assumptions, the red lines in Figure 5-8 show the radiative forcing of the low-GWP alternatives in 2050 is between 0.00026 and 0.00080 W m^{-2}. As a result, radiative forcing resulting from future requirements for refrigerants and blowing agents is significantly reduced. In contrast, the monotonically increasing radiative forcing of long-lived HFCs (the black lines in Figure 5-8 for low and high HFC growth scenarios from Velders et al., 2009) reaches 0.25 to 0.40 W m^{-2} in 2050. The blue lines in Figure 5-8 show the radiative forcing of the long-lived HFCs for scenarios transitioning to low-GWP alternatives; the HFC radiative forcing for this assumption peaks at 0.046 to 0.053 W m^{-2} near 2030 and decreases to 0.026 to 0.031 W m^{-2} in 2050. The resulting reduction in radiative forcing on climate in 2030 is significant, between 0.04 and 0.07 W m^{-2} (Wuebbles et al., 2013), comparable to the savings of the regulatory black carbon reduction measures, or a sizable fraction of the savings of the technological black carbon reduction measures and CH$_4$ reduction measures recently suggested (Shindell et al., 2012). By 2050, Figure 5-8 shows that the savings could be as large as 0.37 W m^{-2}. Comparably, a recent study by Rigby et al. (2014) suggests that reducing HFC use under the Montreal Protocol could reduce radiative forcing in 2050 by 0.05 to 0.24 W m^{-2}. Some fraction of the replacements could possibly be not-in-kind gases, leading to the possibility for even more reduction in radiative forcing (if those replacements are not greenhouse gases).
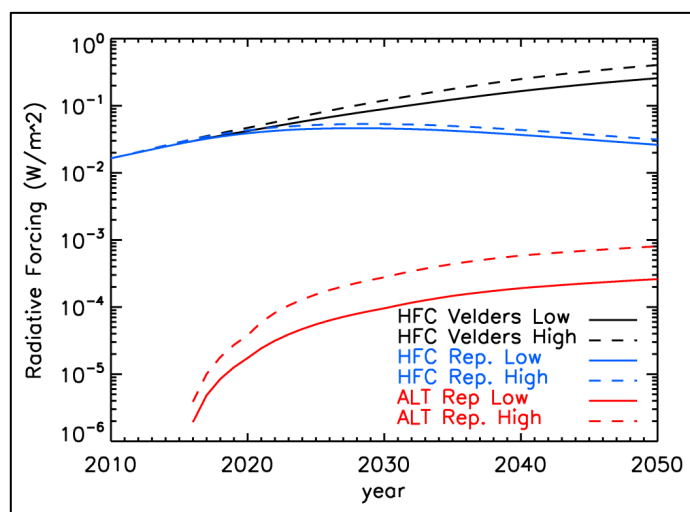
Figure 5-8. Radiative forcing (in W m^{-2}) from 2010–2050 for various scenarios of future HFC usage: high-GWP HFC scenario (Velders et al., 2009; black lines); scenarios for transitioning long-lived high-GWP HFCs to low-GWP alternatives (based on Wuebbles et al., 2013; blue lines) and low-GWP replacement scenarios based on the use of low-GWP alternative compounds (based on Wuebbles et al., 2013; red lines).

Radiative forcing of HFCs would soon be less than that of today if the current mix of HFCs (mean lifetime ~15 yrs) were hypothetically to be entirely replaced within the next few years by a mix of replacements with lifetimes less than 1 month (Velders et al., 2012) but such a rapid transition may be difficult, if not unrealistic. Assuming the slower transition process, the blue lines in Figure 5-8, the radiative forcing due to long-lived HFCs emitted would essentially be the only remaining meaningful direct climate forcing contribution due to the chemicals used in refrigeration and blowing agents. Nonetheless, the quicker the long-lived HFCs are phased out, the less radiative forcing there would be.

Because the applications using HFCs are, in general, less emissive than were those of the CFCs at the same stage, the amount of HFCs stored in existing applications (banks) is projected to be a much larger fraction of annual production (or cumulative production) than was the case for CFCs. As a result, there is an additional future commitment to climate change from HFC banks that would not be apparent if only radiative forcing for a given period is analyzed (Velders et al., 2014). By 2050, HFC banks are estimated to grow to 40 and 65 GtCO$_2$-eq in the high and low scenarios from Velders et al. (2009). In both cases, these bank sizes are approximately 25% of the cumulative production through 2050. Figure 5-9 shows the cumulative production and emissions and their comparisons with the bank sizes for the two scenarios from Velders et al. (2009). While the emissions and forcing from these scenarios are higher than for other published projections, the larger relative importance of the banks compared with the historical CFC situation should hold for all reasonable HFC scenarios. The implication is that earlier phase-outs of HFC production may play a somewhat larger role in mitigating climate forcing than previous estimates have suggested.

Figure 5-9. Projected growth of HFC production, emissions, and banks for two future scenarios (Velders et al., 2014). Figures show the magnitude of the future banks relative to cumulate emissions and production. For example, a phase-out of production in 2020 rather than 2030 would lead to a production decrease of 27–42 GtCO$_2$-eq, of which 8–15 GtCO$_2$ would have remained in banks at the end of that decade and 19–27 GtCO$_2$-eq would have been emitted to the atmosphere during that decade.
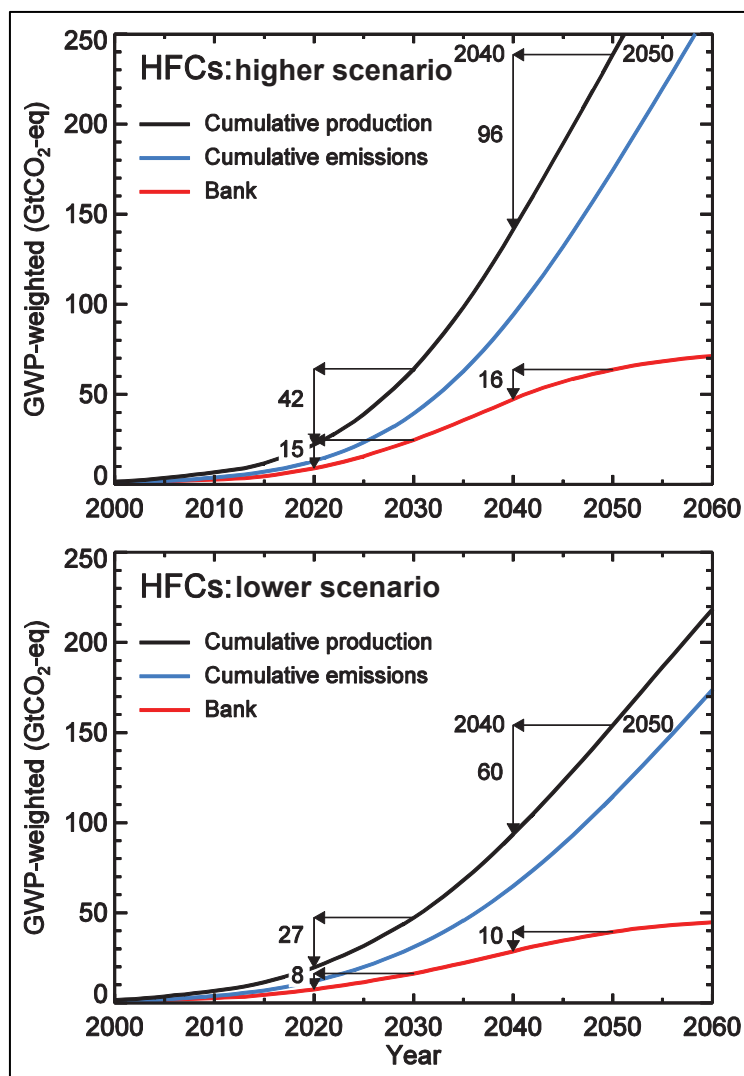
REFERENCES

Anderson, J.G., D.M. Wilmouth, J.B. Smith, and D.S. Sayres, UV dosage levels in summer: Increased risk of ozone loss from convectively injected water vapor, *Science*, *337* (6096), 835-839, doi: 10.1126/science.1222978, 2012.

Azar, C., and D.J.A. Johansson, On the relationship between metrics to compare greenhouse gases – the case of IGTP, GWP and SGTP, *Earth Syst. Dynam.*, *3* (2), 139-147, doi: 10.5194/esd-3-139-2012, 2012.

Benesch, J.A., M.S. Gustin, G.R. Cramer, and T.M. Cahill, Investigation of effects of trifluoroacetate on vernal pool ecosystems, *Environ. Toxicol. Chem.*, *21* (3), 640-647, doi: 10.1002/etc.5620210325, 2002.

Boucher, O., Comparison of physically-and economically-based CO_2-equivalences for methane, *Earth Syst. Dynam.*, *3* (1), 49-61, doi: 10.5194/esd-3-49-2012, 2012.

Boucher, O., P. Friedlingstein, B. Collins, and K.P. Shine, The indirect global warming potential and global temperature change potential due to methane oxidation, *Env. Res. Lett.*, *4* (4), 044007, doi: 10.1088/1748-9326/4/4/044007, 2009.

Boutonnet, J.C., P. Bingham, D. Calamari, C. de Rooij, J. Franklin, T. Kawano, J.-M. Libre, A. McCulloch, G. Malinverno, J.M. Odom, G.M. Rusch, K. Smythe, I. Sobolev, R. Thompson, and J.M. Tiedje, Environmental risk assessment of trifluoroacetic acid, *Hum. Ecol. Risk Assess.*, *5* (1), 59-124, 1999.

Brasseur, G., and S. Solomon, *Aeronomy of the Middle Atmosphere*, 3rd ed., Dordrecht, The Netherlands, 2005.

Brasseur, G.P., M. Schultz, C. Granier, M. Saunois, T. Diehl, M. Botzet, E. Roeckner, and S. Walters, Impact of climate change on the future chemical composition of the global troposphere, *J. Clim.*, *19* (16), 3932-3951, doi: 10.1175/JCLI3832.1, 2006.

Brasseur, G.P., A. Gettelman, M. Jacobson, P. Minnis, J. Penner, R. Prinn, H.B. Selkirk, N. Unger, H.-W. Wong, D.J. Wuebbles, P. Yang, R. Halthore, and S.D. Jacob, *Aviation Climate Change Research Initiative (ACCRI) Phase II Report*, Federal Aviation Administration, Washington, D.C., 2013.

Bridgeman, C.H., J.A. Pyle, and D E. Shallcross, A three-dimensional model calculation of the ozone depletion potential of 1-bromopropane (1-C_3H_7Br), *J. Geophys. Res.*, *105* (D21), 26493-26502, doi: 10.1029/2000 JD900293, 2000.

Brioude, J., R.W. Portmann, J.S. Daniel, O.R. Cooper, G.J. Frost, K.H. Rosenlof, C. Granier, A.R. Ravishankara, S.A. Montzka, and A. Stohl, Variations in ozone depletion potentials of very short-lived substances with season and emission region, *Geophys. Res. Lett.*, *37* (19), L19804, doi: 10.1029/2010GL044856, 2010.

Brown, J.S., C. Zilio, and A. Cavallini, The fluorinated olefin R-1234ze(Z) as a high-temperature heat pumping refrigerant, *International Journal of Refrigeration*, *32* (6), 1412-1422, doi: 10.1016/j.ijrefrig.2009.03.002, 2009.

Brühl, C., J. Lelieveld, P.J. Crutzen, and H. Tost, The role of carbonyl sulphide as a source of stratospheric sulphate aerosol and its impact on climate, *Atmos. Chem. Phys.*, *12* (3), 1239-1253, doi: 10.5194/acp-12-1239-2012, 2012.

Canty, T., N.R. Mascioli, M.D. Smarte, and R.J. Salawitch, An empirical model of global climate – Part 1: A critical evaluation of volcanic cooling, *Atmos. Chem. Phys.*, *13* (8), 3997-4031, doi: 10.5194/acp-13-3997-2013, 2013.

Crutzen, P.J., Albedo enhancement by stratospheric sulfur injections: A contribution to resolve a policy dilemma?, *Clim. Change*, *77* (3-4), 211-220, doi: 10.1007/s10584-006-9101-y, 2006.

Daniel, J.S., S. Solomon, and D.L. Albritton, On the evaluation of halocarbon radiative forcing and global warming potentials, *J. Geophys. Res.*, *100* (D1), 1271-1285, 1995.

Daniel, J.S., E.L. Fleming, R.W. Portmann, G.J.M. Velders, C.H. Jackman, and A.R. Ravishankara, Options to accelerate ozone recovery: Ozone and climate benefits, *Atmos. Chem. Phys.*, *10* (16), 7697-7707, doi: 10.5194/acp-10-7697-2010, 2010.

Davis, S.M., and K.H. Rosenlof, A multidiagnostic intercomparison of tropical-width time series using reanalyses and satellite observations, *J. Climate*, *25* (4), 1061-1078, doi: 10.1175/JCLI-D-11-00127.1, 2012.

Dessens, O., G. Zeng, N. Warwick, and J. Pyle, Short-lived bromine compounds in the lower stratosphere; impact of climate change on ozone, *Atmos. Sci. Lett.*, *10* (3), 201-206, doi: 10.1002/asl.236, 2009.

Dessler, A.E., M.R. Schoeberl, T. Wang, S.M. Davis, and K.H. Rosenlof,, Stratospheric water vapor feedback, *Proc. Natl. Acad. Sci.*, *110* (45), 18087-18091, doi: 10.1073/pnas.1310344110, 2013.

Eyring, V., J.M. Arblaster, I. Cionni, J. Sedláček, J. Perlwitz, P.J. Young, S. Bekki, D. Bergmann, P. Cameron-Smith, W.J. Collins, G. Faluvegi, K.-D. Gottschaldt, L.W. Horowitz, D.E. Kinnison, J.-F. Lamarque, D.R. Marsh, D. Saint-Martin, D.T. Shindell, K. Sudo, S. Szopa, and S. Watanabe, Long-term ozone changes and associated climate impacts in CMIP5 simulations, *J. Geophys. Res.*, *118* (10), 5029-5060, doi: 10.1002/jgrd.50316, 2013.

FAA (Federal Aviation Administration), *2011 U.S. Commercial Space Transportation Developments and Concepts:*

Vehicles, Technologies, and Spaceports, 103 pp., Washington D.C., http://www.faa.gov/about/office_org/headquarters_offices/ast/media/111355.pdf, 2011.

FAA (Federal Aviation Administration), *2013 Commercial Space Transportation Forecasts*, FAA Commercial Space Transportation (AST) and the Commercial Space Transportation Advisory Committee (COMSTAC), 96 pp., Washington D.C., http://www.faa.gov/go.ast, 2013.

FAO (Food and Agriculature Organisation), *The State of World Fisheries and Aquaculture 2012*, Food and Agriculture Organisation of the United Nations, Fisheries and Aquaculture Department, 209 pp., Rome, http://www.fao.org/docrep/016/i2727e/i2727e00.htm, 2012.

Feng, W., M.P. Chipperfield, S. Dhomse, B.M. Monge-Sanz, X. Yang, K. Zhang, and M. Ramonet, Evaluation of cloud convection and tracer transport in a three-dimensional chemical transport model, *Atmos. Chem. Phys*., *11* (12), 5783-5803, doi: 10.5194/acp-11-5783-2011, 2011.

Ferraro, A.J., E.J. Highwood, and A.J. Charlton-Perez, Stratospheric heating by potential geoengineering aerosols, *Geophys. Res. Lett.*, *38* (24), L24706, doi: 10.1029/2011GL049761, 2011.

Fleming, E.L., C.H. Jackman, R.S. Stolarski, and A.R. Douglass, A model study of the impact of source gas changes on the stratosphere for 1850-2100, *Atmos. Chem. Phys*., *11* (16), 8515-8541, doi: 10.5194/acp-11-8515-2011, 2011.

Free, M., and J. Lanzante, Effect of volcanic eruptions on the vertical temperature profile in radiosonde data and climate models, *J. Clim.*, *22* (11), 2925-2939, doi: 10.1175/2008JCLI2562.1, 2009.

Gillett, N.P., and H.D. Matthews, Accounting for carbon cycle feedbacks in a comparison of the global warming effects of greenhouse gases, *Environ. Res. Lett.*, *5* (3), 034011, doi: 10.1088/1748-9326/5/3/034011, 2010.

Graf, H.-F., B. Langmann, and J. Feichter, The contribution of Earth degassing to the atmospheric sulfur budget, *Chemical Geology*, *147* (1-2), 131-145, doi: 10.1016/S0009-2541(97)00177, 1998.

Grooß, J.-U. and R. Müller, Do cosmic-ray-driven electron-induced reactions impact stratospheric ozone depletion and global climate change?, *Atmos. Environ.*, *45* (20), 3508-3514, doi: 10.1016/j.atmosenv.2011.03.059, 2011.

Gschrey, B., W. Schwarz, C. Elsner, and R. Engelhardt, High increase of global F-gas emissions until 2050, *Greenhouse Gas Measurement and Management, 1* (2), 85-92, doi: 10.1080/20430779.2011.579352, 2011.

Haigh, J.D., and J.A. Pyle, A two-dimensional calculation including atmospheric carbon dioxide and stratospheric ozone, *Nature*, *279*, 222-224, doi: 10.1038/279222a0, 1979.

Harris, N.R, J.C. Farman, and D.W. Fahey, Comment on "Effects of cosmic rays on atmospheric chlorofluorocarbon dissociation and ozone depletion," *Phys. Rev. Lett.*, *89* (21), 219801, doi: 10.1103/PhysRevLett.89.219803, 2002.

Heckendorn, P., D. Weisenstein, S. Fueglistaler, B.P. Luo, E. Rozanov, M. Schraner, L.W. Thomason, and T. Peter, Impact of geoengineering aerosols on stratospheric temperature and ozone, *Env. Res. Lett.*, *4* (4), 045108, doi: 10.1088/1748-9326/4/4/045108, 2009.

Henne, S., D.E. Shallcross, S. Reimann, P. Xiao, D. Brunner, S. O'Doherty, and B. Buchmann, Future emissions and atmospheric fate of HFC-1234yf from mobile air conditioners in Europe, *Environ. Sci. Technol.*, *46* (3), 1650-1658, doi: 10.1021/es2034608, 2012.

Hodnebrog, Ø., M. Etminan, J.S. Fuglestvedt, G. Marston, G. Myhre, C.J. Nielsen, K.P. Shine, and T.J. Wallington, Global warming potentials and radiative efficiencies of halocarbons and related compounds: A comprehensive review, *Rev. Geophys.*, *51* (2), 300-378, doi: 10.1002/rog.20013, 2013.

Holmes, C.D., Q. Tang, and M.J. Prather, Uncertainties in climate assessment for the case of aviation NO, *Proc. Natl. Acad. Sci. USA*, *108* (27), 10997-11002, doi: 10.1073/pnas.1101458108, 2011.

Hossaini, R., M.P. Chipperfield, S. Dhomse, C. Ordóñez, A. Saiz-Lopez, N.L. Abraham, A. Archibald, P. Braesicke, P. Telford, N. Warwick, X. Yang, and J. Pyle, Modelling future changes to the stratospheric source gas injection of biogenic bromocarbons, *Geophys. Res. Lett.*, *39* (20), L20813, doi: 10.1029/2012GL053401, 2012a.

Hossaini, R., M.P. Chipperfield, W. Feng, T.J. Breider, E. Atlas, S.A. Montzka, B.R. Miller, F. Moore, and J. Elkins, The contribution of natural and anthropogenic very short-lived species to stratospheric bromine, *Atmos. Chem. Phys.*, *12* (1), 371-380, doi: 10.5194/acp-12-371-2012, 2012b.

Hoyle, C.R., V. Marécal, M.R. Russo, G. Allen, J. Arteta, C. Chemel, M.P. Chipperfield, F. D'Amato, O. Dessens, W. Feng, J.F. Hamilton, N.R.P. Harris, J.S. Hosking, A.C. Lewis, O. Morgenstern, T. Peter, J.A. Pyle, T. Reddmann, N.A.D. Richards, P.J. Telford, W. Tian, S. Viciani, A. Volz-Thomas, O. Wild, X. Yang, and G. Zeng, Representation of tropical deep convection in atmospheric models - Part 2: Tracer transport, *Atmos. Chem. Phys.*, *11* (15), 8103-8131, doi: 10.5194/acp-11-8103-2011, 2011.

Hurley, M.D., J.C. Ball, and T.J. Wallington, Atmospheric chemistry of the Z and E isomers of $CF_3CF=CHF$; Kinetics, mechanisms, and products of gas-phase reactions with Cl atoms, OH radicals, and O_3, *J. Phys. Chem. A*, *111* (39), 9789-9795, doi: 10.1021/jp0753530, 2007.

IPCC (Intergovernmental Panel on Climate Change), *Climate Change: The IPCC Scientific Assessment*, edited by J.T. Houghton, G.J. Jenkins, and J.J. Ephraums, 364 pp., Cambridge University Press, Cambridge, U.K., 1990.

IPCC (Intergovernmental Panel on Climate Change), *Climate Change, 1994: Radiative Forcing of Climate Change and an Evaluation of the IPCC IS92 Emission Scenarios*, edited by J.T. Houghton, L.G. Meira Filho, J. Bruce, H. Lee, B.A. Callander, E. Haites, N. Harris, and K. Maskell, 339 pp., Cambridge University Press, Cambridge, U.K., 1995.

IPCC (Intergovernmental Panel on Climate Change), *Climate Change 1995: The Science of Climate Change*, edited by J.T. Houghton, L.G. Meira Filho, B.A. Callander, N. Harris, A. Kattenberg, and K. Maskell, 572 pp., Cambridge University Press, Cambridge, U.K., 1996.

IPCC (Intergovernmental Panel on Climate Change), *Aviation and the Global Atmosphere*, A Special Report of the Intergovernmental Panel on Climate Change, edited by J.E. Penner, D. Lister, D.J. Griggs, D.J. Dokken, and M. McFarland, 373 pp., Cambridge University Press, Cambridge, U.K., doi: 10.2277/0521664047, 1999.

IPCC (Intergovernmental Panel on Climate Change), *Emissions Scenarios. A Special Report of Working Group III of the Intergovernmental Panel on Climate Change*, edited by N. Nakicenovic and R. Swart, 570 pp., Cambridge University Press, Cambridge, U.K., and New York, NY, U.S.A., 2000.

IPCC (Intergovernmental Panel on Climate Change), *Climate Change 2001: The Scientific Basis, Contribution of Working Group I to the Third Assessment Report of the Intergovernmental Panel on Climate Change*, edited by J.T. Houghton, Y. Ding, D.J. Griggs, M. Noguer, P.J. van der Linden, X. Dai, K. Maskell, and C.A. Johnson, 881 pp., Cambridge University Press, Cambridge, U.K., 2001.

IPCC (Intergovernmental Panel on Climate Change), *Climate Change 2007: The Physical Science Basis: Contribution of Working Group I to the Fourth Assessment Report of the Intergovernmental Panel on Climate Change*, edited by Solomon, S., D. Qin, M. Manning, Z. Chen, M. Marquis, K.B. Averyt, M. Tignor, and H.L. Miller, 996 pp., Cambridge University Press, Cambridge, U.K., and New York, NY, U.S.A., 2007.

IPCC (Intergovernmental Panel on Climate Change), *Summary Report of the IPCC Expert Meeting on the Science of Alternative Metrics*, 18–20 March 2009, Oslo, Norway. IPCC-XXX/Doc.13 (31.III.2009), http://www.ipcc.ch/meetings/session30/doc13.pdf, 2009.

IPCC (Intergovernmental Panel on Climate Change), *Climate Change 2013: The Physical Science Basis: Contribution of Working Group I to the Fifth Assessment Report of the Intergovernmental Panel on Climate Change*, edited by T.F. Stocker, D. Qin, G.-K. Plattner, M. Tignor, S.K. Allen, J. Boschung, A. Nauels, Y. Xia, V. Bex, and P.M. Midgley, 1535 pp., Cambridge University Press, Cambridge, UK and New York, NY, USA, 2013.

IPCC/TEAP (Intergovernmental Panel on Climate Change/Technology and Economic Assessment Panel), *IPCC/TEAP Special Report on Safeguarding the Ozone Layer and the Global Climate System: Issues Related to Hydrofluorocarbons and Perfluorocarbons*, prepared by Working Groups I and III of the Intergovernmental Panel on Climate Change, and the Technical and Economic Assessment Panel, Cambridge University Press, Cambridge, U.K. and New York, NY, U.S.A., 2005.

John, J.G., A.M. Fiore, V. Naik, L.W. Horowitz, and J.P. Dunne, Climate versus emission drivers of methane lifetime against loss by tropospheric OH from 1860–2100, *Atmos. Chem. Phys.*, *12* (24), 12021-12036, doi: 10.5194/acp-12-12021-2012, 2012.

Joos, F., R. Roth J.S. Fuglestvedt G.P. Peters, I.G. Enting, W. von Bloh, V. Brovkin, E.J. Burke, M. Eby, N.R. Edwards, T. Friedrich, T.L. Frölicher, P.R. Halloran, P.B. Holden, C. Jones, T. Kleinen, F.T. Mackenzie, K. Matsumoto, M. Meinshausen, G.-K. Plattner, A. Reisinger, J. Segschneider, G. Shaffer, M. Steinacher, K. Strassmann, K. Tanaka, A. Timmermann, and A.J. Weaver, Carbon dioxide and climate impulse response functions for the computation of greenhouse gas metrics: A multi-model analysis, *Atmos. Chem. Phys.*, *13* (5), 2793-2825, doi: 10.5194/acp-13-2793-2013, 2013.

Katz, J.I., Stratospheric albedo modification, *Energy Environ. Sci.*, *3* (11), 1634-1644, doi: 10.1039/C002441D, 2010.

Kawase, H., T. Nagashima, K. Sudo, and T. Nozawa, Future changes in tropospheric ozone under Representative Concentration Pathways (RCPs), *Geophys. Res. Lett.*, *38* (5), L05801, doi: 10.1029/2010GL046402, 2011.

Kravitz, B., A. Robock, O. Boucher, H. Schmidt, K.E. Taylor, G. Stenchikov, and M. Schulz, The Geoengineering Model Intercomparison Project (GeoMIP), *Atm. Sci. Lett.*, *12* (2), 162-167, doi: 10.1002/asl.316, 2011.

Lary, D.J., Catalytic destruction of stratospheric ozone, *J. Geophys. Res.*, *102* (D17), 21515-21526, doi: 10.1029/97JD00912, 1997.

Laube, J.C., A. Keil, H. Bönisch, A. Engel, T. Röckmann, C.M. Volk, and W.T. Sturges, Observation-based assessment of stratospheric fractional release, lifetimes, and ozone depletion potentials of ten important source gases, *Atmos. Chem. Phys.*, *13* (5), 2779-2791, doi: 10.5194/acp-13-2779-2013, 2013.

Lee, D.S., D.W. Fahey, P.M. Forster, P.J. Newton, R.C.N. Wit, L.L. Lim, B. Owen, and R. Sausen, Aviation and global climate change in the 21st century, *Atmos. Environ.*, *43* (22-23), 3520-3537, doi: 10.1016/j.atmosenv. 2009.04.024, 2009.

Leedham, E.C., C. Hughes, F.S.L. Keng, S.-M. Phang, G. Malin, and W.T. Sturges, Emission of atmospherically significant halocarbons by naturally occurring and farmed tropical macroalgae, *Biogeosciences*, *10* (6), 3615-3633, doi: 10.5194/bg-10-3615-2013, 2013.

Li, F., R.S. Stolarski, and P.A. Newman, Stratospheric ozone in the post-CFC era, *Atmos. Chem. Phys.*, *9* (6), 2207-2213, doi: 10.5194/acp-9-2207-2009, 2009.

Lu, Q.-B., Cosmic-ray-driven reaction and greenhouse effect of halogenated molecules: Culprits for atmospheric ozone depletion and global climate change, *Int. J. Mod. Phys. B*, *27* (17), 1350073, doi: 10.1142/S0217979 213500732, 2013.

Lu, Q.-B., Reply to "Comment on 'Cosmic-ray-driven reaction and greenhouse effect of halogenated molecules: Culprits for atmospheric ozone depletion and global climate change' by Rolf Müller and Jens-Uwe Grooß," *Int. J. Mod. Phys. B*, *28* (13), 1482002, doi: 10.1142/S0217979214820025, 2014.

Luecken, D.J., R.L. Waterland, S. Papasavva, K.N. Taddonio, W.T. Hutzel, J.P. Rugh, and S.O. Andersen, Ozone and TFA impacts in North America from degradation of 2,3,3,3-tetrafluoropropene (HFO-1234yf), a potential greenhouse gas replacement, *Environ. Sci. Technol.*, *44* (1), 343-348, doi: 10.1021/es902481f, 2010.

Miller, B.R., and L.J.M. Kuijpers, Projecting future HFC-23 emissions, *Atmos. Chem. Phys.*, *11* (24), 13259-13267, doi: 10.5194/acp-11-13259-2011, 2011.

Müller, R., and J.-U. Grooß, Comment on "Cosmic-ray-driven reaction and greenhouse effect of halogenated molecules: Culprits for atmospheric ozone depletion and global climate change," *Int. J. Mod. Phys. B*, *28* (13), 1482001, doi: 10.1142/S0217979214820013, 2014.

Myhre, G., D. Shindell, F.-M. Bréon, W. Collins, J. Fuglestvedt, J. Huang, D. Koch, J.-F. Lamarque, D. Lee, B. Mendoza, T. Nakajima, A. Robock, G. Stephens, T. Takemura, and H. Zhang, Anthropogenic and natural radiative forcing, Chapter 8 in *Climate Change 2013: The Physical Science Basis. Contribution of Working Group I to the Fifth Assessment Report of the Intergovernmental Panel on Climate Change*, edited by Stocker, T.F., D. Qin, G.-K. Plattner, M. Tignor, S.K. Allen, J. Boschung, A. Nauels, Y. Xia, V. Bex and P.M. Midgley, Cambridge University Press, Cambridge, U.K. and New York, NY, 2013.

Nagai, T., B. Liley, T. Sakai, T. Shibata, and O. Uchino, Post-Pinatubo evolution and subsequent trend of the stratospheric aerosol layer observed by mid-latitude lidars in both hemispheres, *SOLA*, *6*, 69-72, doi: 10.2151/sola.2010-018, 2010.

Neely III, R.R., O.B. Toon, S. Solomon, J.-P. Vernier, C. Alvarez, J.M. English, K.H. Rosenlof, M.J. Mills, C.G. Bardeen, J.S. Daniel, and J.P. Thayer, Recent anthropogenic increases in SO_2 from Asia have minimal impact on stratospheric aerosol, *Geophys. Res. Lett.*, *40* (5), 999-1004, doi: 10.1002/grl.50263, 2013.

Newman, P.A., E.R. Nash, S.R. Kawa, S.A. Montzka, and S.M. Schauffler, When will the Antarctic ozone hole recover?, *Geophys. Res. Lett.*, *33*, L12814, doi: 10.1029/2005GL025232, 2006.

Newman, P.A., J.S. Daniel, D.W. Waugh, and E.R. Nash, A new formulation of equivalent effective stratospheric chlorine (EESC), *Atmos. Chem. Phys.*, *7* (17), 4537-4522, doi: 10.5194/acp-7-4537-2007, 2007.

Newman, P.A., E.R. Nash, A.R. Douglass, J.E. Nielsen, and R.S. Stolarski, Estimating when the Antarctic ozone hole will recover, in *Twenty Years of Ozone Decline, Proceedings of the Symposium for the 20th Anniversary of the Montreal Protocol*, edited by C. Zerefos, G. Contopoulos, and G. Skalkeas, Springer Publishing, Dordrecht, The Netherlands, doi: 10.1007/978-90-481-2469-5, p. 191-200, 2009.

Olivié, D.J.L., and G.P. Peters, Variations in emission metrics due to variation in CO_2 and temperature impulse response functions, *Earth Syst. Dynam.*, *4* (2), 267-286, doi: 10.5194/esd-4-267-2013, 2013.

Olsen, S.C., B.J. Hannegan, X. Zhu, and M.J. Prather, Evaluating ozone depletion from very short-lived halocarbons, *Geophys. Res. Lett.*, *27* (10), 1475-1478, doi: 10.1029/1999GL011040, 2000.

Olsen, S.C., G.P. Brasseur, D.J. Wuebbles, S.R.H. Barrett, H. Dang, S.D. Eastham, M.Z. Jacobson, A. Khodayari, H. Selkirk, A. Sokolov, and N. Unger, Comparison of model estimates of the effects of aviation emissions on atmospheric ozone and methane, *Geophys. Res. Lett.*, *40* (22), 6004-6009, doi: 10.1002/2013GL057660, 2013.

O'Neill, B.C., The jury is still out on global warming potentials, *Clim. Change*, *44* (4), 427-443, doi: 10.1023/A:1005582929198, 2000.

Papadimitriou, V.C., Y.G. Lazarou, R.K. Talukdar, and J.B. Burkholder, Atmospheric chemistry of $CF_3CF{=}CH_2$ and (Z)-$CF_3CF{=}CHF$: Cl and NO_3 rate coefficients, Cl reaction product yields, and thermochemical calculations, *J. Phys. Chem. A*, *115* (2), 167-181, doi: 10.1021/jp110021u, 2011.

Papadimitriou, V.C., M.R. McGillen, S.C. Smith, A.M. Jubb, R.W. Portmann, B.D. Hall, E.L. Fleming, C.H. Jackman, and J.B. Burkholder, 1,2-dichlorohexafluoro-cyclobutane (1,2-c-$C_4F_6Cl_2$, R-316c) a potent ozone

depleting substance and greenhouse gas: Atmospheric loss processes, lifetimes, and ozone depletion and global warming potentials for the (*E*) and (*Z*) stereoisomers, *J. Phys. Chem. A*, *117* (43), 11049-11065, doi: 10.1021/jp407823k, 2013.

Papanastasiou, D.K., N.R. Carlon, J.A. Neuman, E.L. Fleming, C.H. Jackman, and J.B. Burkholder, Revised UV absorption spectra, ozone depletion potentials, and global warming potentials for the ozone-depleting substances CF_2Br_2, CF_2ClBr, and CF_2BrCF_2Br, *Geophys. Res. Lett.*, *40* (2), 464-469, doi: 10.1002/grl.50121, 2013.

Patra, P.K., and M.S. Santhanam, Comment on "Effects of cosmic rays on atmospheric chlorofluorocarbon dissociation and ozone depletion," *Phys. Rev. Lett.*, *89*, 219803, doi: 10.1103/PhysRevLett.89.219803, 2002.

Patten, K.O., and D.J. Wuebbles, Atmospheric lifetimes and Ozone Depletion Potentials of trans-1-chloro-3,3,3-trifluoropropylene and trans-1,2-dichloroethylene in a three-dimensional model, *Atmos. Chem. Phys.*, *10* (22), 10867-10874, doi: 10.5194/acp-10-10867-2010, 2010.

Patten, K.O., V.G. Khamaganov, V.L. Orkin, S.L. Baughcum, and D.J. Wuebbles, OH reaction rate constant, IR absorption spectrum, ozone depletion potentials and global warming potentials of 2-bromo-3,3,3-trifluoropropene, *J. Geophys. Res.*, *116* (D24), D24307, doi: 10.1029/2011JD016518, 2011.

Peters, G.P., B. Aamaas, T. Bernsten, and J.S. Fuglestvedt, The integrated global temperature change potential (iGTP) and relationships between emission metrics, *Environ. Res. Lett.*, *6* (4), 044021, doi: 10.1088/1748-9326/6/4/044021, 2011.

Pisso, I., P.H. Haynes, and K.S. Law, Emission location dependent ozone depletion potentials for very short-lived halogenated species, *Atmos. Chem. Phys.*, *10* (24), 12025-12036, doi: 10.5194/acp-10-12025-2010, 2010.

Pitari, G., V. Aquila, B. Kravitz, A. Robock, S. Watanabe, I. Cionni, N. De Luca, G. Di Genova, E. Mancini, and S. Tilmes, Stratospheric ozone response to sulfate geoengineering: Results from the Geoengineering Model Intercomparison Project (GeoMIP), *J. Geophys. Res.*, *119* (5), 2629-2653, doi: 10.1002/2013JD020566, 2014.

Ploeger, F., G. Günther, P. Konopka, S. Fueglistaler, R. Müller, C. Hoppe, A. Kunz, R. Spang, J.-U. Grooß, and M. Riese, Horizontal water vapor transport in the lower stratosphere from subtropics to high latitudes during boreal summer, *J. Geophys. Res.*, *118* (14), 8111-8127, doi: 10.1002/jgrd.50636, 2013.

Plummer, D.A., J.F. Scinocca, T.G. Shepherd, M.C. Reader, and A.I. Jonsson, Quantifying the contributions of stratospheric ozone changes from ozone depleting substances and greenhouse gases, *Atmos. Chem. Phys.*, *10* (18), 8803-8820, doi: 10.5194/acp-10-8803-2010, 2010.

Pope, F.D., P. Braesicke, R.G. Grainger, M. Kalberer, I.M. Watson, P.J. Davidson, and R.A. Cox, Stratospheric aerosol particles and solar-radiation management, *Nature Clim. Change*, *2* (10), 713-719, doi: 10.1038/nclimate1528, 2012.

Prather, M.J., Lifetimes and eigenstates in atmospheric chemistry, *Geophys. Res. Lett.*, *21* (9), 801-804, doi: 10.1029/94GL00840, 1994.

Prather, M.J., Time scales in atmospheric chemistry: Coupled perturbations to N_2O, NO_y, and O_3, *Science*, *279* (5355), 1339-1341, doi: 10.1126/science.279.5355.1339, 1998.

Prather, M.J., Lifetimes of atmospheric species: Integrating environmental impacts, *Geophys. Res. Lett.*, *29* (22), 2063, doi: 10.1029/2002GL016299, 2002.

Prather, M.J., and J. Hsu, Coupling of nitrous oxide and methane by global atmospheric chemistry, *Science*, *330* (6006), 952-954, doi: 10.1126/science.1196285, 2010.

Pyle, J.A., N.J. Warwick, N.R.P. Harris, M.R. Abas, A.T. Archibald, M.J. Ashfold, K. Ashworth, M.P. Barkley, G.D. Carver, K. Chance, J.R. Dorsey, D. Fowler, S. Gonzi, B. Gostlow, C.N. Hewitt, T.P. Kurosu, J.D. Lee, S.B. Langford, G. Mills, S. Moller, A.R. MacKenzie, A.J. Manning, P. Misztal, M.S.M. Nadzir, E. Nemitz, H.M. Newton, L.M. O'Brien, S. Ong, D. Oram, P.I. Palmer, L.K. Peng, S.M. Phang, R. Pike, T.A.M. Pugh, N.A. Rahman, A.D. Robinson, J. Sentian, A. Abu Samah, U. Skiba, H.E. Ung, S.E. Yong, and P.J. Young, The impact of local surface changes in Borneo on atmospheric composition at wider spatial scales: Coastal processes, land-use change and air quality, *Phil. Trans. R. Soc. B*, *366* (1582), 3210-3224, doi: 10.1098/rstb.2011.0060, 2011.

Randel, W.J., and E.J. Jensen, Physical processes in the tropical tropopause layer and their roles in a changing climate, *Nature Geosci.*, *6* (3), 169-176, doi: 10.1038/ngeo1733, 2013.

Ravishankara, A.R., A.A. Turnipseed, N.R. Jensen, S. Barone, M. Mills, C.J. Howard, and S. Solomon, Do hydrofluorocarbons destroy stratospheric ozone?, *Science*, *263*, 71-75, 1994.

Ravishankara, A.R., J.S. Daniel, and R.W. Portmann, Nitrous oxide (N_2O): The dominant ozone-depleting substance emitted in the 21st century, *Science*, *326* (5949), 123-125, doi: 10.1126/science.1176985, 2009.

Reisinger, A., M. Meinshausen, M. Manning, and G. Bodeker, Uncertainties of global warming metrics: CO_2 and CH_4, *Geophys. Res. Lett.*, *37* (14), L14707, doi: 10.1029/2010GL043803, 2010.

Reisinger, A., M. Meinshausen, and M. Manning, Future changes in global warming potentials under representative concentration pathways, *Environ. Res. Lett.*, *6* (2), 024020, doi: 10.1088/1748-9326/6/2/024020, 2011.

Revell L.E., G.E. Bodeker, P.E. Huck, B.E. Williamson, and E. Rozanov, The sensitivity of stratospheric ozone changes through the 21st century to N_2O and CH_4, *Atmos. Chem. Phys.*, *12* (23), 11309-11317, doi: 10.5194/acp-12-11309-2012, 2012.

Rex, M., I. Wohltmann, T. Ridder, R. Lehmann, K. Rosenlof, P. Wennberg, D. Weisenstein, J. Notholt, K. Krüger, V. Mohr, and S. Tegtmeier, A tropical West Pacific OH minimum and implications for stratospheric composition, *Atmos. Chem. Phys.*, *14* (9), 4827-4841, doi: 10.5194/acp-14-4827-2014, 2014.

Rigby, M., R.G. Prinn, S. O'Doherty, B.R. Miller, D. Ivy, J. Mühle, C.M. Harth, P.K. Salameh, T. Arnold, R.F. Weiss, P.B. Krummel, L.P. Steele, P.J. Fraser, D. Young, and P.G. Simmonds, Recent and future trends in synthetic greenhouse gas radiative forcing, *Geophys. Res. Lett.*, *41* (7), 2623-2630, doi: 10.1002/2013 GL059099, 2014.

Rosenfield, J.E., and A.R. Douglass, Doubled CO_2 effects on NO_y in a coupled 2D model, *Geophys. Res. Lett.*, *25* (23), 4381-4384, doi: 10.1029/1998GL900147, 2013.

Ross, M., D. Toohey, M. Peinemann, and P. Ross, Limits on the space launch market related to stratospheric ozone depletion, *Astropolitics*, *7* (1), 50-82, doi: 10.1080/14777620902768867, 2009.

Sander, S.P., J. Abbatt, J.R. Barker, J.B. Burkholder, R.R. Friedl, D.M. Golden, R.E. Huie, C.E. Kolb, M.J. Kurylo, G.K. Moortgat, V.L. Orkin and P.H. Wine, *Chemical Kinetics and Photochemical Data for Use in Atmospheric Studies*, *Evaluation Number 17*, JPL Publication 10-6, Jet Propulsion Laboratory, Pasadena, California, http://jpldataeval.jpl.nasa.gov, 2011.

Schofield, R., S. Fueglistaler, I. Wohltmann, and M. Rex, Sensitivity of stratospheric Br_y to uncertainties in very short lived substance emissions and atmospheric transport, *Atmos. Chem. Phys.*, *11* (4), 1379-1392, doi: 10.5194/acp-11-1379-2011, 2011.

Schwartz, M.J., W.G. Read, M.L. Santee, N.J. Livesey, L. Froidevaux, A. Lambert, and G.L. Manney, Convectively injected water vapor in the North American summer lowermost stratosphere, *Geophys. Res. Lett.*, *40* (10), 2316-2321, doi: 10.1002/grl.50421, 2013.

Shindell, D., J.C.I. Kuylenstierna, E. Vignati, R. van Dingenen, M. Amann, Z. Klimont, S.C. Anenberg, N. Muller, G. Janssens-Maenhout, F. Raes, J. Schwartz, G. Faluvegi, L. Pozzoli, K. Kupiainen, L. Höglund-Isaksson, L. Emberson, D. Streets, V. Ramanathan, K. Hicks, N.T. Kim Oanh, G. Milly, M. Williams, V. Demkine, and D. Fowler, Simultaneously mitigating near-term climate change and improving human health and food security, *Science*, *335* (6065), 183-189, doi: 10.1126/science.1210026, 2012.

Shine, K.P., J.S. Fuglestvedt, K. Hailemariam, and N. Stuber, Alternatives to the global warming potential for comparing climate impacts of emissions of greenhouse gases, *Clim. Change*, *68,* 281-302, doi: 10.1007/s10584-005-1146-9, 2005.

Shine, K.P., T.K. Berntsen, J.S. Fuglestvedt, R.B. Skeie, and N. Stuber, Comparing the climate effect of emissions of short-and long-lived climate agents, *Phil. Trans. R. Soc. A*, *365* (1856), 1903-1914, doi: 10.1098/rsta.2007.2050, 2007.

Siddaway, J.M., and S.V. Petelina, Transport and evolution of the 2009 Australian Black Saturday bushfire smoke in the lower stratosphere observed by OSIRIS on Odin, *J. Geophys. Res.*, *116* (D6), D06203, doi: 10.1029/2010JD015162, 2011.

Skowron, A., D.S. Lee, and R.R. DeLeòn, The assessment of the impact of aviation NO_x on ozone and other radiative forcing responses - The importance of representing cruise altitudes accurately, *Atmos. Environ.*, *74*, 159-168, doi: 10.1016/j.atmosenv.2013.03.034, 2013.

Solomon, S., M. Mills, L.E. Heidt, W.H. Pollock, and A.F. Tuck, On the evaluation of ozone depletion potentials, *J. Geophys. Res.*, *97* (D1), 825-842, doi: 10.1029/91JD02613, 1992.

Solomon, S., R.W. Portmann, R.R. Garcia, L.W. Thomason, L.R. Poole, and M.P. McCormick, The role of aerosol variations in anthropogenic ozone depletion at northern midlatitudes, *J. Geophys. Res.*, *101 (D3)*, 6713-6727, doi: 10.1029/95JD03353, 1996.

Solomon, S., J.S. Daniel, R.R. Neely III, J.-P. Vernier, E.G. Dutton, and L.W. Thomason, The persistently variable "background" stratospheric aerosol layer and global climate change, *Science*, *333* (6044), 866-870, doi: 10.1126/science.1206027, 2011.

SPARC CCMVal (Stratosphere-troposphere Processes And their Role in Climate), *SPARC Report on the Evaluation of Chemistry-Climate Models*, edited by V. Eyring, T.G. Shepherd, and D.W. Waugh, SPARC Report No. 5, WCRP-132, WMO/TD-No. 1526, 478 pp., http://www.atmosp.physics.utoronto.ca/SPARC/ccmval_final/index.php, 2010.

SPARC (Stratosphere-troposphere Processes And their Role in Climate), *SPARC Report on the Lifetimes of Stratospheric Ozone-Depleting Substances, Their Replacements, and Related Species*, edited by M. Ko, P. Newman, S. Reimann, and S. Strahan, SPARC Report No. 6, WCRP-15/2013, 2013.

Stevenson, D., R. Doherty, M. Sanderson, C. Johnson, B. Collins, and D. Derwent, Impacts of climate change and variability on tropospheric ozone and its precursors, *Faraday Discuss.*, *130*, 41-57, doi: 10.1039/b417412g, 2005.

Sulbaek Andersen, M.P., E.J.K. Nilsson, O.J. Nielsen, M.S. Johnson, M.D. Hurley, and T.J. Wallington, Atmospheric chemistry of *trans*-$CF_3CH=CHCl$: Kinetics of the gas-phase reactions with Cl atoms, OH radicals, and O_3, *J. Photochem. Photobio. A: Chemistry*, *199* (1), 92-97, doi: 10.1016/j.jphotochem.2008.05.013, 2008.

Tegtmeier, S., K. Krüger, B. Quack, E.L. Atlas, I. Pisso, A. Stohl, and X. Yang, Emission and transport of bromocarbons: From the West Pacific ocean into the stratosphere, *Atmos. Chem. Phys.*, *12* (22), 10633-10648, doi: 10.5194/acp-12-10633-2012, 2012.

Tilmes, S., R. Müller, and R. Salawitch, The sensitivity of polar ozone depletion to proposed geoengineering schemes, *Science*, *320*, 1201-1204, 2008.

Tilmes, S., R.R. Garcia, D.E. Kinnison, A. Gettelman, and P.J. Rasch, Impact of geoengineered aerosols on the troposphere and stratosphere, *J. Geophys. Res.*, *114*, D12305, doi: 10.1029/2008JD011420, 2009.

Tilmes, S., D.E. Kinnison, R.R. Garcia, R. Salawitch, T. Canty, J. Lee-Taylor, S. Madronich, and K. Chance, Impact of very short-lived halogens on stratospheric ozone abundance and UV radiation in a geo-engineered atmosphere, *Atmos. Chem. Phys.*, *12* (22), 10945-10955, doi: 10.5194/acp-12-10945-2012, 2012.

UNEP (United Nations Environment Programme), *Assessment of Alternatives to HCFCs and HFCs and Update of the TEAP 2005 Supplement Report Data*, Report of the UNEP Technology and Economic Assessment Panel, Task Force Decision XX/8 Report, 129 pp., Nairobi, Kenya, http://ozone.unep.org/teap/Reports/TEAP_Reports/teap-may-2009-decisionXX-8-task-force-report.pdf, 2009.

UNEP (United Nations Environment Programme), *Environmental Effects of Ozone Depletion and Its Interactions with Climate Change: 2010 Assessment*, Report of the UNEP Environmental Effects Assessment Panel, Nairobi, Kenya, http://ozone.unep.org/Assessment_Panels/EEAP/eeap-report2010.pdf, 2010.

UNEP (United Nations Environment Programme), *HFCs: A Critical Link in Protecting Climate and the Ozone Layer*, 36 pp., Nairobi, Kenya, http://www.unep.org/dewa/Portals/67/pdf/HFC_report.pdf, 2011.

UNEP (United Nations Environment Programme), *Volume 2, Additional Information on Alternatives to ODS*, Report of the UNEP Technology and Economic Assessment Panel, ISBN: 978-9966-20-017-4, Nairobi, Kenya, http://ozone.unep.org/Assessment_Panels/TEAP/Reports/TEAP_Reports/TEAP_TaskForce%20XXIV-7-September2013.pdf, 2013.

van Vuuren, D.P., J. Edmonds, M. Kainuma, K. Riahi, A. Thomson, K. Hibbard, G.C. Hurtt, T. Kram, V. Krey, J.-F. Lamarque, T. Masui, M. Meinshausen, N. Nakicenovic, S.J. Smith, and S.K. Rose, The representative concentration pathways: An overview, *Clim. Change*, *109*, 5-31, doi: 10.1007/s10584-011-0148-z, 2011.

Velders, G.J.M., and J.S. Daniel, Uncertainty analysis of projections of ozone-depleting substances: Mixing ratios, EESC, ODPs, and GWPs, *Atmos. Chem. Phys.*, *14* (6), 2757-2776, doi: 10.5194/acp-14-2757-2014, 2014.

Velders, G.J.M., D.W. Fahey, J.S. Daniel, M. McFarland, and S.O. Andersen, The large contribution of projected HFC emissions to future climate forcing, *Proc. Natl. Acad. Sci.*, *106* (27), 10949-10954, doi: 10.1073/pnas.0902817106, 2009.

Velders, G.J.M. A.R. Ravishankara, M.K. Miller, M.J. Molina, J. Alcamo, J.S. Daniel, D.W. Fahey, S.A. Montzka, and S. Reimann, Preserving Montreal Protocol climate benefits by limiting HFCs, *Science*, *335* (6071), 922-923, doi: 10.1126/science.1216414, 2012.

Velders, G.J.M., S. Solomon, and J.S. Daniel, Growth in climate change commitments from HFC banks and emissions, *Atmos. Chem. Phys.*, *14* (9), 4563-4572, doi: 10.5194/acp-14-4563-2014, 2014.

Vernier, J.P., J.P. Pommereau, A. Garnier, J. Pelon, N. Larsen, J. Nielsen, T. Christensen, F. Cairo, L.W. Thomason, T. Leblanc, and I.S. McDermid, Tropical stratospheric aerosol layer from CALIPSO lidar observations, *J. Geophys. Res.*, *114*, D00H10, doi: 10.1029/2009JD011946, 2009.

Vernier, J.-P., L.W. Thomason, J.-P. Pommereau, A. Bourassa, J. Pelon, A. Garnier, A. Hauchecorne, L. Blanot, C. Trepte, D. Degenstein, and F. Vargas, Major influence of tropical volcanic eruptions on the stratospheric aerosol layer during the last decade, *Geophys. Res. Lett.*, *38* (12), L12807, doi: 10.1029/2011GL047563, 2011.

Voigt, Ch., U. Schumann, K. Graf, and K.-D. Gottschaldt, Impact of rocket exhaust plumes on atmospheric composition and climate ― an overview, *Progress in Propulsion Physics*, *4*, 657-670, doi: 10.1051/eucass/201304657, 2013.

Voulgarakis, A., V. Naik, J.-F. Lamarque, D.T. Shindell, P.J. Young, M.J. Prather, O. Wild, R.D. Field, D. Bergmann, P. Cameron-Smith, I. Cionni, W.J. Collins, S.B. Dalsøren, R.M. Doherty, V. Eyring, G. Faluvegi,

G.A. Folberth, L.W. Horowitz, B. Josse, I.A. MacKenzie, T. Tagashima, D.A. Plummer, M. Righi, S.T. Rumbold, D.S. Stevenson, S.A. Strode, K. Sudo, S. Szopa, and G. Zeng, Analysis of present day and future OH and methane lifetime in the ACCMIP simulations, *Atmos. Chem. Phys.*, *13* (5), 2563-2587, doi: 10.5194/acp-13-2563-2013, 2013.

Wallington, T.J., W.F. Schneider, D.R. Worsnop, O.J. Nielsen, J. Sehested, W.J. DeBruyn, and J.A. Shorter, The environmental impact of CFC replacements – HFCs and HCFCs, *Environ. Sci. Technol.*, *28* (7), 320A-326A, doi: 10.1021/es00056a002, 1994.

Wallington, T.J., M.P. Sulbaek Andersen, and O.J. Nielsen, Estimated photochemical ozone creation potentials (POCPs) of $CF_3CF=CH_2$ (HFO-1234yf) and related hydrofluoroolefins (HFOs), *Atmos. Environ.*, *44* (11), 1478-1481, doi: 10.1016/j.atmosenv.2010.01.040, 2010.

Wigley, T.M.L., A combined mitigation/geoengineering approach to climate stabilization, *Science*, *314* (5798), 452-454, doi: 10.1126/science.1131728, 2006.

WMO (World Meteorological Organization), *Scientific Assessment of Ozone Depletion: 1994*, Global Ozone Research and Monitoring Project–Report No. 37, Geneva, Switzerland, 1995.

WMO (World Meteorological Organization), *Scientific Assessment of Ozone Depletion: 1998*, Global Ozone Research and Monitoring Project–Report No. 44, Geneva, Switzerland, 1999.

WMO (World Meteorological Organization), *Scientific Assessment of Ozone Depletion: 2002*, Global Ozone Research and Monitoring Project–Report No. 47, Geneva, Switzerland, 2003.

WMO (World Meteorological Organization), *Scientific Assessment of Ozone Depletion: 2006*, Global Ozone Research and Monitoring Project–Report No. 50, 572 pp., Geneva, Switzerland, 2007.

WMO (World Meteorological Organization), *Scientific Assessment of Ozone Depletion: 2010*, *Global Ozone Research and Monitoring Project–Report No. 52*, Geneva, Switzerland, 2011.

Wuebbles, D.J., *The Relative Efficiency of a Number of Halocarbons for Destroying Stratospheric Ozone*, 11 pp., Lawrence Livermore National Laboratory, Livermore, CA, 1981.

Wuebbles, D.J., Chlorocarbon emission scenarios: Potential impact on stratospheric ozone, *Geophys. Res. Lett.*, *88* (C2), 1433-1443, 1983.

Wuebbles, D.J., Weighing functions for ozone depletion and greenhouse gas effects on climate, *Annual Reviews of Energy and the Environment*, *20*, 45-70, doi: 10.1146/annurev.eg.20.110195.000401, 1995.

Wuebbles, D.J., R. Kotamarthi, and K.O. Patten, Updated evaluation of ozone depletion potentials for chlorobromomethane (CH_2ClBr) and 1-bromo-propane ($CH_2BrCH_2CH_3$), *Atmos. Environ.*, *33* (10), 1641-1643, doi: 10.1016/S1352-2310(98)00249-0, 1999.

Wuebbles, D.J., K.O. Patten, M.T. Johnson, and R. Kotamarthi, New methodology for Ozone Depletion Potentials of short-lived compounds: n-Propyl bromide as an example, *J. Geophys. Res.*, *106* (D13), 14551-14571, doi: 10.1029/2001JD900008, 2001.

Wuebbles, D.J., D. Youn, K. Patten, D. Wang, and M. Martinez-Aviles, Metrics for ozone and climate: Three-dimensional modeling studies of ozone depletion potentials and indirect global warming potentials, in *Twenty Years of Ozone Decline*, *Proceedings of the Symposium for the 20th Anniversary of the Montreal Protocol*, edited by C. Zerefos, G. Contopoulos, and G. Skalkeas, 297-326, Springer, Netherlands, doi: 10.1007/978-90-481-2469-5_23, 2009.

Wuebbles, D.J., K.O. Patten, D. Wang, D. Youn, M. Martínez-Avilés, and J.S. Francisco, Three-dimensional model evaluation of the Ozone Depletion Potentials for n-propyl bromide, trichloroethylene and perchloroethylene, *Atmos. Chem. Phys.*, *11* (5), 2371-2380, doi: 10.5194/acp-11-2371-2011, 2011.

Wuebbles, D.J., D. Wang, K.O. Patten, and S.C. Olsen, Analyses of short-lived replacements for HFCs with large GWPs, *Geophys. Res. Lett.*, *40* (17), 4767-4771, doi: 10.1002/grl.50908, 2013.

Youn, D., K.O. Patten, D.J. Wuebbles, H. Lee, and C.-W. So, Potential impacts of iodinated replacement compounds CF_3I and CH_3I on atmospheric ozone: A three-dimensional modeling study, *Atmos. Chem. Phys.*, *10* (20), 10129-10144, doi: 10.5194/acp-10-10129-2010, 2010.

Young, C.J., and S.A. Mabury, Atmospheric perfluorinated acid precursors: Chemistry, occurrence, and impacts, *Rev. of Environ. Contam. Toxicology*, *208*, 1-109, doi: 10.1007/978-1-4419-6880-7_1, 2010.

APPENDIX 5A

5A-1. ANALYSES OF GWPs AND GTPs

Table 5A-1. Atmospheric lifetimes / adjustment times, radiative efficiencies (RE), and GWP values for 20 and 100 years, and GTP values for 20, 50 and 100 years (from IPCC, 2013). Climate-carbon feedbacks are included for CO_2 while no climate feedbacks are included for the other components (see IPCC (2013) for further details). The derivation of GTP assumes a climate sensitivity of 1.06 K (W m^{-2})$^{-1}$, equivalent to a 3.9 K equilibrium response to 2 x CO_2, toward the higher end of the uncertainty in climate sensitivity. For a complete list of chemical names and Chemical Abstracts Service (CAS) numbers, and for accurate replications of metric values, plus further details on the specific values used, see Supplementary Material Section S8.13 and references therein in IPCC (2013). Also see Hodnebrog et al. (2013) for analyses of radiative efficiencies for the halocarbons and related compounds.

Industrial Designation or Chemical Name	Chemical Formula	Lifetime (years)	Radiative Efficiency (W m^{-2} ppb^{-1})	GWP 20-yr	GWP 100-yr	GTP 20-yr	GTP 50-yr	GTP 100-yr
Carbon dioxide	CO_2	See *	1.37e-5	1	1	1	1	1
Methane	CH_4	12.4$^+$	3.63e-4	84	28	67	14	4
Fossil methane #	CH_4	12.4$^+$	3.63e-4	85	30	68	15	6
Nitrous oxide	N_2O	121$^+$	3.00e-3	264	265	277	282	234
Chlorofluorocarbons								
CFC-11	CCl_3F	45.0	0.26	6,900	4,660	6,890	4,890	2,340
CFC-12	CCl_2F_2	100.0	0.32	10,800	10,200	11,300	11,000	8,450
CFC-13	$CClF_3$	640.0	0.25	10,900	13,900	11,700	14,200	15,900
CFC-113	CCl_2FCClF_2	85.0	0.30	6,490	5,820	6,730	6,250	4,470
CFC-114	$CClF_2CClF_2$	190.0	0.31	7,710	8,590	8,190	9,020	8,550
CFC-115	$CClF_2CF_3$	1,020.0	0.20	5,860	7,670	6,310	7,810	8,980
Hydrochlorofluorocarbons								
HCFC-21	$CHCl_2F$	1.7	0.15	543	148	192	26	20
HCFC-22	$CHClF_2$	11.9	0.21	5,280	1,760	4,200	832	262
HCFC-122	$CHCl_2CF_2Cl$	1.0	0.17	218	59	70	10	8
HCFC-122a	$CHFClCFCl_2$	3.4	0.21	945	258	426	48	36
HCFC-123	$CHCl_2CF_3$	1.3	0.15	292	79	98	14	11
HCFC-123a	$CHClFCF_2Cl$	4.0	0.23	1,350	370	659	72	51
HCFC-124	$CHClFCF_3$	5.9	0.20	1,870	527	1,120	121	74

Industrial Designation or Chemical Name	Chemical Formula	Lifetime (years)	Radiative Efficiency (W m^{-2} ppb^{-1})	GWP 20-yr	GWP 100-yr	GTP 20-yr	GTP 50-yr	GTP 100-yr
HCFC-132c	CH_2FCFCl_2	4.3	0.17	1,230	338	624	67	47
HCFC-141b	CH_3CCl_2F	9.2	0.16	2,550	782	1,850	271	111
HCFC-142b	CH_3CClF_2	17.2	0.19	5,020	1,980	4,390	1,370	356
HCFC-225ca	$CHCl_2CF_2CF_3$	1.9	0.22	469	127	170	22	18
HCFC-225cb	$CHClFCF_2CClF_2$	5.9	0.29	1,860	525	1,110	120	73
(E)-1-Chloro-3,3,3-trifluoroprop-1-ene	trans-$CF_3CH=CHCl$	26.0 days	0.04	5	1	2	<1	<1
Hydrofluorocarbons								
HFC-23	CHF_3	222.0	0.18	10,800	12,400	11,500	13,000	12,700
HFC-32	CH_2F_2	5.2	0.11	2,430	677	1,360	145	94
HFC-41	CH_3F	2.8	0.02	427	116	177	21	16
HFC-125	CHF_2CF_3	28.2	0.23	6,090	3,170	5,800	2,980	967
HFC-134	CHF_2CHF_2	9.7	0.19	3,580	1,120	2,660	412	160
HFC-134a	CH_2FCF_3	13.4	0.16	3,710	1,300	3,050	703	201
HFC-143	CH_2FCHF_2	3.5	0.13	1,200	328	549	62	46
HFC-143a	CH_3CF_3	47.1	0.16	6,940	4,800	6,960	5,060	2,500
HFC-152	CH_2FCH_2F	0.4	0.04	60	16	18	3	2
HFC-152a	CH_3CHF_2	1.5	0.10	506	138	174	24	19
HFC-161	CH_3CH_2F	66.0 days	0.02	13	4	4	<1	<1
HFC-227ca	$CF_3CF_2CHF_2$	28.2	0.27	5,080	2,640	4,830	2,480	806
HFC-227ea	CF_3CHFCF_3	38.9	0.26	5,360	3,350	5,280	3,440	1,460
HFC-236cb	$CH_2FCF_2CF_3$	13.1	0.23	3,480	1,210	2,840	636	185
HFC-236ea	CHF_2CHFCF_3	11.0	0.30	4,110	1,330	3,190	573	195
HFC-236fa	$CF_3CH_2CF_3$	242.0	0.24	6,940	8,060	7,400	8,400	8,380
HFC-245ca	$CH_2FCF_2CHF_2$	6.5	0.24	2,510	716	1,570	176	100
HFC-245cb	$CF_3CF_2CH_3$	47.1	0.24	6,680	4,620	6,690	4,870	2,410
HFC-245ea	$CHF_2CHFCHF_2$	3.2	0.16	863	235	378	44	33
HFC-245eb	$CH_2FCHFCF_3$	3.1	0.20	1,070	290	460	54	40
HFC-245fa	$CHF_2CH_2CF_3$	7.7	0.24	2,920	858	1,970	245	121
HFC-263fb	$CH_3CH_2CF_3$	1.2	0.10	278	76	92	13	10
HFC-272ca	$CH_3CF_2CH_3$	2.6	0.07	530	144	213	26	20
HFC-329p	$CHF_2CF_2CF_2CF_3$	28.4	0.31	4,510	2,360	4,290	2,220	725
HFC-365mfc	$CH_3CF_2CH_2CF_3$	8.7	0.22	2,660	804	1,890	262	114
HFC-43-10mee	$CF_3CHFCHFCF_2CF_3$	16.1	0.42	4,310	1,650	3,720	1,070	281
HFC-1132a	$CH_2=CF_2$	4.0 days	0.004	<1	<1	<1	<1	<1
HFC-1141	$CH_2=CHF$	2.1 days	0.002	<1	<1	<1	<1	<1
(Z)-HFC-1225ye	$CF_3CF=CHF(Z)$	8.5 days	0.02	<1	<1	<1	<1	<1

Industrial Designation or Chemical Name	Chemical Formula	Lifetime (years)	Radiative Efficiency (W m^{-2} ppb^{-1})	GWP 20-yr	GWP 100-yr	GTP 20-yr	GTP 50-yr	GTP 100-yr
(E)-HFC-1225ye	$CF_3CF=CHF(E)$	4.9 days	0.01	**<1**	**<1**	**<1**	**<1**	**<1**
(Z)-HFC-1234ze	$CF_3CH=CHF(Z)$	10.0 days	0.02	**1**	**<1**	**<1**	**<1**	**<1**
HFC-1234yf	$CF_3CF=CH_2$	10.5 days	0.02	**1**	**<1**	**<1**	**<1**	**<1**
(E)-HFC-1234ze	trans-$CF_3CH=CHF$	16.4 days	0.04	**4**	**<1**	**<1**	**<1**	**<1**
(Z)-HFC-1336	$CF_3CH=CHCF_3(Z)$	22.0 days	0.07	**6**	**2**	**2**	**<1**	**<1**
HFC-1243zf	$CF_3CH=CH_2$	7.0 days	0.01	**<1**	**<1**	**<1**	**<1**	**<1**
HFC-1345zfc	$C_2F_5CH=CH_2$	7.6 days	0.01	**<1**	**<1**	**<1**	**<1**	**<1**
3,3,4,4,5,5,6,6,6-Nonafluorohex-1-ene	$C_4F_9CH=CH_2$	7.6 days	0.03	**<1**	**<1**	**<1**	**<1**	**<1**
3,3,4,4,5,5,6,6,7,7,8,8,8-Tridecafluorooct-1-ene	$C_6F_{13}CH=CH_2$	7.6 days	0.03	**<1**	**<1**	**<1**	**<1**	**<1**
3,3,4,4,5,5,6,6,7,7,8,8,9,9,10,10,10-Heptadecafluorodec-1-ene	$C_8F_{17}CH=CH_2$	7.6 days	0.03	**<1**	**<1**	**<1**	**<1**	**<1**
Chlorocarbons and Hydrochlorocarbons								
Methyl chloroform	CH_3CCl_3	5.0	0.07	**578**	**160**	**317**	**34**	**22**
Carbon tetrachloride	CCl_4	26.0	0.17	**3,480**	**1,730**	**3,280**	**1,570**	**479**
Methyl chloride	CH_3Cl	1.0	0.01	**45**	**12**	**15**	**2**	**2**
Methylene chloride	CH_2Cl_2	0.4	0.03	**33**	**9**	**10**	**2**	**1**
Chloroform	$CHCl_3$	0.4	0.08	**60**	**16**	**18**	**3**	**2**
1,2-Dichloroethane	CH_2ClCH_2Cl	65.0 days	0.01	**3**	**<1**	**<1**	**<1**	**<1**
Bromocarbons, Hydrobromocarbons and Halons								
Methyl bromide	CH_3Br	0.8	0.004	**9**	**2**	**3**	**<1**	**<1**
Methylene bromide	CH_2Br_2	0.3	0.01	**4**	**1**	**1**	**<1**	**<1**
Halon-1201	$CHBrF_2$	5.2	0.15	**1,350**	**376**	**756**	**80**	**52**
Halon-1202	CBr_2F_2	2.9	0.27	**848**	**231**	**356**	**42**	**32**
Halon-1211	$CBrClF_2$	16.0	0.29	**4,590**	**1,750**	**3,950**	**1,130**	**297**
Halon-1301	$CBrF_3$	65.0	0.30	**7,800**	**6,290**	**7,990**	**6,750**	**4,170**
Halon-2301	CH_2BrCF_3	3.4	0.14	**635**	**173**	**286**	**33**	**24**
Halon-2311 / Halothane	$CHBrClCF_3$	1.0	0.13	**151**	**41**	**49**	**7**	**6**
Halon-2401	$CHFBrCF_3$	2.9	0.19	**674**	**184**	**283**	**34**	**25**
Halon-2402	$CBrF_2CBrF_2$	20.0	0.31	**3,440**	**1,470**	**3,100**	**1,150**	**304**
Fully Fluorinated Species								
Nitrogen trifluoride	NF_3	500.0	0.20	**12,800**	**16,100**	**13,700**	**16,500**	**18,100**
Sulphur hexafluoride	SF_6	3,200.0	0.57	**17,500**	**23,500**	**18,900**	**23,800**	**28,200**

Industrial Designation or Chemical Name	Chemical Formula	Lifetime (years)	Radiative Efficiency (W m^{-2} ppb^{-1})	GWP 20-yr	GWP 100-yr	GTP 20-yr	GTP 50-yr	GTP 100-yr
(Trifluoromethyl)sulfur pentafluoride	SF_5CF_3	800.0	0.59	13,500	17,400	14,500	17,800	20,200
Sulfuryl fluoride	SO_2F_2	36.0	0.20	6,840	4,090	6,690	4,140	1,650
PFC-14	CF_4	50,000.0	0.09	4,880	6,630	5,270	6,690	8,040
PFC-116	C_2F_6	10,000.0	0.25	8,210	11,100	8,880	11,200	13,500
PFC-c216	$c-C_3F_6$	3,000.0	0.23	6,850	9,200	7,400	9,310	11,000
PFC-218	C_3F_8	2,600.0	0.28	6,640	8,900	7,180	9,010	10,700
PFC-318	$c-C_4F_8$	3,200.0	0.32	7,110	9,540	7,680	9,660	11,500
PFC-31-10	C_4F_{10}	2,600.0	0.36	6,870	9,200	7,420	9,320	11,000
Perfluorocyclopentene	$c-C_5F_8$	31.0 days	0.08	7	2	2	<1	<1
PFC-41-12	$n-C_5F_{12}$	4,100.0	0.41	6,350	8,550	6,860	8,650	10,300
PFC-51-14	$n-C_6F_{14}$	3,100.0	0.44	5,890	7,910	6,370	8,010	9,490
PFC-61-16	$n-C_7F_{16}$	3,000.0	0.50	5,830	7,820	6,290	7,920	9,380
PFC-71-18	C_8F_{18}	3,000.0	0.55	5,680	7,620	6,130	7,710	9,140
PFC-91-18	$C_{10}F_{18}$	2,000.0	0.55	5,390	7,190	5,820	7,290	8,570
Perfluorodecalin (Z)	$(Z)-C_{10}F_{18}$	2,000.0	0.56	5,430	7,240	5,860	7,340	8,630
Perfluorodecalin (E)	$(E)-C_{10}F_{18}$	2,000.0	0.48	4,720	6,290	5,090	6,380	7,500
PFC-1114	$CF_2=CF_2$	1.1 days	0.002	<1	<1	<1	<1	<1
PFC-1216	$CF_3CF=CF_2$	4.9 days	0.01	<1	<1	<1	<1	<1
Perfluorobuta-1,3-diene	$CF_2=CFCF=CF_2$	1.1 days	0.003	<1	<1	<1	<1	<1
Perfluorobut-1-ene	$CF_3CF_2CF=CF_2$	6.0 days	0.02	<1	<1	<1	<1	<1
Perfluorobut-2-ene	$CF_3CF=CFCF_3$	31.0 days	0.07	6	2	2	<1	<1
Halogenated Alcohols and Ethers								
HFE-125	CHF_2OCF_3	119.0	0.41	12,400	12,400	13,000	13,200	10,900
HFE-134 (HG-00)	CHF_2OCHF_2	24.4	0.44	11,600	5,560	10,800	4,900	1,430
HFE-143a	CH_3OCF_3	4.8	0.18	1,890	523	1,020	108	73
HFE-227ea	$CF_3CHFOCF_3$	51.6	0.44	8,900	6,450	8,980	6,850	3,630
HCFE-235ca2 (enflurane)	CHF_2OCF_2CHFCl	4.3	0.41	2,120	583	1,080	116	81
HCFE-235da2 (isoflurane)	$CHF_2OCHClCF_3$	3.5	0.42	1,800	491	822	93	68
HFE-236ca	$CHF_2OCF_2CHF_2$	20.8	0.56	9,710	4,240	8,820	3,400	912
HFE-236ea2 (desflurane)	$CHF_2OCHFCF_3$	10.8	0.45	5,550	1,790	4,280	753	260
HFE-236fa	$CF_3CH_2OCF_3$	7.5	0.36	3,350	979	2,240	273	138
HFE-245cb2	$CF_3CF_2OCH_3$	4.9	0.33	2,360	654	1,280	136	91
HFE-245fa1	$CHF_2CH_2OCF_3$	6.6	0.31	2,900	828	1,820	206	116
HFE-245fa2	$CHF_2OCH_2CF_3$	5.5	0.36	2,910	812	1,670	179	114
2,2,3,3,3-Pentafluoropropan-1-ol	$CF_3CF_2CH_2OH$	0.3	0.14	69	19	21	3	3
HFE-254cb1	$CH_3OCF_2CHF_2$	2.5	0.26	1,110	301	438	54	42

Industrial Designation or Chemical Name	Chemical Formula	Lifetime (years)	Radiative Efficiency (W m^{-2} ppb^{-1})	GWP 20-yr	GWP 100-yr	GTP 20-yr	GTP 50-yr	GTP 100-yr
HFE-263fb2	$CF_3CH_2OCH_3$	23.0 days	0.04	5	1	1	0	0
HFE-263m1	$CF_3OCH_2CH_3$	0.4	0.13	108	29	33	5	4
3,3,3-Trifluoropropan-1-ol	$CF_3CH_2CH_2OH$	12.0 days	0.02	1	0	0	0	0
HFE-329mcc2	$CHF_2CF_2OCF_2CF_3$	22.5	0.53	6,720	3,070	6,180	2,580	718
HFE-338mmz1	$(CF_3)_2CHOCHF_2$	21.2	0.44	5,940	2,620	5,410	2,130	575
HFE-338mcf2	$CF_3CH_2OCF_2CF_3$	7.5	0.44	3,180	929	2,120	259	131
Sevoflurane (HFE-347mmz1)	$(CF_3)_2CHOCH_2F$	2.2	0.32	795	216	302	38	30
HFE-347mcc3 (HFE-7000)	$CH_3OCF_2CF_2CF_3$	5.0	0.35	1,910	530	1,050	111	74
HFE-347mcf2	$CHF_2CH_2OCF_2CF_3$	6.6	0.42	2,990	854	1,880	212	120
HFE-347pcf2	$CHF_2CF_2OCH_2CF_3$	6.0	0.48	3,150	889	1,900	206	124
HFE-347mmy1	$(CF_3)_2CFOCH_3$	3.7	0.32	1,330	363	624	69	51
HFE-356mec3	$CH_3OCF_2CHFCF_3$	3.8	0.30	1,410	387	673	74	54
HFE-356mff2	$CF_3CH_2OCH_2CF_3$	105.0 days	0.17	62	17	18	3	2
HFE-356pcf2	$CHF_2CH_2OCF_2CHF_2$	5.7	0.37	2,560	719	1,500	162	101
HFE-356pcf3	$CHF_2OCH_2CF_2CHF_2$	3.5	0.38	1,640	446	747	84	62
HFE-356pcc3	$CH_3OCF_2CF_2CHF_2$	3.8	0.32	1,510	413	718	79	57
HFE-356mmz1	$(CF_3)_2CHOCH_3$	97.1 days	0.15	50	14	15	2	2
HFE-365mcf3	$CF_3CF_2CH_2OCH_3$	19.3 days	0.05	3	<1	<1	<1	<1
HFE-365mcf2	$CF_3CF_2OCH_2CH_3$	0.6	0.26	215	58	66	10	8
HFE-374pc2	$CHF_2CF_2OCH_2CH_3$	5.0	0.30	2,260	627	1,240	132	88
4,4,4-Trifluorobutan-1-ol	$CF_3(CH_2)_2CH_2OH$	4.0 days	0.01	<1	<1	<1	<1	<1
2,2,3,3,4,4,5,5-Octafluorocyclopentanol	$-(CF_2)_4CH(OH)-$	0.3	0.16	47	13	14	2	2
HFE-43-10pccc124 (H-Galden 1040x, HG-11)	$CHF_2OCF_2OC_2F_4OCHF_2$	13.5	1.02	8,010	2,820	6,600	1,530	436
HFE-449s1 (HFE-7100)	$C_4F_9OCH_3$	4.7	0.36	1,530	421	809	86	59
n-HFE-7100	$n-C_4F_9OCH_3$	4.7	0.42	1,760	486	934	99	68
i-HFE-7100	$i-C_4F_9OCH_3$	4.7	0.35	1,480	407	783	83	57
HFE-569sf2 (HFE-7200)	$C_4F_9OC_2H_5$	0.8	0.30	209	57	66	10	8
n-HFE-7200	$n-C_4F_9OC_2H_5$	0.8	0.35	237	65	75	11	9
i-HFE-7200	$i-C_4F_9OC_2H_5$	0.8	0.24	163	44	52	8	6
HFE-236ca12 (HG-10)	$CHF_2OCF_2OCHF_2$	25.0	0.65	11,000	5,350	10,300	4,770	1,420
HFE-338pcc13 (HG-01)	$CHF_2OCF_2CF_2OCHF_2$	12.9	0.86	8,430	2,910	6,860	1,500	442
1,1,1,3,3,3-Hexafluoropropan-2-ol	$(CF_3)_2CHOH$	1.9	0.26	668	182	243	32	25
HG-02	$HF_2C-(OCF_2CF_2)_2-OCF_2H$	12.9	1.24	7,900	2,730	6,430	1,410	415

Industrial Designation or Chemical Name	Chemical Formula	Lifetime (years)	Radiative Efficiency (W m^{-2} ppb^{-1})	GWP 20-yr	GWP 100-yr	GTP 20-yr	GTP 50-yr	GTP 100-yr
HG-03	$HF_2C–(OCF_2CF_2)_3–OCF_2H$	12.9	1.76	8,270	2,850	6,730	1,480	434
HG-20	$HF_2C–(OCF_2)_2–OCF_2H$	25.0	0.92	10,900	5,300	10,200	4,730	1,400
HG-21	$HF_2C–OCF_2CF_2OCF_2OCF_2O–CF_2H$	13.5	1.71	11,100	3,890	9,110	2,120	602
HG-30	$HF_2C–(OCF_2)_3–OCF_2H$	25.0	1.65	15,100	7,330	14,100	6,530	1,940
1-Ethoxy-1,1,2,2,3,3,3-heptafluoropropane	$CF_3CF_2CF_2OCH_2CH_3$	0.8	0.28	223	61	70	10	8
Fluoroxene	$CF_3CH_2OCH=CH_2$	3.6 days	0.01	<1	<1	<1	<1	<1
1,1,2,2-Tetrafluoro-1-(fluoromethoxy)ethane	$CH_2FOCF_2CF_2H$	6.2	0.34	3,080	871	1,880	207	122
2-Ethoxy-3,3,4,4,5-pentafluorotetrahydro-2,5-bis[1,2,2,2-tetrafluoro-1-(trifluoromethyl)ethyl]-furan	$C_{12}H_5F_{19}O_2$	1.0	0.49	204	56	66	10	8
Fluoro(methoxy)methane	CH_3OCH_2F	73.0 days	0.07	46	13	14	2	2
Difluoro(methoxy)methane	CH_3OCHF_2	1.1	0.17	528	144	173	25	20
Fluoro(fluoromethoxy)methane	CH_2FOCH_2F	0.9	0.19	479	130	153	22	18
Difluoro(fluoromethoxy)methane	CH_2FOCHF_2	3.3	0.30	2,260	617	1,010	115	86
Trifluoro(fluoromethoxy)methane	CH_2FOCF_3	4.4	0.33	2,730	751	1,400	150	105
HG'-01	$CH_3OCF_2CF_2OCH_3$	2.0	0.29	815	222	301	39	31
HG'-02	$CH_3O(CF_2CF_2O)_2CH_3$	2.0	0.56	868	236	320	42	33
HG'-03	$CH_3O(CF_2CF_2O)_3CH_3$	2.0	0.76	812	221	299	39	31
HFE-329me3	$CF_3CFHCF_2OCF_3$	40.0	0.48	7,170	4,550	7,090	4,690	2,040
3,3,4,4,5,5,6,6,7,7,7-Undecafluoroheptan-1-ol	$CF_3(CF_2)_4CH_2CH_2OH$	20.0 days	0.06	2	<1	<1	<1	<1
3,3,4,4,5,5,6,6,7,7,8,8,9,9,9-Pentadecafluorononan-1-ol	$CF_3(CF_2)_6CH_2CH_2OH$	20.0 days	0.07	1	<1	<1	<1	<1
3,3,4,4,5,5,6,6,7,7,8,8,9,9,10,10,11,11,11-Nonadecafluoroundecan-1-ol	$CF_3(CF_2)_8CH_2CH_2OH$	20.0 days	0.05	<1	<1	<1	<1	<1
2-Chloro-1,1,2-trifluoro-1-methoxyethane	CH_3OCF_2CHFCl	1.4	0.21	449	122	153	21	17
PFPMIE (perfluoropolymethylisopropyl ether)	$CF_3OCF(CF_3)CF_2OCF_2OCF_3$	800.0	0.65	7,500	9,710	8,070	9,910	11,300
HFE-216	$CF_3OCF=CF_2$	8.4 days	0.02	<1	<1	<1	<1	<1

Industrial Designation or Chemical Name	Chemical Formula	Lifetime (years)	Radiative Efficiency ($W\ m^{-2}\ ppb^{-1}$)	GWP 20-yr	GWP 100-yr	GTP 20-yr	GTP 50-yr	GTP 100-yr
Trifluoromethyl formate	$HCOOCF_3$	3.5	0.31	2,150	588	984	111	82
Perfluoroethyl formate	$HCOOCF_2CF_3$	3.5	0.44	2,130	580	971	110	81
Perfluoropropyl formate	$HCOOCF_2CF_2CF_3$	2.6	0.50	1,380	376	555	68	52
Perfluorobutyl formate	$HCOOCF_2CF_2CF_2CF_3$	3.0	0.56	1,440	392	613	72	54
2,2,2-Trifluoroethyl formate	$HCOOCH_2CF_3$	0.4	0.16	123	33	37	6	5
3,3,3-Trifluoropropyl formate	$HCOOCH_2CH_2CF_3$	0.3	0.13	64	17	19	3	2
1,2,2,2-Tetrafluoroethyl formate	$HCOOCHFCF_3$	3.2	0.35	1,720	470	755	87	65
1,1,1,3,3,3-Hexafluoropropan-2-yl formate	$HCOOCH(CF_3)_2$	3.2	0.33	1,220	333	535	62	46
Perfluorobutyl acetate	$CH_3COOCF_2CF_2CF_2CF_3$	21.9 days	0.12	6	2	2	<1	<1
Perfluoropropyl acetate	$CH_3COOCF_2CF_2CF_3$	21.9 days	0.11	6	2	2	<1	<1
Perfluoroethyl acetate	$CH_3COOCF_2CF_3$	21.9 days	0.10	8	2	2	<1	<1
Trifluoromethyl acetate	CH_3COOCF_3	21.9 days	0.07	8	2	2	<1	<1
Methyl carbonofluoridate	$FCOOCH_3$	1.8	0.07	350	95	126	17	13
1,1-Difluoroethyl carbonofluoridate	$FCOOCF_2CH_3$	0.3	0.17	99	27	30	5	4
1,1-Difluoroethyl 2,2,2-trifluoroacetate	$CF_3COOCF_2CH_3$	0.3	0.27	113	31	34	5	4
Ethyl 2,2,2-trifluoroacetate	$CF_3COOCH_2CH_3$	21.9 days	0.05	5	1	1	<1	<1
2,2,2-Trifluoroethyl 2,2,2-trifluoroacetate	$CF_3COOCH_2CF_3$	54.8 days	0.15	25	7	7	1	<1
Methyl 2,2,2-trifluoroacetate	CF_3COOCH_3	0.6	0.18	192	52	60	9	7
Methyl 2,2-difluoroacetate	HCF_2COOCH_3	40.1 days	0.05	12	3	4	<1	<1
Difluoromethyl 2,2,2-trifluoroacetate	$CF_3COOCHF_2$	0.3	0.24	99	27	30	5	4
2,2,3,3,4,4,4-Heptafluorobutan-1-ol	$C_3F_7CH_2OH$	0.6	0.20	124	34	38	6	5
1,1,2-Trifluoro-2-(trifluoromethoxy)-ethane	$CHF_2CHFOCF_3$	9.8	0.35	3,970	1,240	2,960	467	178
1-Ethoxy-1,1,2,3,3,3-hexafluoropropane	$CF_3CHFCF_2OCH_2CH_3$	0.4	0.19	86	23	26	4	3
1,1,1,2,2,3,3-Heptafluoro-3-(1,2,2,2-tetrafluoroethoxy)-propane	$CF_3CF_2CF_2OCHFCF_3$	67.0	0.58	7,940	6,490	8,140	6,960	4,380
2,2,3,3-Tetrafluoro-1-propanol	$CHF_2CF_2CH_2OH$	91.2 days	0.11	48	13	14	2	2
2,2,3,4,4,4-Hexafluoro-1-butanol	$CF_3CHFCF_2CH_2OH$	94.9 days	0.19	63	17	19	3	2
2,2,3,3,4,4,4-Heptafluoro-1-butanol	$CF_3CF_2CF_2CH_2OH$	0.3	0.16	60	16	18	3	2
1,1,2,2-Tetrafluoro-3-methoxy-propane	$CHF_2CF_2CH_2OCH_3$	14.2 days	0.03	2	<1	<1	<1	<1
Perfluoro-2-methyl-3-pentanone	$CF_3CF_2C(O)CF(CF_3)_2$	7.0 days	0.03	<1	<1	<1	<1	<1

Industrial Designation or Chemical Name	Chemical Formula	Lifetime (years)	Radiative Efficiency (W m^{-2} ppb^{-1})	GWP 20-yr	GWP 100-yr	GTP 20-yr	GTP 50-yr	GTP 100-yr
3,3,3-Trifluoro-propanal	CF_3CH_2CHO	2.0 days	0.004	**<1**	**<1**	**<1**	**<1**	**<1**
2-Fluoroethanol	CH_2FCH_2OH	20.4 days	0.02	**3**	**<1**	**<1**	**<1**	**<1**
2,2-Difluoroethanol	CHF_2CH_2OH	40.0 days	0.04	**11**	**3**	**3**	**<1**	**<1**
2,2,2-Trifluoroethanol	CF_3CH_2OH	0.3	0.10	**73**	**20**	**22**	**3**	**3**
1,1'-Oxybis[2-(difluoromethoxy)-1,1,2,2-tetrafluoroethane	$HCF_2O(CF_2CF_2O)_2\text{-}CF_2H$	26.0	1.15	**9,910**	**4,920**	**9,320**	**4,460**	**1,360**
1,1,3,3,4,4,6,6,7,7,9,9,10,10,12,12-Hexadecafluoro-2,5,8,11-tetraoxadodecane	$HCF_2O(CF_2CF_2O)_3\text{-}CF_2H$	26.0	1.43	**9,050**	**4,490**	**8,520**	**4,080**	**1,250**
1,1,3,3,4,4,6,6,7,7,9,9,10,10,12,12,13,13,15,15-Eicosafluoro-2,5,8,11,14-pentaoxapentadecane	$HCF_2O(CF_2CF_2O)_4\text{-}CF_2H$	26.0	1.46	**7,320**	**3,630**	**6,880**	**3,300**	**1,010**

For CH_4 we estimate an uncertainty of ±30% and ±40% for 20- and 100-year time horizons, respectively (for 90% uncertainty range). The uncertainty is dominated by AGWP for CO_2 and indirect effects. The uncertainty in GWP for N_2O is estimated to be ±20% and ±30% for 20- and 100-year time horizons, with the largest contributions from CO_2. The uncertainty in GWP for HFC-134a is estimated to be ±25% and ±35% for 20- and 100-year time horizons while for CFC-11, the GWP corresponding uncertainties are approximately ±20% and ±35% (not accounting for the indirect effects). For CFC-12 the corresponding numbers are ±20 and ±30. The uncertainties estimated for HFC-134a and CFC-11 are assessed as representative for most other gases with similar or longer lifetimes. For shorter-lived gases, the uncertainties will be larger. For GTP, few estimates are available in the literature. The uncertainty is assessed to be of the order of ±75% for the methane 100-year GTP.

* No single lifetime can be given. The impulse response function for CO_2 from Joos et al. (2013) has been used. See also Supplementary Material Section S8.11 in IPCC (2013).

+ Perturbation lifetime is used in calculation of metrics; not the lifetime of the atmospheric burden.

Metric values for CH_4 of fossil origin include the oxidation to CO_2 (based on Boucher et al. (2009)). In applications of these values, inclusion of the CO_2 effect of fossil methane must be done with caution to avoid any double counting, since CO_2 emissions numbers are often based on total carbon content. For non-fossil CH_4 we assume balance between CO_2 taken up by the biosphere and CO_2 produced from CH_4 oxidation.

5A-2. BASELINE SCENARIO MIXING RATIOS

Table 5A-2. Mixing ratios (ppt) of the ODSs considered in the baseline (A1) scenario. Values are for the beginning of the corresponding year (see Chapter 1). Potentially important short-lived gases that may currently contribute 5 (2–8) ppt of stratospheric bromine and 95 (50–145) ppt of stratospheric chlorine (see Chapter 1) are not shown in the table. Note: Areas are shaded for compounds in years when mixing ratio values are forced to equal global average estimates inferred from observations (see Chapter 1, Figure 1-1).

Year	CFC-11	CFC-12	CFC-113	CFC-114	CFC-115	CCl$_4$	CH$_3$CCl$_3$	HCFC-22	HCFC-141b	HCFC-142b	halon-1211	halon-1202	halon-1301	halon-2402	CH$_3$Br	CH$_3$Cl
1955	3.3	14.3	1.3	2.6	0.0	42.3	0.1	1.0	0.0	0.0	0.00	0.00	0.00	0.00	6.3	491.3
1960	9.5	29.5	1.9	3.8	0.0	52.1	1.5	2.1	0.0	0.0	0.00	0.00	0.00	0.00	6.5	510.3
1965	23.5	58.8	3.1	5.0	0.0	64.4	4.7	4.9	0.0	0.0	0.00	0.00	0.00	0.00	6.7	528.1
1970	52.8	114.3	5.5	6.5	0.2	75.9	16.3	12.1	0.0	0.0	0.02	0.00	0.00	0.02	7.0	539.9
1975	106.1	203.1	10.4	8.3	0.6	85.5	40.0	23.8	0.0	0.2	0.12	0.01	0.04	0.06	7.4	545.8
1980	161.9	297.1	19.0	10.7	1.5	92.9	82.0	42.5	0.0	0.4	0.69	0.01	0.36	0.15	7.8	548.4
1981	170.5	312.1	21.5	11.1	1.7	94.3	89.0	46.6	0.0	0.5	0.81	0.01	0.43	0.17	7.9	548.6
1982	179.2	330.5	24.5	11.6	2.0	95.7	94.1	50.7	0.0	0.6	0.95	0.01	0.51	0.19	8.0	548.9
1983	187.6	346.4	28.0	12.0	2.3	97.0	98.0	54.8	0.0	0.6	1.09	0.02	0.60	0.21	8.0	549.1
1984	196.4	363.7	32.2	12.4	2.7	98.5	102.0	58.8	0.0	0.7	1.23	0.02	0.71	0.23	8.1	549.3
1985	206.2	378.5	36.7	12.9	3.0	99.9	106.5	62.7	0.0	0.7	1.40	0.02	0.85	0.26	8.2	549.4
1986	216.2	397.9	41.8	13.4	3.4	101.3	110.3	66.9	0.0	0.8	1.59	0.02	1.03	0.27	8.3	549.5
1987	227.2	416.4	47.5	14.0	3.9	103.0	113.5	71.5	0.0	0.8	1.77	0.02	1.24	0.29	8.4	549.6
1988	238.7	439.0	54.0	14.5	4.3	104.0	118.7	76.7	0.0	0.9	1.96	0.02	1.45	0.31	8.5	549.7
1989	248.8	459.3	60.9	15.0	4.7	104.8	123.5	82.5	0.0	1.1	2.14	0.02	1.64	0.34	8.6	549.8
1990	256.4	476.4	67.6	15.4	5.2	105.6	127.3	88.2	0.0	1.2	2.32	0.03	1.80	0.37	8.7	549.8
1991	262.0	489.7	73.3	15.7	5.6	105.9	130.8	93.7	0.0	1.8	2.52	0.03	1.95	0.39	8.8	549.9
1992	265.4	500.7	78.2	15.8	6.0	105.8	133.6	99.8	0.1	2.8	2.72	0.03	2.09	0.42	8.9	549.9
1993	267.8	510.0	81.2	16.0	6.4	105.3	130.3	103.9	0.4	3.9	2.92	0.03	2.23	0.44	9.0	549.9
1994	268.1	516.5	83.0	16.1	6.8	104.4	121.9	109.1	1.5	5.1	3.11	0.03	2.35	0.46	9.2	550.0
1995	267.8	523.0	83.8	16.1	7.1	103.7	110.5	113.6	2.8	6.2	3.35	0.04	2.45	0.47	9.2	555.2
1996	267.0	528.7	84.0	16.2	7.4	102.6	98.2	119.4	4.5	7.2	3.53	0.04	2.53	0.48	9.2	539.3
1997	266.0	532.9	83.8	16.3	7.7	101.6	84.1	124.2	6.4	8.3	3.69	0.05	2.61	0.49	9.1	529.6
1998	264.6	536.4	83.4	16.4	7.9	100.7	71.0	128.9	8.2	9.4	3.82	0.05	2.69	0.49	9.3	554.3
1999	263.3	539.3	82.9	16.4	8.0	99.6	59.4	134.3	10.1	10.4	3.96	0.04	2.76	0.49	9.3	555.5
2000	261.6	541.4	82.3	16.5	8.1	98.5	49.7	139.2	11.8	11.4	4.08	0.04	2.84	0.49	9.0	542.8
2001	260.0	542.8	81.7	16.5	8.2	97.5	41.5	144.7	13.5	12.5	4.18	0.03	2.88	0.49	8.5	534.8
2002	258.2	543.6	81.1	16.6	8.3	96.5	34.5	150.5	14.8	13.3	4.24	0.02	2.91	0.49	8.3	533.6

Year	CFC-11	CFC-12	CFC-113	CFC-114	CFC-115	CCl$_4$	CH$_3$CCl$_3$	HCFC-22	HCFC-141b	HCFC-142b	halon-1211	halon-1202	halon-1301	halon-2402	CH$_3$Br	CH$_3$Cl
2003	256.0	543.6	80.4	16.6	8.3	95.5	28.8	155.4	16.1	13.9	4.28	0.02	2.97	0.49	8.2	539.6
2004	253.8	543.4	79.7	16.6	8.3	94.5	24.0	160.5	17.0	14.6	4.31	0.02	3.02	0.49	8.1	536.2
2005	251.5	542.5	79.0	16.6	8.4	93.5	20.0	165.7	17.5	15.2	4.34	0.01	3.05	0.49	7.9	539.9
2006	249.4	541.6	78.4	16.5	8.4	92.5	16.7	171.9	17.8	15.9	4.34	0.01	3.08	0.48	7.8	536.9
2007	247.2	539.6	77.7	16.5	8.4	91.4	14.0	179.1	18.5	16.9	4.32	0.01	3.11	0.48	7.6	543.7
2008	245.0	537.5	76.9	16.5	8.4	90.2	11.7	187.3	19.1	18.1	4.28	0.00	3.15	0.47	7.5	545.3
2009	243.0	535.3	76.2	16.5	8.4	88.9	9.8	195.2	19.6	19.3	4.22	0.00	3.17	0.47	7.3	541.0
2010	241.1	532.7	75.5	16.4	8.4	87.6	8.2	202.5	20.1	20.0	4.16	0.00	3.19	0.46	7.1	538.4
2011	239.0	530.1	74.8	16.4	8.4	86.5	6.9	210.0	20.9	20.8	4.08	0.00	3.22	0.45	7.1	533.5
2012	237.0	527.4	74.1	16.4	8.4	85.2	5.7	216.1	21.9	21.5	4.01	0.00	3.24	0.45	7.0	538.1
2013	234.7	525.0	73.4	16.3	8.4	84.1	4.8	221.5	22.9	21.9	3.91	0.00	3.26	0.44	7.0	539.5
2014	232.4	520.9	72.7	16.2	8.4	82.9	4.0	233.8	23.8	22.7	3.81	0.00	3.27	0.43	7.0	539.5
2015	229.9	516.7	71.9	16.1	8.4	81.6	3.3	244.8	24.6	23.5	3.71	0.00	3.28	0.43	7.0	539.5
2016	227.5	512.4	71.2	16.1	8.4	80.3	2.7	254.7	25.5	24.2	3.60	0.00	3.29	0.42	7.0	539.5
2017	224.9	508.0	70.5	16.0	8.4	78.9	2.2	262.9	26.4	24.8	3.49	0.00	3.30	0.41	7.0	539.5
2018	222.4	503.6	69.7	16.0	8.4	77.4	1.8	269.8	27.2	25.3	3.38	0.00	3.31	0.41	7.0	539.5
2019	219.9	499.1	69.0	15.9	8.4	75.9	1.5	275.5	28.0	25.8	3.27	0.00	3.31	0.40	7.0	539.5
2020	217.3	494.6	68.3	15.8	8.4	74.4	1.2	280.3	28.7	26.2	3.15	0.00	3.31	0.39	7.0	539.5
2025	204.2	472.0	64.7	15.5	8.4	66.6	0.4	282.2	31.5	27.0	2.60	0.00	3.29	0.35	7.0	539.5
2030	190.9	449.8	61.4	15.1	8.4	58.8	0.2	251.9	32.0	26.0	2.09	0.00	3.24	0.32	7.0	539.5
2035	177.8	428.5	58.2	14.7	8.3	51.3	0.1	198.8	29.8	23.3	1.66	0.00	3.16	0.28	7.0	539.5
2040	165.1	408.1	55.1	14.3	8.3	44.4	0.0	142.9	26.0	19.6	1.30	0.00	3.06	0.25	7.0	539.5
2045	152.8	388.6	52.3	14.0	8.3	38.1	0.0	98.7	21.7	16.0	1.01	0.00	2.95	0.22	7.0	539.5
2050	141.1	370.0	49.5	13.6	8.2	32.6	0.0	66.4	17.7	12.7	0.77	0.00	2.83	0.19	7.0	539.5
2055	130.0	352.3	46.9	13.3	8.2	27.7	0.0	44.2	14.1	9.9	0.59	0.00	2.71	0.17	7.0	539.5
2060	119.6	335.5	44.5	12.9	8.1	23.4	0.0	29.3	11.1	7.7	0.45	0.00	2.58	0.15	7.0	539.5
2065	109.8	319.4	42.1	12.6	8.0	19.8	0.0	19.3	8.6	5.9	0.34	0.00	2.45	0.13	7.0	539.5
2070	100.7	304.1	39.9	12.2	8.0	16.6	0.0	12.8	6.7	4.5	0.26	0.00	2.32	0.11	7.0	539.5
2075	92.3	289.6	37.9	11.9	7.9	14.0	0.0	8.4	5.1	3.4	0.19	0.00	2.20	0.10	7.0	539.5
2080	84.5	275.7	35.9	11.6	7.9	11.7	0.0	5.6	3.9	2.6	0.14	0.00	2.07	0.08	7.0	539.5
2085	77.2	262.5	34.0	11.3	7.8	9.8	0.0	3.7	3.0	2.0	0.11	0.00	1.96	0.07	7.0	539.5
2090	70.6	250.0	32.2	11.0	7.7	8.2	0.0	2.4	2.3	1.5	0.08	0.00	1.84	0.06	7.0	539.5
2095	64.4	238.0	30.5	10.7	7.7	6.8	0.0	1.6	1.7	1.2	0.06	0.00	1.73	0.05	7.0	539.5
2100	58.8	226.6	28.9	10.5	7.6	5.7	0.0	1.1	1.3	0.9	0.04	0.00	1.63	0.04	7.0	539.5